Performance of Alternative Diamond Interchange Forms

Volume 1
Research Report

Andrew P. Tarko, Mario A. Romero, Afia Sultana

AUTHORS

Andrew P. Tarko, PhD
Professor of Civil Engineering
Lyles School of Civil Engineering
Purdue University
(765) 494-5027
tarko@purdue.edu
Corresponding Author

Mario A. Romero
Research Scientist
Lyles School of Civil Engineering
Purdue University

Afia Sultana
Graduate Research Assistant
Lyles School of Civil Engineering
Purdue University

NOTICE

The contents of this report reflect the views of the authors, who are responsible for the facts and the accuracy of the data presented herein. The contents do not necessarily reflect the official views and policies of the Indiana Department of Transportation or the Federal Highway Administration. The report does not constitute a standard, specification, or regulation.

1. Report No.	2. Government Accession No.	3. Recipient's Catalog No.
FHWA/IN/JTRP-2016/01		

4. Title and Subtitle	5. Report Date
Performance of Alternative Diamond Interchange Forms: Volume I—Research Report	January 2017
	6. Performing Organization Code

7. Names	8. Performing Organization Report No.
Andrew P. Tarko, Mario A. Romero, Afia Sultana	FHWA/IN/JTRP-2016/01

9. Performing Organization Name and Address	10. Work Unit No.
Joint Transportation Research Program Purdue University 550 Stadium Mall Drive West Lafayette, IN 47907-2051	
	11. Contract or Grant No. SPR-3866

12. Sponsoring Agency Name and Address	13. Type of Report and Period Covered
Indiana Department of Transportation State Office Building 100 North Senate Avenue Indianapolis, IN 46204	Final Report
	14. Sponsoring Agency Code

15. Supplementary Notes

Prepared in cooperation with the Indiana Department of Transportation and Federal Highway Administration.

16. Abstract

Service interchanges connect freeways to arterial roads and are the backbone of the U.S. road network. Improving the operations of service interchanges is possible by applying one of several new solutions: diverging diamond, single point interchanges, and double or single roundabout diamonds.

VISSIM was used to perform 13,500 experiments to simulate the traffic performance of the studied alternative interchanges during a typical day for a wide range of geometry and traffic scenarios. Five performance measures were investigated: daily-average delay, level of service of critical movement, daily-average number of stops, longest off-ramp queue, and longest crossing road queue. The obtained daily-average delays at the alternative interchanges were consistent with expectations. Roundabouts had the highest average delay while single-point interchanges had the lowest average delays. Roundabouts exhibited the lowest numbers of stops among all the alternatives in the low traffic range up to non-freeway 30,000 veh/day. Diverging diamonds tended to have the shortest and roundabouts tended to have the longest queues on their off-ramps. Overall, single-point interchanges had the shortest queues among all the alternatives.

The study developed guidelines for early stage screening of alternative diamond. The guidelines exhibit performance measures for 25 traffic and geometric scenarios and a wide range of traffic volumes. The guidelines provide a fair comparison procedure for alternative diamond interchanges in the preliminary planning and conceptual design stages.

17. Key Words	18. Distribution Statement
service interchanges, capacity, level of service, traffic performance, geometric design, alternative diamond interchanges, transportation planning	No restrictions. This document is available to the public through the National Technical Information Service, Springfield, VA 22161.

19. Security Classif. (of this report)	20. Security Classif. (of this page)	21. No. of Pages	22. Price
Unclassified	Unclassified	73	

Form DOT F 1700.7 (8-69)

EXECUTIVE SUMMARY

PERFORMANCE OF ALTERNATIVE DIAMOND INTERCHANGE FORMS: VOLUME 1—RESEARCH REPORT

Introduction

Service interchanges connect freeways to arterial roads and are the backbone of the U.S. road network. Improving the operations of service interchanges is possible by increasing the capacity of the off-ramp intersections with a crossing road and eliminating or reducing the traffic interference between these two closely spaced intersections. Recently proposed solutions use three different methods: (1) eliminating the interference by merging the two intersections into a single one (single-point interchange), (2) adding roundabouts to eliminate traffic signals (single- or dual-roundabout diamond), or (3) improving the traffic flow by swapping the directions of traffic within the interchange area and redesigning traffic signals (diverging diamond). In addition, tight diamonds are proposed where space restrictions in the developed areas force planners and designers to reduce the interchange footprint. Together with a traditional diamond interchange, decision makers have available several forms of service interchanges.

These alternatives may perform quite differently depending on traffic and local conditions. The existing research for selecting alternative diamond interchange forms is incomplete for site-specific conditions. This study investigated the operational performance of six alternative diamond interchange forms: conventional diamond (DI), tight diamond (TDI), diverging diamond (DDI), single point (SPI), and double and single roundabout (RA). Performance comparison has been used for developing guidelines (Volume 2 of this report) for early stage screening of diamond forms. The guidelines will help identify the traffic and/or geometric conditions that support the use of one type of interchange over another, focusing on the traffic performance.

Findings

VISSIM has been used to perform 13,500 experiments to simulate the traffic performance of the studied alternative interchanges during a typical day for 25 geometry and traffic scenarios. Five measures of effectiveness (MOEs) were chosen for the alternative interchange performance comparison of the alternative diamond interchanges. These MOEs can effectively demonstrate the actual time lost at signalized and unsignalized interchange intersections and the queue spillback onto the freeway and adjacent surface intersections, as well as the perception of the traffic conditions by drivers. Five performance measures were investigated in this research: daily-average delay, level of service (LOS) of critical movement, daily-average number of stops, longest off-ramp queue, and longest crossing road queue.

Daily-Average Delay

- The obtained daily-average delays at the alternative interchanges were consistent with expectations.

- Roundabouts had the highest average delay across all off-ramp and crossing road traffic shares; TDI had the second highest average delay; and with an increase in the off-ramp volume share, DDI exhibited a lower average delay.
- Overall, SPI had the lowest average delay among all the alternatives.

Level of Service (LOS) of Critical Movement

- Roundabouts outperformed DI and TDI in terms of critical movement delay for 20 and 30 percent off-ramp volumes in the lower range of non-freeway flow rates.
- With the increased share of off-ramp traffic, DDI exhibited lower critical movement delays.
- With 50 percent and 60 percent off-ramp shares, DDI exhibited critical movement delays similar to SPI's.

Daily-Average Number of Stops

- Roundabouts had the lowest number of average stops among all the alternatives up to 30,000 non-freeway AADT across all off-ramp and crossing road traffic shares.
- DI, TDI, and roundabouts had almost double the number of stops of DDI and SPI.
- With an increase in the off-ramp traffic share, DDI exhibited a smaller number of stops.
- Overall, SPI had the lowest number of average stops among all the alternatives.

Longest Off-Ramp Queue

- DDI had the shortest and roundabouts had the longest queues on the off-ramp among all the alternatives across all off-ramp and crossing road traffic shares.
- With an increased share of off-ramp traffic, SPI exhibited queues on off-ramps shorter than DI and TDI.

Longest Crossing Road Queue

- TDI had shorter queues on the crossing road DDI, DI, and roundabouts up to 3,500 veh/hr across all off-ramp and crossing road traffic shares.
- With the increased share of off-ramp traffic, DDI exhibited shorter queues on the crossing road.
- Overall, SPI had the shortest queues among all the alternatives.

Implementation

The results of this study were used to develop guidelines (Volume 2 of this report) that exhibit operational performance of six alternative diamond interchanges for 25 traffic and geometric scenarios and a wide range of traffic volumes. Each of these scenarios involve five performance measures (average delay, critical movement delay, average stops, longest queue on the off-ramp, and longest queue on the crossing road) to compare the alternative interchanges against each other. The guidelines provide a fair comparison procedure for alternative diamond interchanges in the preliminary planning and conceptual design stages.

CONTENTS

LIST OF TABLES

LIST OF FIGURES

1. INTRODUCTION

Service interchanges connect freeways to arterial roads and are the backbone of the U.S. road network. The first interchange was implemented in 1928 to demonstrate that grade separations could greatly improve the traffic capacity of road intersections (Garber & Fontaine, 2000). Interchanges became a standard component of road design through the years, and in the 1960s, they were systemically incorporated in the design of the interstate highway system. Today, as state transportation agencies face the critical challenges of ever-increasing traffic demand, limited space, and funding constraints, planners and designers are looking to new design solutions that offer higher capacities and better user performance at relatively low construction cost as they construct new facilities and replace existing interchanges.

Improving the operations of service interchanges is possible by increasing the capacity of the off-ramp intersections with a crossing road and eliminating or reducing the traffic interference between these two closely spaced intersections. Recently proposed solutions use three different methods: (1) eliminating the interference by merging the two intersections into a single one (single-point interchange), (2) adding roundabouts to eliminate traffic signals (single- or dual-roundabout diamond), or (3) improving the traffic flow by swapping the directions of traffic within the interchange area and redesigning traffic signals (diverging diamond). In addition, space restrictions in the developed areas force designers to reduce the interchange footprint by designing tight or compressed diamonds. Together with a traditional diamond interchange, planners and designers have available several various forms of service interchanges. These alternatives may perform quite differently in different traffic and local conditions. No single alternative is universally superior; and specific alternatives may be preferred under certain traffic demands and spatial restrictions.

With several alternative design forms, road designers face a difficult dilemma: (1) designing all the alternatives at a high cost in order to select the best one or (2) limiting the number of design alternatives early in decision making at the increased risk of eliminating the best solution. Guidelines are needed to assist in making a good initial selection to identify the promising design alternatives and to reduce effort invested in ill-suited solutions.

The Indiana Department of Transportation (INDOT) intends to use alternative intersection designs to improve the capacity of service interchanges where the traditional diamond design is insufficient or can be outperformed by alternative designs. These improvements are particularly needed for urban and suburban interchanges where the on and off traffic flows of freeways are sizeable and may exceed the capacity of the terminal intersections. INDOT is currently going through the process of selecting the optimal diamond interchange forms for their local geometry and traffic conditions. Therefore, this study focused on assisting with this selection by developing guidelines for early stage screening of alternative diamond forms prior to the detailed analysis of operational performance and cost as well as a fair comparison procedure for alternatives diamond interchange in the preliminary planning and conceptual design stages.

The scope of this research was to evaluate the performance measures of six alternative diamond interchanges: single point interchange (SPI), tight diamond interchange (TDI), diverging diamond interchange (DDI), single roundabout interchange (SRI), double roundabout interchange (DRI), and conventional diamond interchange (DI). The goal of this research was to develop guidelines that identify traffic and/or geometric conditions that support the use of one type of interchange over another while focusing on the following aspects of traffic performance at diamond interchanges:

- Level of service of the weakest interchange movement
- Queue spillback onto the freeway main lanes
- Vehicle average delays
- Average number of stops
- Queue spillback blocking adjacent intersections

This report is organized in seven chapters. Chapter 1 discusses the motivation for this study and its objectives. Chapter 2 reviews the past literature pertaining to the focus area of this study. Chapter 3 briefly describes the research scope and method. Chapter 4 discusses the micro-simulation experiment design details. Chapter 5 discusses the statistical models for predicting the performance of alternatives designs. Chapter 6 presents the statistical model results with graphical examples for the various alternatives. Finally, Chapter 7 presents the conclusions of this study and recommendations for future work.

2. LITERATURE REVIEW

2.1 Study Interchanges

Service interchanges are the connection between access-controlled facilities and arterials and are a key element of an efficient and effective transportation system. The most common type of service interchange in Indiana is the diamond, which is generally applicable for a wide range of conditions. Diamonds can be categorized based on the ramp separation distance, the ramp terminal control strategy, and the crossing road cross-section. In this presented study, six alternative diamond interchanges were investigated. Other forms of diamond interchanges, such as folded diamond, were not included in this research. This study also does not cover hybrid diamond interchange forms such as partial cloverleafs. For each alternative interchange, several geometry configurations were considered based on the number of lanes on the crossing roads and off-ramps. A brief overview of each interchange configuration is provided in the following sections.

2.1.1 Conventional Diamond Interchange (DI)

The typical intersection spacing between two ramp terminals of a conventional DI is 800 to 1,200 ft

Figure 2.1 Conventional diamond interchange.

(FHWA, 2012). The radii of the left-turning roadways range from 50 ft to 75 ft and the right-turn radii are usually from 35 to 75 ft (Leisch, Urbanik, & James, 1989). DIs may use signalization for traffic control at the two ramp terminal intersections with the crossing road. Lower volume ramps simply may be stop-controlled for the off-ramp approaches. Adequate sight distance is a key factor in the bridge design at an interchange in the case of unsignalized control (AASHTO, 2001). To accommodate potential future traffic growth, consideration should be given to coordination of the signals and the needed lengths of left-turn bays on the crossing road. The cost of constructing a conventional DI is governed by the bridge width, size, earthwork and other factors. Figure 2.1 shows a simulation snapshot of the conventional DI layout.

2.1.2 Diverging Diamond Interchange (DDI)

Missouri was the first state in the U.S. to implement the DDI as part of an interchange project (Hughes, Jagannathan, Sengupta, & Hummer, 2010). The DDI is a relatively new design in Indiana. INDOT has two in operations now. Through-traffic on the arterial crosses from the right side to the left side at the signal prior to the interchange bridge and then crosses back after the signal. This allows left turns from the exit ramps to flow freely without a protected signal phase, which in turn reduces the number of signal phases from three to two. This advantage makes the signal operation more efficient, resulting in better operations, higher capacities, and better user performance.

Figure 2.2 shows a simulated snapshot of the DDI layout. There are two on-ramps and two off-ramps that connect the crossing road and the freeway. The distance between the two crossover intersections is typically 500 ft (Bared, Edara, & Jagannathan, 2005) but can vary

depending on the site condition. The crossing road generally has two through-lanes and one dedicated right-turn lane in each direction. Two signalized intersections are situated at the two crossover locations.

2.1.3 Tight Diamond Interchange (TDI)

The TDI, a type of compressed DI, is mostly used in urban and suburban areas where the right-of-way is a constraint. Figure 2.3 shows a TDI which has two closely spaced signalized intersections at the junction of the ramp terminals and the crossing road. Typical TDI designs provide 200 to 400 ft (Jones & Selinger, 2003) of separation between the signal-controlled intersections. Generally, the bridge design of a TDI spans between 140 and 180 ft (Leisch et al., 1989) depending on the various geometries of the interchange bridge. Because of the closely spaced intersections, mostly both intersections are signalized and coordinated to allow through-traffic to pass through both intersections with one stop at most.

2.1.4 Single-Point Interchange (SPI)

The single-point urban diamond interchange (SPI) (Figure 2.4) consolidates all the left-turn movements to and from the entrance and exit ramps into a single intersection in the center of the interchange. SPI is also referenced as a SPUI (single point urban interchange) and SPDI (single point diamond interchange). The left turning radii of SPIs can range from 170 to 400 ft and the right-turn radii from 70 to 200 ft (Bonneson & Messer, 1989).The advantages of a SPI (FHWA, 2012) include:

- One signalized intersection on the crossing road, compared to two in conventional DIs, and typically involves improved operations and reduced delay.

Figure 2.2 Diverging diamond interchange.

Figure 2.3 Tight diamond interchange.

- Curve radii for left-turn movements through the inter-section are significantly flatter than at conventional interchanges, which therefore accommodates more efficient discharge of left-turning vehicles and trucks.

The primary disadvantages of the SPI are its higher cost because of the need for a larger structure and the need for careful design of the channelization for left turns to minimize driver confusion.

2.1.5 Double Roundabout Interchange (DRI)

Double roundabouts are two roundabouts at the two modern ramps-crossing road junctions (see Figure 2.5).

Figure 2.4 Single point interchange.

Figure 2.5 Double roundabout diamond interchange.

Roundabouts include counterclockwise circulatory traffic movements and vehicles entering the roundabout at low speed. A DI is also called a dumbbell interchange. Under selected traffic and site-specific conditions, the design has a number of advantages over the signalized interchanges (Gitbooks, 2015).

- Narrower bridge as it does not have storage turn lanes.
- No signal control at the interchange.
- Significantly less delays than signalized intersections at low traffic volumes.

- Effective tool for managing speed and creating a transition area that moves traffic from a high-speed to a low-speed environment.

2.1.6 Single Roundabout Interchange (SRI)

Roundabouts and other unconventional intersection designs have gained popularity in the U.S. in the past 20 years. Free-flow arterial through-movements are provided by using a single roundabout on a separate

Figure 2.6 Single roundabout interchange.

grade to accommodate off-ramp left and right turns and all the movements on the crossing road. SRI (see Figure 2.6) is sometimes referenced as a dogbone interchange. SRI can handle more than four intersecting roadways and can serve as a frontage road for adjacent interchange parcels (Gitbooks, 2015). The single roundabout design is particularly suitable in built-up urban areas with moderate capacity requirements. Single roundabout interchanges are considered most often where five or more roadways intersect and/or where the right-of-way on the arterial and/or cross streets is very restricted. A single roundabout also possesses all the advantages of a double roundabout.

2.2 Review of Interchange Performance in Previous Research

Interchanges provide access between arterial crossing roads and access-controlled facilities. The interstate and principal arterial system in the U.S. accounts for only about 5.3% of the roadway miles but carries up to 54% of the vehicle miles of travel (FHWA, 2013). Due to their major impact on connectivity, past researchers compared the operational performance of alternative interchanges in pairs; and most of them compared the alternatives to the conventional DI.

Few studies compared the performance of the SPI and the DI (Fang, 2008; Gerber & Fontaine, 2000; Smith & Gerber, 1998). Smith and Gerber (1998) studied the operations of the SPI and the DI using the simulation program TRAFNETSIM. They developed ten volume scenarios ranging from a low end of 2,700 veh/hr and a high volume of 6,000 veh/hr and simulated both interchanges to analyze the effect of various traffic patterns on the relative operational performance of each

interchange type. The authors concluded that the major factors contributing to the selection of the SPI over the DI were: (1) increased capacity and decreased congestion, (2) efficient phasing to minimize delay, (3) simplified arterial coordination because of single-signal design, and (4) presence of high left-turn volumes.

Several researchers studied the operational performance of the TDI and the SPI (Bonneson & Lee, 2002; Fowler, 1993; Jones & Selinger, 2003; Leisch, et al., 1989; Sharp & Selinger, 2000). Jones and Selinger (2003) provided a comprehensive comparison of the operations of a four-lane crossing road with two left-turning lanes and a two-lane off-ramp SPI and TDI. Fifteen analysis scenarios were used based on three volume patterns and five volume intensities. Each simulation was run for a 60-min duration. The analysis was conducted with three traffic engineering software programs: Synchro 5.0, Passer III-98, and CORSIM. Their results showed that SPI provided greater traffic operation performance than TDI for the geometric and volume conditions tested. SPI had higher average travel speeds, fewer phase failures, a lower percentage of stops, and a considerably higher capability to serve traffic. TDI reached capacity conditions when the SPI was operating in average conditions.

Fowler (1993) developed 12 traffic volume scenarios and utilized a spreadsheet volume-to-capacity ratio analysis. Variations in the traffic volume characteristics affected the relative capacities of two interchanges. Comparison of the volume-to-capacity ratios and intersection delays prompted the following two conclusions: (1) SPI provided greater capacity than TDI for most volume conditions, and (2) TDI was more sensitive to variations in the traffic volume.

Click, Berry, and Mahendran (2001) compared the relative performance of five traditional and five nontraditional

interchange treatments at two common sites using three volume scenarios. They conducted micro-simulation wherein they increased the base year hourly traffic volume by 120%, 150%, and 190%. Instead of the delay and running speed, the average travel speed was used as a performance measure criterion for comparing the alternatives. The TDI tended toward poor performance (low speeds) and resulted in long queues, especially when the left-turn volumes were high. DRI was the worst performer of all the treatments evaluated in this study and failed first at all three sites and then had the worst performance in each of the study scenarios. The SPI was the best performer and the DDI was the second best among the ten alternatives.

The DDI involves an exclusive concept that requires traffic on the arterial road to cross on the opposite side of the road between the ramp intersections. Many researchers conducted extensive research on traffic modeling to determine if this solution would work in the U.S. A DDI was typically compared with the performance of a conventional DI.

In Chlewicki's (2003) research the interchange of I-695 (Baltimore Beltway) at MD140 (Reisterstown Road) in Baltimore County, Maryland was chosen as the test interchange to compare a DDI with a conventional DI. Simulations were conducted to compare the delays and total stops of these designs to other conventional designs. The results showed that the total delay for the conventional DI was about three times greater than the delay for the DDI. The stop delays were over four times worse for the conventional DI. There were approximately twice as many total stops for the conventional DI compared to the DDI designs.

MoDOT (Chilukuri, Siromaskul, Trueblood, & Ryan, 2011) conducted an operational analysis of the at-grade intersections of a DDI using VISSIM. A key element of this study was the development of traffic simulation models to assess the operational characteristics of a DDI and compared it to a conventional DI. Delays and travel speeds were compared; and the results showed that the DDI provided roadway users with an overall design and operations that minimized traffic delay and was capable of recovering more quickly from events and incidents.

Bared et al. (2005) evaluated the performance of a DDI in six different traffic scenarios using VISSIM. Two designs of DDI were analyzed: four-lane DDI and six-lane DDI. The conventional and DDI signal timing had a fixed cycle length of 70 s for lower to medium flows and 100 s for higher flows. The optimal cycle lengths were obtained using TRANSYT-7F and PASSER-3. The experimental traffic volume ranged from 1,700 to 8,600 vehicle/hr. DDI performed better than conventional DI, which included higher levels of service, shorter delays, less stops, smaller queues, and higher throughput. However, for lower volumes, the performance of DDIs and conventional intersections were similar.

A group of researchers from Iowa State University (Sharma & Chatterjee, 2007) conducted a comparative study between a DDI and conventional DI. The base model for the interchanges was coded in VISSIM, and the traffic signal timings were obtained using Synchro for signal optimization. For the DI, a three-phase signal was used, and a two-phase signal was used for the DDI. The two alternatives were studied for a range of volume scenarios (1,700–6,200 veh/hr) including balanced and unbalanced flows. The VISSIM simulation models for the two interchanges were run for 60 m, and data were collected for delays and queue lengths. Better performance was reported in each DDI scenario in terms of delay, travel time, maximum queue length, etc.

Siromaskul and Speth (2008) studied the operational benefits of a DDI compared to a DI and a SPI. Synchro was used to develop an optimum timing plan for each traffic scenario. The traffic signals were coded as pre-timed to reduce the variability in results. The traffic operations of the three interchange designs were compared for four different volume scenarios in order to obtain a good understanding of the conditions that affected each of the interchange types. Capacity and delay were compared with varied traffic patterns such as high balanced ramp volumes, high unbalanced ramp volumes, heavy arterial volumes, mid-to heavy level overall volumes, and a real-world projected condition. The DDI performed better in terms of average vehicle delay and queue length with more volume, especially when the ramp volume was increased.

Afshar, Bared, Wolf, and Edara (2009) conducted a traffic comparison between SPI and DDI in VISSIM using MOEs of throughput, delay, and number of stops. The analysis was conducted for the crossing road and ramps (excluding the freeway through traffic). The authors employed a wide variety of hypothetical traffic flow scenarios for each design. Their results suggested that, for balanced conditions, SPI's capacity was superior to the capacity of DDI. For unbalanced conditions, the sum of the critical lane volume for the DDI was found to gradually increase to a level comparable to the SPI. When the imbalance of the crossing road's opposing volumes was 30–70% and greater, the DDI outperformed the SPI. This research also revealed that the DDI had shorter delays than the SPI, but the SPI generated less stops compared to the DDI design.

Focusing on the issue of estimating the extra traffic volume that can be generated from new development, Leong et al. (2015) conducted VISSIM micro-simulation to investigate the design and operational performance of a DDI for different traffic scenarios and pre-timed signal settings. The vehicle delay, stop delay, stops, and travel time of vehicles in the network, were compared with the conventional DI. The results indicated that for the DDI, vehicles tended to make more stops but experienced much less total delay and travel time compared to the existing networks with conventional DIs. The network with a DDI performed better for future traffic demand generated by the proposed development.

The safety and traffic operations of DIs could be improved by replacing the stop or signal-controlled intersections with well-designed roundabouts for low and moderate traffic volumes (Bared & Kaiser, 2000).

Several traffic scenarios were applied to compare the control delay between a DI and interchanges with double and single roundabouts. The selected scenarios were compared using models for roundabout traffic operations and for signalized intersections. Based on the modeling efforts of the given case studies, roundabout interchanges provided noticeable reductions in control delay, which makes then economically advantageous to operational costs and also can result in substantial savings in bridge construction cost.

LeBas (2015) evaluated roundabout designs as alternatives to improve the traffic flow through a currently congested corridor. Three alternatives were considered: the existing signalized corridor, a partial two-lane roundabout corridor, and a partial three-lane roundabout corridor. Field data were used to model the alternatives in VISSIM. The following average vehicle travel time, average delay per vehicle for each corridor, and average delay per vehicle at each intersection were the considered performance measures. The study corridor with a roundabout interchange provided better performance than the existing signalized corridor for the existing traffic volumes tested. The partial three-lane roundabout in their study provided the lowest vehicle travel times and lowest average delays due to the added capacity. For the higher traffic volumes at the interchange, the partial two-lane roundabout had a higher average vehicle travel time (VTT) at the exit ramp than the existing corridor.

Roundabout interchanges are being considered as an alternative to the traditional signalized DI as a safety treatment. Scant information is available that specifies the conditions under which the roundabout interchange should be considered instead of the signalized DI. Li, DeAmico, Chitturi, Bill, and Noyce (2013) conducted a comprehensive operational comparison between roundabout and signalized interchanges in VISSIM. The capacities at each roundabout entrance of the entire interchange were calibrated and validated via the critical and follow-up headways for passenger and heavy vehicles. A total of 3,520 different scenarios were simulated for roundabout and signalized interchanges with different ramp and arterial volumes, ramp spacing, and heavy vehicle percentages. The roundabout performed better than the conventional DI at low volumes.

2.3 Summary of Previous Research

Past studies focused on the performance evaluation of an alternative interchange solution to existing conventional DIs. Different micro-simulation programs (VISSIM, CORSIM, and TRAFNETSIM) were used for generating performance results. Non-freeway portion of the interchange (excluding the freeway main line) were taken into consideration, and very few (six to ten) traffic patterns were simulated for one hour. Average delay, control delay, number of stops, stops per vehicle, and speed were the performance evaluation criteria utilized. All the past studies concluded that the alternative interchange solutions performed better than the

conventional DI; and the SPI typically outperformed the DDI, TDI, DI, DRI, and SRI.

2.4 Limitations of Previous Research

AADT along with the traffic mix during specific times of the day notably peak travel periods is an important traffic parameter that determines the geometric configuration of an interchange intersection. The operational performance of an interchange is heavily dependent on the traffic volumes entering on the approach and navigating inside the interchange. The research to date has not always done so, and a limited number of hypothetical traffic patterns were considered in past projects for making recommendations. Many of the past studies did not develop statistical models to estimate the performance measures based on the simulated inputs. Moreover, most of the previous studies focused on comparing a conventional DI as if it were replaced by a particular alternative at a specific location, the results of which may not be easily transferrable to other locations and states.

Two performance measures were considered in the current study that had not been considered in the previous studies: critical movement delay, which is a very important indicator of efficient interchange operations, and queue spillback on the freeway mainlines, which is another important parameter for interchange safety.

This study was inspired by JTRP Project No. SPR-3102, "Safety and Operational Impacts of Alternative Intersections," which was completed in December 2008 and delivered critical information and guidance to INDOT on the traffic mobility/operational performance of six surface intersections, including alternative or innovative continuous flow and roundabout forms (Tarko, Inerowicz, & Lang, 2008). The busiest movement delay, the average intersection delay, and the average stop per vehicles were the studied performance measures. However, a limitation of that study was that it studied alternative intersections in isolation, rather than as integral elements of interchanges.

3. RESEARCH SCOPE AND METHOD

3.1 Measure of Effectiveness (MOE)

Five MOEs were chosen for the alternative interchange performance comparison: daily-average delay, critical movement delay, daily-average stops, longest queue length on crossing road, and longest queue length on off-ramp. These MOEs can effectively demonstrate the actual time lost at signals and the queue spillback onto the freeway and adjacent surface intersections, as well as the poor perception of the traffic conditions by drivers.

3.1.1 Non-freeway Daily-Average Delay

The average interchange delay is an important performance measure for selecting an alternative interchange from an economic point of view. The total delay, which includes geometry delay, was calculated by the

difference between the minimum travel time and the actual travel time. The minimum travel time was calculated along two straight segments that connected the center of the interchange with the beginning and the end of the path. The centers and footprints of the interchanges were identical. In order to accommodate a common reference, the minimum travel time was calculated on a straight path via the center of the interchange. A lognormal model estimated the expected total daily delay at the interchange level. This expected daily delay then was used to calculate the daily-average delay.

Delay Calculation. Daily delay was measured as the difference between the actual travel time with all the traffic and geometric conditions present in the network and the computed minimum travel time between the origin and the destination on the shortest path via the center of the interchange for ten different interchange movements. The minimum travel time is the travel time which could be achieved if there are no other vehicles and/or no signal controls or other reasons for stops and a straight path via the center of the interchange was available. The average delay at the interchange during the entire day was calculated based on 15-min periods that represented the actual periods. The vehicle delay was calculated as follows:

$$D_{24} = \sum_{w \in W} e_w \sum_{j=1}^{10} (T_j - TC_j * Veh_j) \qquad (3.1)$$

where:

D_{24} = vehicle delay at the interchange during the representative day (sec),

e_w = expansion factor to account for the actual length of the periods w; w=morning rush hour, afternoon rush hour, off-peak periods, see,

T_j = Total travel time of all the vehicles in movement j obtained from the VISSIM object Travel Time Measurement,

TC= computed minimum travel time of movement j between origin and destination via the center of the interchange,

Veh_j = total number of vehicles on movement j

3.1.2 Critical Movement Delay

In this study, movement delay was calculated for the vehicles that entered the system during the simulation period. The control delay of a vehicle was obtained by subtracting the theoretical (ideal) travel time from the actual travel time. The theoretical travel time is the travel time that could be achieved if there were no other vehicles and/or signal controls or other reasons for stops along the path with the actual geometry.

The highest average vehicle delay among the ten interchange movements is called the "critical movement." If the critical movement delay was greater than 80 sec for a signalized intersection or 50 sec for an unsignalized intersection during the peak 15-min period,

then that movement had a LOS F (TRB, 2010), which indicated a capacity failure for the entire interchange. The average delay on the critical movement was used as an indicator for the capacity failure for the alternative interchanges. Movement delay was obtained through the VISSIM VTT object within the simulated network, but vehicle delays can occur outside the simulated network. In this circumstance, the measured delay needs to be adjusted with the outside network delay. The following section explains the necessity of a delay adjustment.

3.1.3 Non-freeway Daily-Average Stop

The average number of stops at an interchange is another performance measure for selecting an alternative interchange from an economic point of view. A lognormal model was used to estimate the expected number of stops for the entire interchange in a 24-hour period. This expected total number of stops then was used to calculate the daily-average number of stops.

Due to the backward shockwaves at signalized interchanges, a queue can break and form at different points from the system entry to the bottleneck. To be able to count the actual number of stops that occur at different points in the network, several queue counters were placed about 1,000 ft apart in the VISSIM simulated network. Moreover, stops can occur outside the simulated network when the traffic is very congested, which results in stopped vehicles outside the network that are unable to enter. Therefore, the stops recorded must be adjusted with this spillover outside the network.

3.1.4 Longest Queue on Off-Ramp and Crossing-Road

The physical queue length at the external approaches of a non-freeway roadway is useful in evaluating the risk of blocking the adjacent non-freeway intersections. A vehicle is in a queue when its speed is lower than 10 mph.

The length of the ramp is a critical design factor for avoiding an undesirable queue spillback onto the freeway through-lanes. This is a valuable tool for a designer to evaluate the risk of queue spillback when the ramp length is known.

The queue length was measured from the stop line of the interchange through the VISSIM queue counter object. Due to the backward shockwaves at the signalized interchanges, a queue can break and form at different network entry areas to the bottleneck. To be able to track the actual back of the queue, several queue counters were placed about 1,000 ft apart in the network, which is why the queue length recorded from the stop line had to be adjusted with the other queue counters and the queue outside the network.

3.2 Method

Microsimulation, statistical analysis, and guidelines in the form of graphical representation of the performance
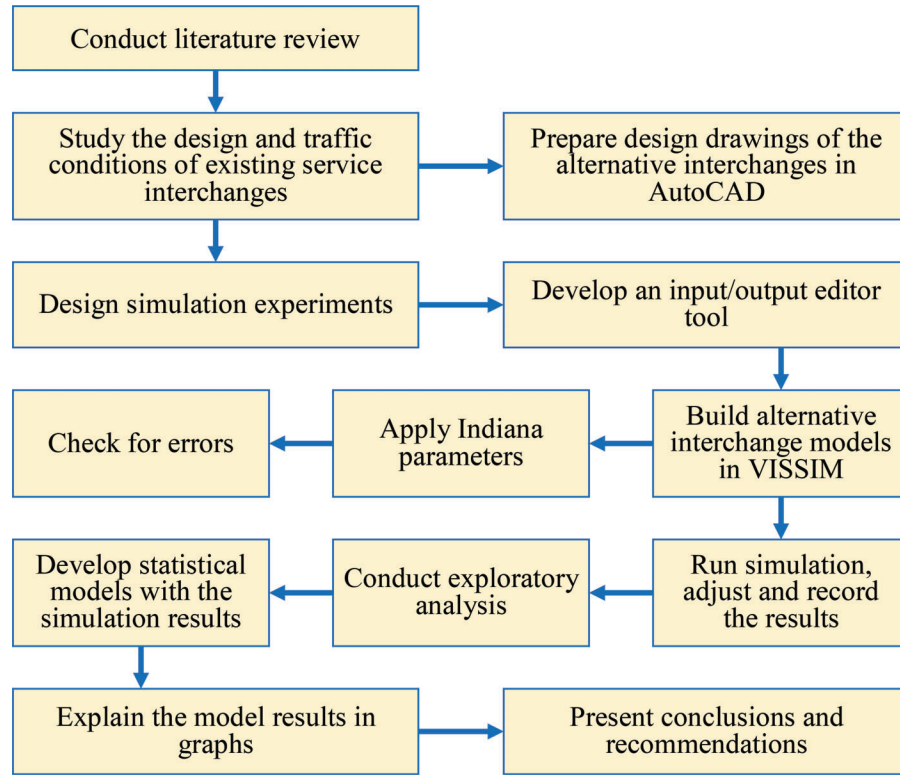
Figure 3.1 Study flowchart.

evaluation results were the three major components of this study.

Figure 3.1 shows the research tasks in a flow chart. The following sections briefly introduce the methods that were employed to evaluate the performance of the six alternative diamond interchanges.

3.2.1 Micro-simulation

Micro-simulation techniques are being implemented around the world to improve traffic control and management. This technique is quite successful and is increasingly being used by transportation agencies to evaluate the traffic performance of existing infrastructure and new transportation facilities. The performance measures of the alternative diamond interchanges were simulated by deploying VISSIM (PTV, 2014). VISSIM incorporates the flexible input of traffic demand, road geometry, and signal operations together to appropriately reflect traffic operations. VISSIM is a trajectory-based micro-simulation software that utilizes a psychophysical driver behavioral model as developed by Wiedemann. For the off-ramps, the VISSIM Wiedemann 1999 model was used, and for the crossing road, the Wiedemann 1974 model was used. All the traffic parameters of VISSIM were calibrated with Indiana conditions. The simulation experiment design details are provided in Chapter 4.

3.2.2 Statistical Model

When the relationship between the independent and dependent variables is non-linear, then log transformation of the variables in a regression model is a very common practice (Benoit, 2011). Logarithmic transformation of the dependent variable also helps to eliminate the negative estimation. Logarithmic transformations are a very useful way of transforming a highly skewed variable into one that is more approximately normal. The general form of the log linear and log-log model is shown in Eq. 3.2 and Eq. 3.4.

$$\text{Log}-\text{linear model}, \; Log\,Y_i = \beta_0 + \beta_i x_i + \in_i \quad (3.2)$$

$$\text{Log}-\text{log model}, \; Log\,Y_i = \beta_0 + \beta_i log x_i + \in_i \quad (3.3)$$

Modified Log$-$linear model,

$$Log\,Y_i = \beta_0 + \beta_i x_i + \beta_i log z_i + \in_i \quad (3.4)$$

In this study a log-linear model was utilized for predicting the critical movement delay, the longest queue lengths on the off-ramps and the crossing road. A modified log-linear model was used for predicting the interchange daily-average delay and stops in order to mitigate the systematic bias between the dependent and independent variables. A detailed description of the

selection process for the appropriate model form is provided in Chapter 5.

Presentation of the Results

The simulation results in this study were summarized through statistical modeling to determine the relationship between crucial design decisions and the performance of an interchange. The expected critical movement delay, daily-average delay and stops, and longest queue on off-ramp and crossing road were calculated with the developed statistical models for all the studied traffic and geometry scenarios and they are presented in Guidelines (Volume 2). The Guidelines can be used to select feasible alternatives (those worthy of further detailed operational analysis) based on a typically limited input available during transportation planning and in early stages of geometric design.

4. MICRO-SIMULATION

Micro-simulation tool VISSIM was used to extract information regarding the performance measures needed for this comparative study of the six alternative interchanges. This chapter provides a detailed description of the interchange geometry, daily traffic profile, traffic parameters, simulation scenarios, signal settings, VISSIM objects, and saved results of the simulation.

4.1 Interchange Geometry

Each of the six alternative DIs investigated in this study had four corresponding geometry cases, which varied by the number of continuous lanes on the ramps and the crossing road and by the number of auxiliary lanes on the off-ramp to the crossing road intersection approaches. The four geometric scenarios presented in Figure 4.1 were studied for each of the alternatives.

A crossing road with six lanes was considered for the four signalized interchanges as it is an unlikely design for roundabout interchanges. The first geometry case had two lanes on the crossing road with one left-turning lane and a one-lane off-ramp with one left- and one right-turning approach lanes at the off-ramp of the non-freeway junction. The second geometry case included four lanes on the crossing road with one left-turning lane and a one-lane off-ramp with two left- and two right-turning approach lanes at the off-ramp of the non-freeway junction. The third geometry case had four lanes on the crossing road with two left-turning lanes and a two-lane off-ramp with one left- and one right-turning approach lanes at the off-ramp of the non-freeway junction. The fourth geometry option had four lanes on the crossing road with two left-turning lanes and a two-lane off-ramp with two left- and two right-turning approach lanes at the off-ramp of the crossing road junction. Figure 4.2 shows an example of the fourth geometry case.

The following rules were applied while generating the geometry cases based on the number of lanes:

1. The number of left-turn lanes on the non-freeway road was equal to the number of lanes on the freeway off-ramp.
2. The maximum number of auxiliary LT lanes was at most equal to the number of receiving ramp lanes.
3. Only a single lane per movement was allowed at an intersection where traffic signals were not used, except roundabouts.
4. The crossing road had one auxiliary right-turn lane.

Freeway traffic passing through the interchange area in the freeway mainline lanes is not affected by the interchange design if the non-freeway part of the interchange operates at a reasonable LOS and without queue spillback onto the freeway. For this reason, the operational performance of an interchange in this study focused on
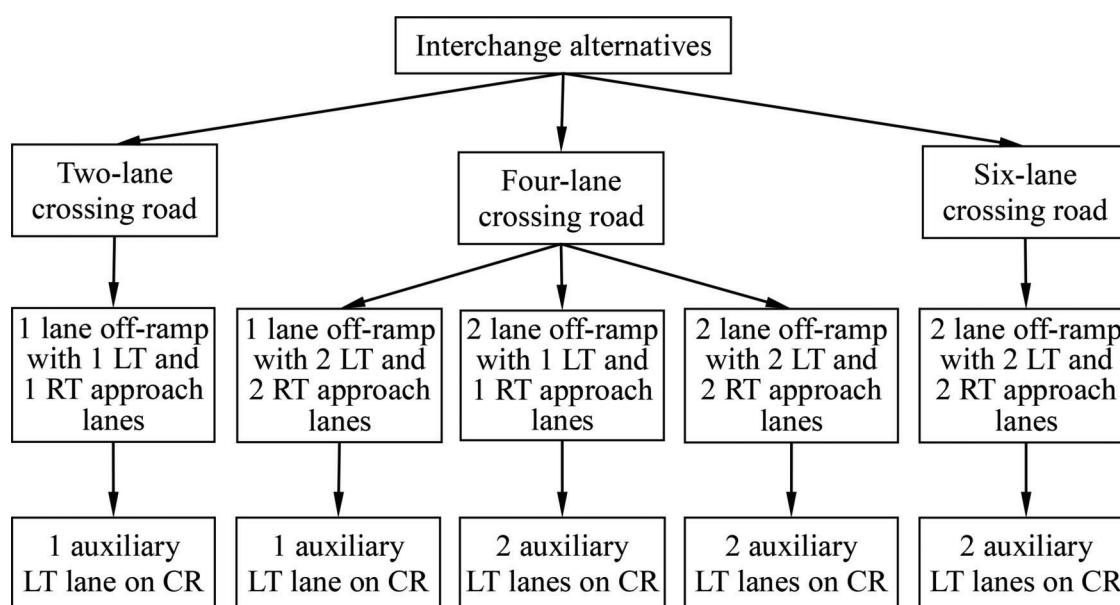
Figure 4.1   Four geometric scenarios for the six alternative interchanges.
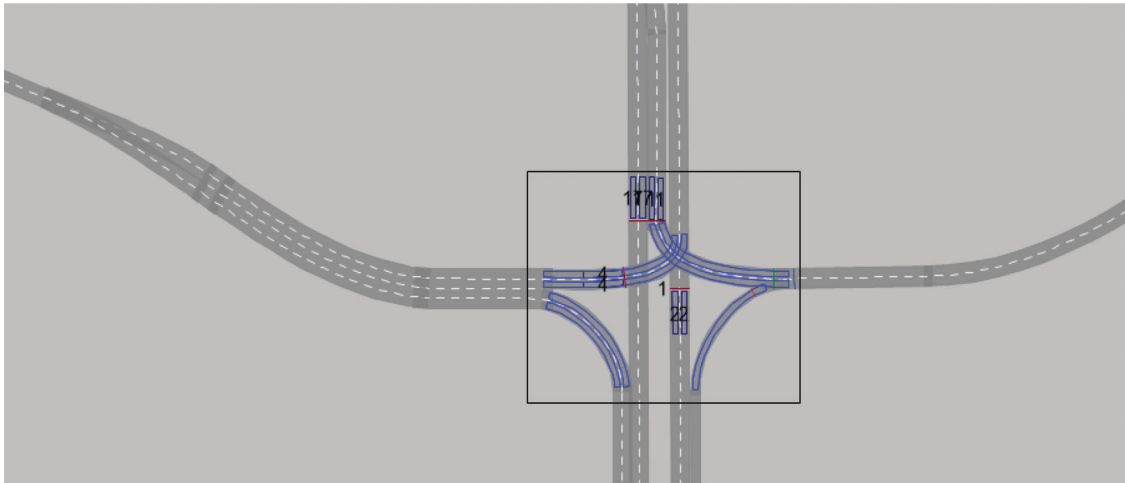
Figure 4.2 Four-lane crossing road with two-lane off-ramp.
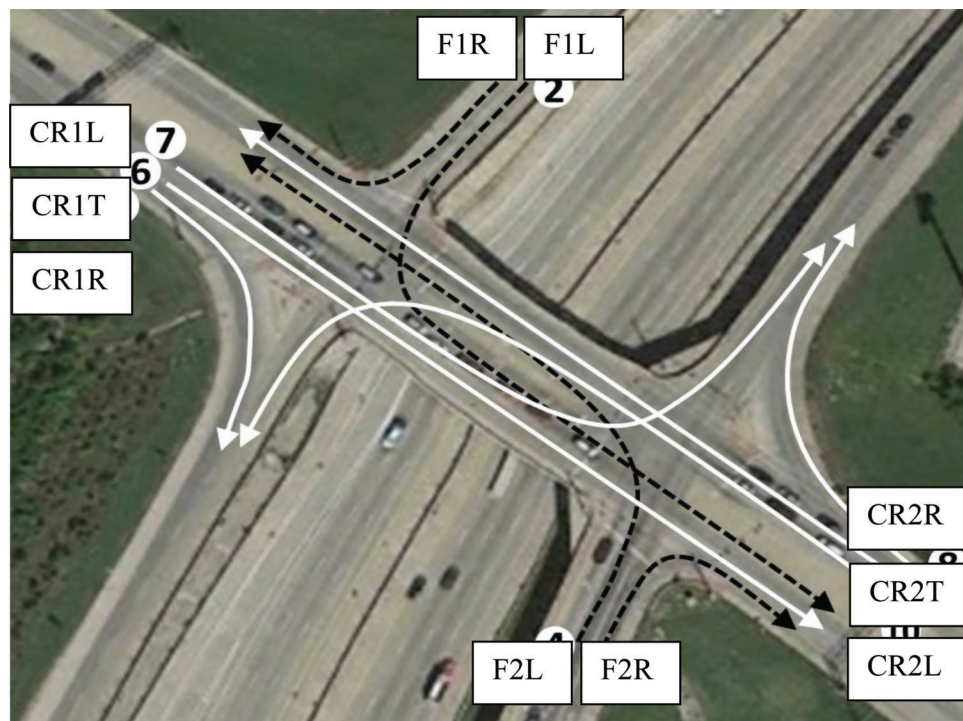
Figure 4.3 Non-freeway movements.

the ten traffic movements on the non-freeway portion that included the non-freeway crossing road and off-ramps where traffic interruptions were expected. Figure 4.3 shows the ten movements that were considered in this study.

4.2 Traffic Pattern

The non-freeway intersections of a freeway interchange include ten traffic movements: six movements from the crossing road (right, through, and left turns) and four movements from the freeway to the crossing road (right and left turns). The total daily traffic, excluding the freeway through movements, is called the non-freeway AADT. A typical daily profile of hourly volumes on a road with prevailing local traffic and no congestion is presented in Figure 4.4.

To reduce the simulation time while accounting for traffic fluctuation during a 24-hour day, a simplified
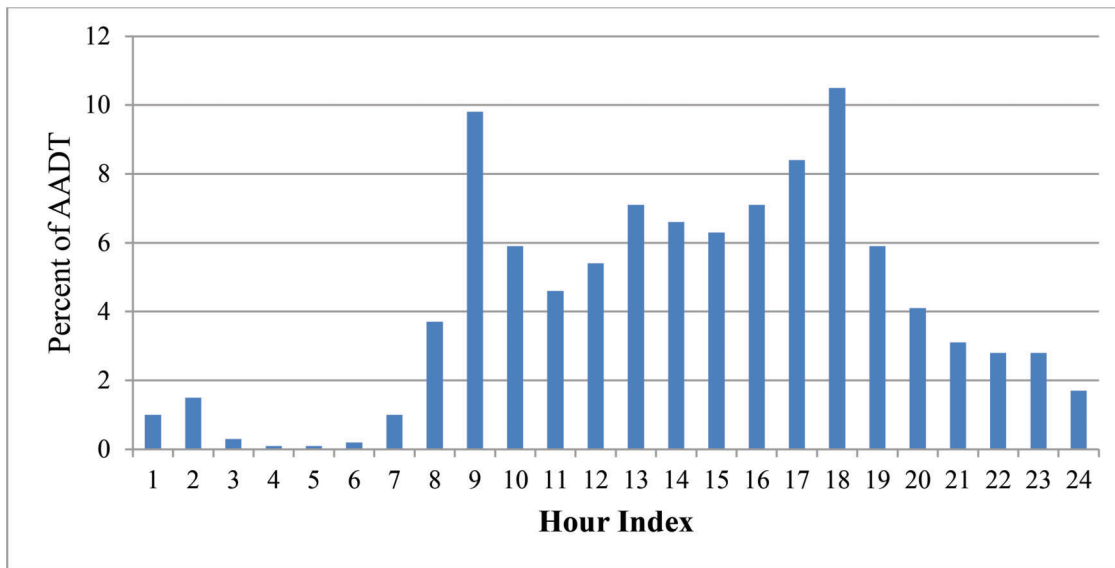
Figure 4.4 Typical daily profile of hourly volumes on a road with prevailing local traffic.

TABLE 4.1
Simplified typical non-freeway AADT profile

			Percent of NON-FREEWAY AADT	
Period	Time	Period Duration	Total Period	15-min Intervals
Off-peak period 1	12 pm–7 am	7 hours	6.78	all 0.242
Off-peak period 2	7–8 am	1 hour	3.20	all 0.800
Morning rush hour	8–9 am	1 hour	9.80	1.99, 3.17, 2.60, 2.04
Off-peak period 3	9 am–4 pm	7 hours	41.30	all 1.472
Off-peak period 4	4–5 pm	1 hour	8.40	all 2.100
Afternoon rush hour	5–6 pm	1 hour	10.50	2.42, 2.74, 3.07, 2.27
Off-peak period 3	6–8 pm	2 hours	11.78	all 1.472
Off-peak period 2	8–10 pm	2 hours	6.40	all 0.800
Off-peak period 1	10–12 pm	2 hours	1.94	all 0.242

daily profile of hourly volumes was assumed (Table 4.1, Figure 4.5 and Figure 4.6). This profile was built in six periods: one morning and one afternoon rush hour with their peaking characteristics and four off-peak periods with assumed uniform traffic intensities. Simulations were run for each full rush hour and for one-half hour of each off-peak period. The daily traffic performance was obtained by aggregating the six obtained performance estimates with weights that accounted for the actual periods during the entire day.

The simplified daily profile is represented by the percent of non-freeway AADT in each 15-min intervals. These percentages were calculated from the known percentages of the morning and afternoon rush-hour traffic and certain assumptions about the typical profile:

P_a = percent of NON-FREEWAY AADT during the morning rush hour,

P_p = percent of NON-FREEWAY AADT during the afternoon rush hour,

P_a^* = typical percent of NON-FREEWAY AADT during the morning rush hour,

P_p^* = typical percent of NON-FREEWAY AADT during the afternoon rush hour,

$P_{o,i}^*$ = typical percent of NON-FREEWAY AADT during a 15-min interval of off-peak period $i = 1..4$.

Calculation of the non-freeway AADT percentage for 15-min intervals was as follows.

1. The actual morning and afternoon rush hour percentages of non-freeway AADT may differ from the typical percentages shown in Table 4.3 Scaling factor S was needed to transform the typical profile to account for the new rush hour percentages:

$$S = \frac{P_{am} + P_{pm} - 800/96}{P_{am}^* + P_{pm}^* - 800/96} \qquad (4.1)$$

2. The percent of non-freeway AADT for each off-peak 15-min interval was rescaled as follows:

$$q_o, i = S \cdot (p_{0,i}^* - 100/96) + 100/96 \qquad (4.2)$$
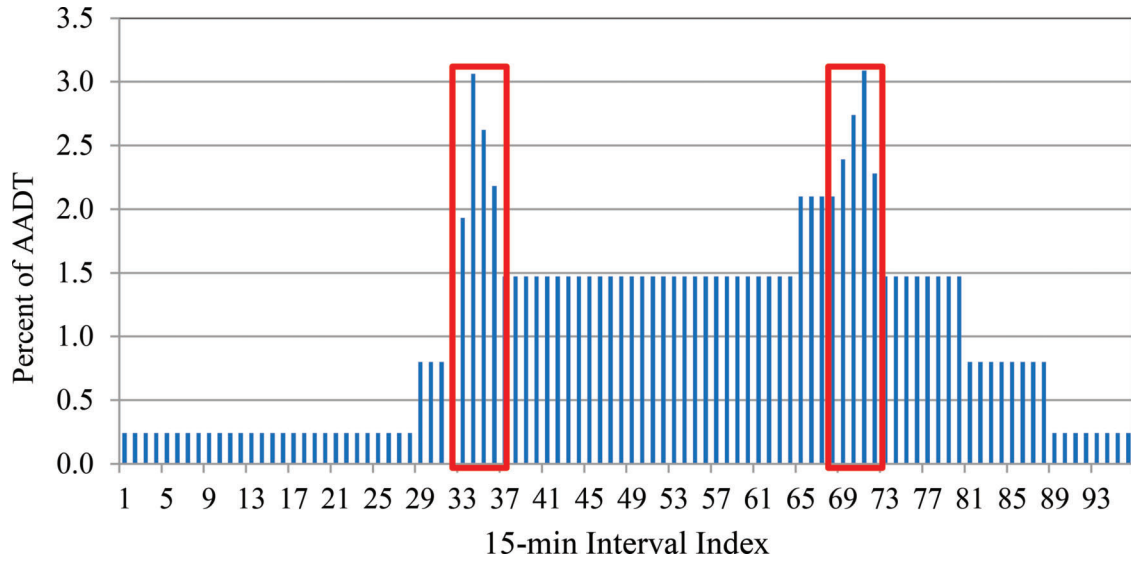
Figure 4.5 Example daily traffic (pronounced rush hours).
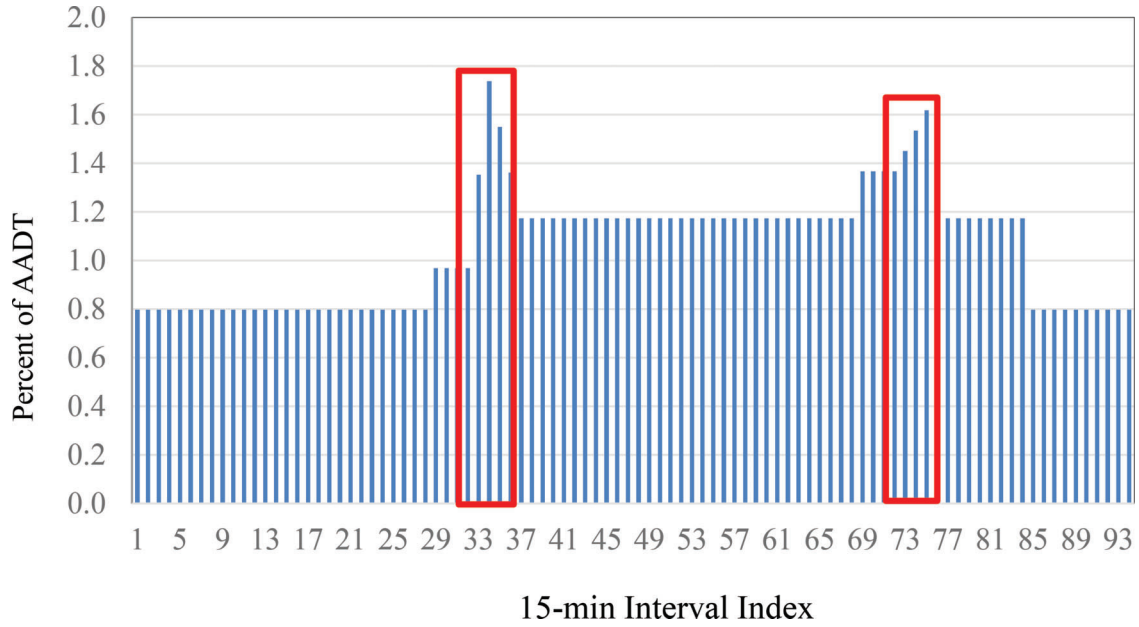
Figure 4.6 Example daily traffic (balanced traffic profile)

3. The percent of non-freeway AADT for each of the four 15-min intervals during the morning rush hour was calculated as follows:

$$p_{a,2} = (2P_a - p_{o,2} - 2p_{o,3})/5 \qquad (4.3)$$

$$p_{a,1} = (p_{a,2} + p_{o,2})/2 \qquad (4.4)$$

$$p_{a,3} = (2p_{a,2} + p_{o,3})/3 \qquad (4.5)$$

$$p_{a,4} = (p_{a,2} + 2p_{o,3})/3 \qquad (4.6)$$

4. The percent of non-freeway AADT for each of the four 15-min intervals during the afternoon rush hour was calculated as follows:

$$p_{p,3} = (2P_p - p_{o,3} - 2p_{o4})/5 \qquad (4.7)$$

$$p_{p,1} = (p_{p,3} + 2p_{o,4})/3 \qquad (4.8)$$

$$p_{p,2} = (2p_{p,3} + p_{o,4})/3 \qquad (4.9)$$

$$p_{p,4} = (p_{p,3} + p_{o,3})/2 \qquad (4.10)$$
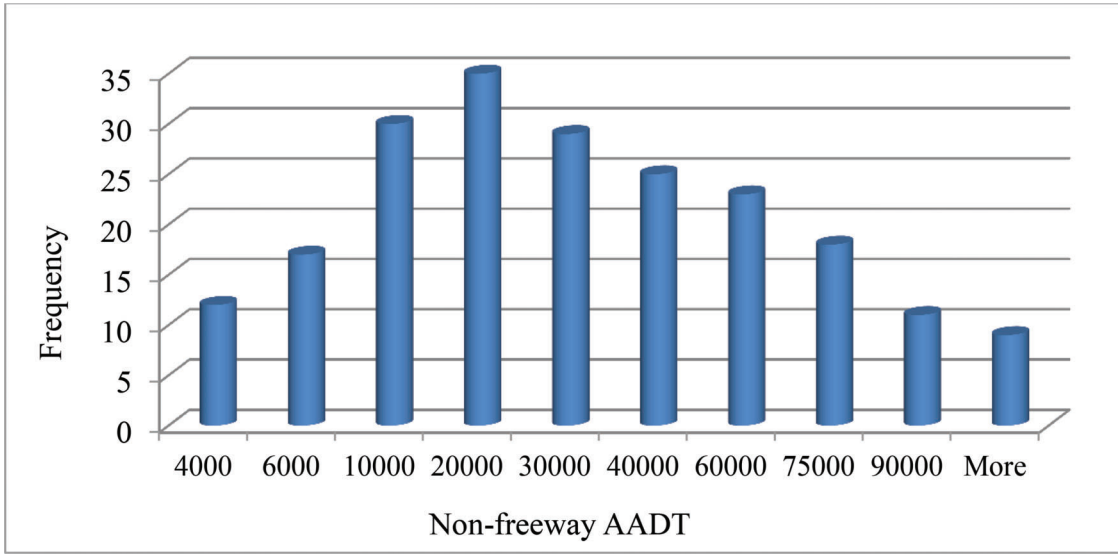
Figure 4.7 Distribution of non-freeway AADT for the studied interchanges

The obtained non-freeway AADT profile is represented with its 96 percentages p corresponding to the 15-min intersection traffic counts q. These 15-min counts q had to be divided among the 10 intersection turning movements m:

$$q_{a,i,m} = u_{a,m} \cdot p_{a,i} \cdot non\_freeway\,AADT / 100 \quad (4.11)$$

$$q_{p,i,m} = u_{a,m} \cdot p_{p,i} \cdot non\_freeway\,AADT / 100 \quad (4.12)$$

$$q_{o,i,m} = (u_{a,m} + u_{p,m}) \cdot p_{o,i} \cdot non\_freeway\,AADT / 200 \quad (4.13)$$

where:

$non\_freeway\ AADT$ = interchange AADT excluding the freeway through traffic (veh/24 hrs),

$q_{a,i,m}$, $q_{p,i,m}$ = movement m traffic count during 15-min interval i of the morning or afternoon rush hour, respectively (veh/15 min), i=1…4, m=1…10,

$q_{o,i,m}$ = movement m traffic count during any 15-min interval of the off-peak period i (veh/15 min), i=1…4, m=1…10,

$u_{a,m}$, $u_{p,m}$= proportion of movement m traffic in the morning or afternoon rush hour traffic, respectively, m=1…10,

$p_{a,i}$, $p_{p,i}$ = percent of intersection traffic during 15-min interval i of the morning or afternoon rush hour, respectively (%), i=1…4,

$p_{o,i}$ = percent of intersection traffic during any 15-min interval of off-peak period i (%), i=1…4.

The values of non-freeway AADT and morning and afternoon turning movements $Q_{a,m}$, $Q_{p,m}$ were obtained from the 2002 Indiana Interchange Planning Study. The distribution of the non-freeway ADDT values is shown in Figure 4.7.

The needed percentages P_a, P_p and proportions $u_{a,m}$ and $a_{p,m}$ were calculated using Eq. 4.14 through Eq. 4.17 below. The statistics for rush hour percentages

P in non-freeway ADDT and the proportions of movement traffic in rush hours are in Table 4.2.

$$P_a = \frac{100 \sum_{m=1}^{10} Q_{a,m}}{Non-freeway\ AADT} \quad (4.14)$$

$$P_p = \frac{100 \sum_{m=1}^{10} Q_{p,m}}{Non-freeway\ AADT} \quad (4.15)$$

$$u_{a,m} = \frac{Q_{a,m}}{\sum_{m=1}^{10} Q_{a,m}} \quad (4.16)$$

$$u_{p,m} = \frac{Q_{p,m}}{\sum_{m=1}^{10} Q_{p,m}} \quad (4.17)$$

Previous studies showed that the best design and operational performance depends on traffic scenarios (Tarko et al., 2008). Therefore, traffic scenarios from the 2002 Indiana Interchange Planning Study were utilized for the evaluation of the operational performance of the six alternative diamond interchanges. Traffic patterns for 225 four-leg service interchanges in Indiana (INDOT, 2002) therefore were utilized in designing simulation experiments to preserve realistic traffic patterns. Table 4.3 shows the descriptive statistics of the morning and afternoon peak hour volume percentages of Indiana's service interchanges.

4.3 Indiana Traffic Parameters

To calibrate the alternative interchanges to the Indiana-specific characteristics, the speed limits of Indiana were incorporated in the simulated network to reflect the field conditions. The desired speed distributions were created based on the posted speed limits and reduced speed areas as per the Indiana standards. The desired speed distributions

TABLE 4.2
Expansion factors for the simulated periods of the representative day

Period w	Time	Period Duration	Simulated Period	Expansion Factor e_w
Off-peak period 1	12 pm–7 am, 10–12 pm	9 hours	0.5 hour	18
Off-peak period 2	7–8 am, 8–10 pm	3 hours	0.5 hour	6
Morning rush hour	8–9 am	1 hour	1 hour	1
Off-peak period 3	9 am–4 pm, 6-8 pm	9 hours	0.5 hour	18
Off-peak period 4	4–5 pm	1 hour	0.5 hour	2
Afternoon rush hour	5–6 pm	1 hour	1 hour	1

TABLE 4.3
Descriptive statistics of the morning and afternoon peak hour volume percentages

Direction of Movement	AM			PM			Covariance AM & PM
	Average	Variance	Std. Dev	Average	Variance	Std. Dev	
$RampVol_{h(1R)}$	0.077	0.003	0.058	0.088	0.006	0.075	0.0029
$RampVol_{h(1L)}$	0.082	0.003	0.055	0.098	0.005	0.071	0.0025
$RampVol_{h(2R)}$	0.088	0.003	0.053	0.112	0.006	0.076	0.0027
$RampVol_{h(2L)}$	0.080	0.003	0.052	0.088	0.004	0.061	0.0021
$CrossVol_{h(1R)}$	0.098	0.005	0.071	0.082	0.003	0.055	0.0025
$CrossVol_{h(1T)}$	0.153	0.008	0.089	0.140	0.006	0.080	0.0050
$CrossVol_{h(1L)}$	0.111	0.006	0.075	0.088	0.003	0.052	0.0027
$CrossVol_{h(2R)}$	0.088	0.004	0.062	0.081	0.003	0.052	0.0022
$CrossVol_{h(2T)}$	0.137	0.006	0.080	0.147	0.008	0.087	0.0048
$CrossVol_{h(2L)}$	0.087	0.006	0.075	0.077	0.003	0.058	0.0029
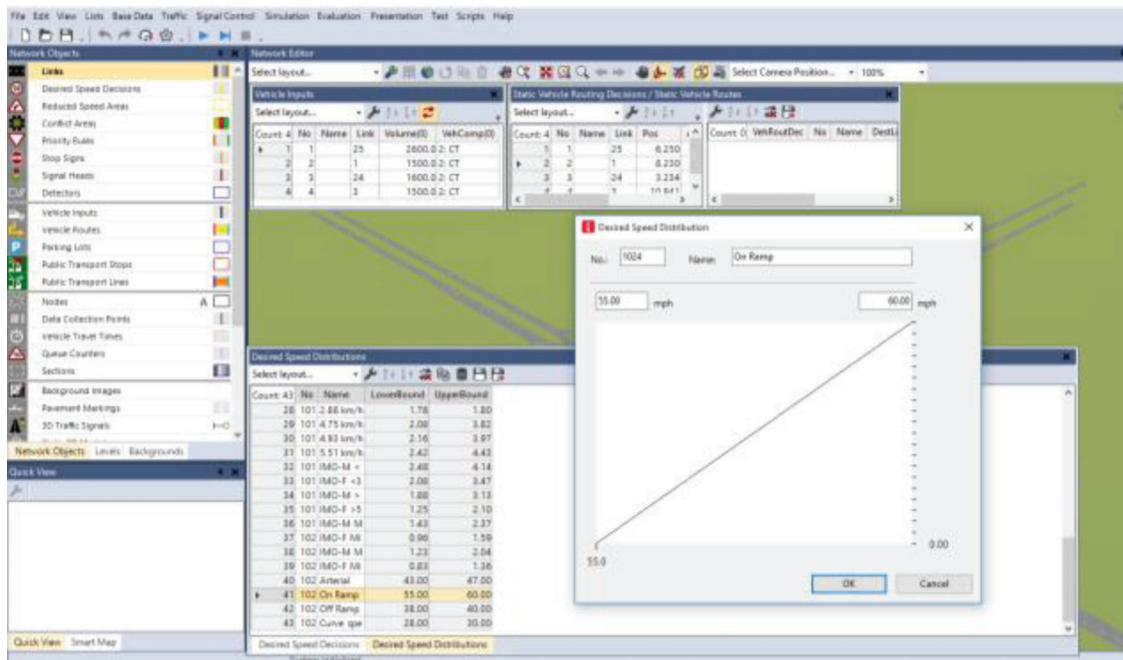
Figure 4.8 Desired speed distribution setup.

were set in ranges to limit traveling vehicles to a specified speed range (see Figure 4.8). Speed reduction areas imitated vehicles slowing down when approaching a turn and speeding up after the turn was completed. Reduced speed areas were placed on the left, the right, the connectors, and inside the roundabout.

The average speeds used in the simulation are presented in Table 4.4.

Indiana-specific capacity parameters were used for evaluating the performance of the alternative diamond interchanges. The saturation flow rate and the corresponding saturation headway time are the most important

TABLE 4.4
Average speed for different entities of interchange system

Entity	Average Speed (mph)
Non-freeway	45
On-ramp	55–60
Off-ramp	40–45
Turning	30
Roundabout approach	25
Roundabout circulating	18

TABLE 4.5
Summary of saturation flow rates for Indiana, pc/h/lane

Parameter	Weighted Average Value	Min–Max Values	Standard Deviation
Through movement	1842	1352–2178	199
Left turns	1844	1764–2079	117

TABLE 4.6
Estimated critical headways (probit method)

Condition	Critical Headways (Sec)
Passenger Car	4.4 (0.98)
Heavy Vehicle	5.2 (0.98)

TABLE 4.7
Calculated follow-up headways (standard deviation in parentheses)

Roundabout	1 Lane Approach	2 Lane Left Lane	Right Lane
Low-speed approach	2.6 (0.4)	2.6 (1.0)	2.5 (0.9)
Heavy vehicle	3.3	–	–

TABLE 4.8
Sensitivity analysis of minimum gap time for critical and follow-up headway

Experiment ID	Parameter Minimum Gap (s)	Result t_c(s)	t_f(s)
1	3.0	3.74	2.81
2	3.5	4.24	2.82
3	4.0	4.68	2.82
4	4.3	4.90	2.84
5	4.5	5.04	2.84
6	5.0	5.39	2.84
7	5.5	5.72	2.86

parameters of the capacity of signalized streams (Tarko et al., 2008). Table 4.5 provides the saturation flow rate used in a previous study conducted for Indiana (Perez-Cartagena & Tarko, 2004) for simulating the performance of alternative intersections.

The saturation flow rate depends on the population in the area where the intersection was located. Since non-freeway AADT tends to grow with the size of the population served by the interchange, the saturation flow rate grows as well (Perez-Cartagena & Tarko, 2004). To reflect the relationship, two ranges of saturation flow rate were used in this study:

1. A saturation flow rate range of 1400–2000 pc/h/lane was associated with non-freeway AADT lower than 25,000 veh/day.
2. A saturation flow rate range of 1600–2200 pc/h/lane was associated with non-freeway AADT equal to or higher than 25,000 veh/day.

Once the saturation flow rate was randomly selected from the proper range, the corresponding saturation time headway for passenger cars was calculated (h) as:

$$h = \frac{3600}{s} \qquad (4.18)$$

Similarly, the critical time headway and the follow-up time are important for unsignalized streams. The double roundabout has two roundabouts at the ramp terminals. The SRA has a peanut shape structure where the interstate runs across the middle. Minor street through and left turn movements navigate through the roundabouts. Roundabout interchanges are controlled by priority rules where the critical headway and follow-up time play a significant role in roundabout capacity. Critical headway is the shortest time headway between two consecutive vehicles on the circulatory roadways and acceptable to an average driver waiting to enter the roundabout safely. The follow-up headway is the average time headway between two consecutive vehicles on the approach roadway entering the roundabout by accepting the same available headway. Table 4.6 presents the critical headways and Table 4.7 shows the follow-up on state roads in Indiana (Matin & Tarko, 2015).

Calibrating roundabout models according to the Indiana traffic characteristics is key to analyze the performance measures. Roundabout interchanges are controlled by the priority rule. Critical (t_c) and follow-up (t_f) headway is represented in the priority rules through minimum gap time. Applying the Indiana driver behavior, the minimum gap was calculated by interpolation of the t_c values of Table 4.8 (Li et al., 2013). Minimum gap time was 3.7 sec for passenger cars and 4.7 sec for heavy vehicles for Indiana conditions.

4.4 Interchange Simulation Scenarios

Interchange alternative, geometry, non-freeway AADT, and daily traffic pattern defined the number of simulation scenario.

- Four signalized diamond alternatives with five geometry cases and two unsignalized diamond interchanges with four geometry cases.
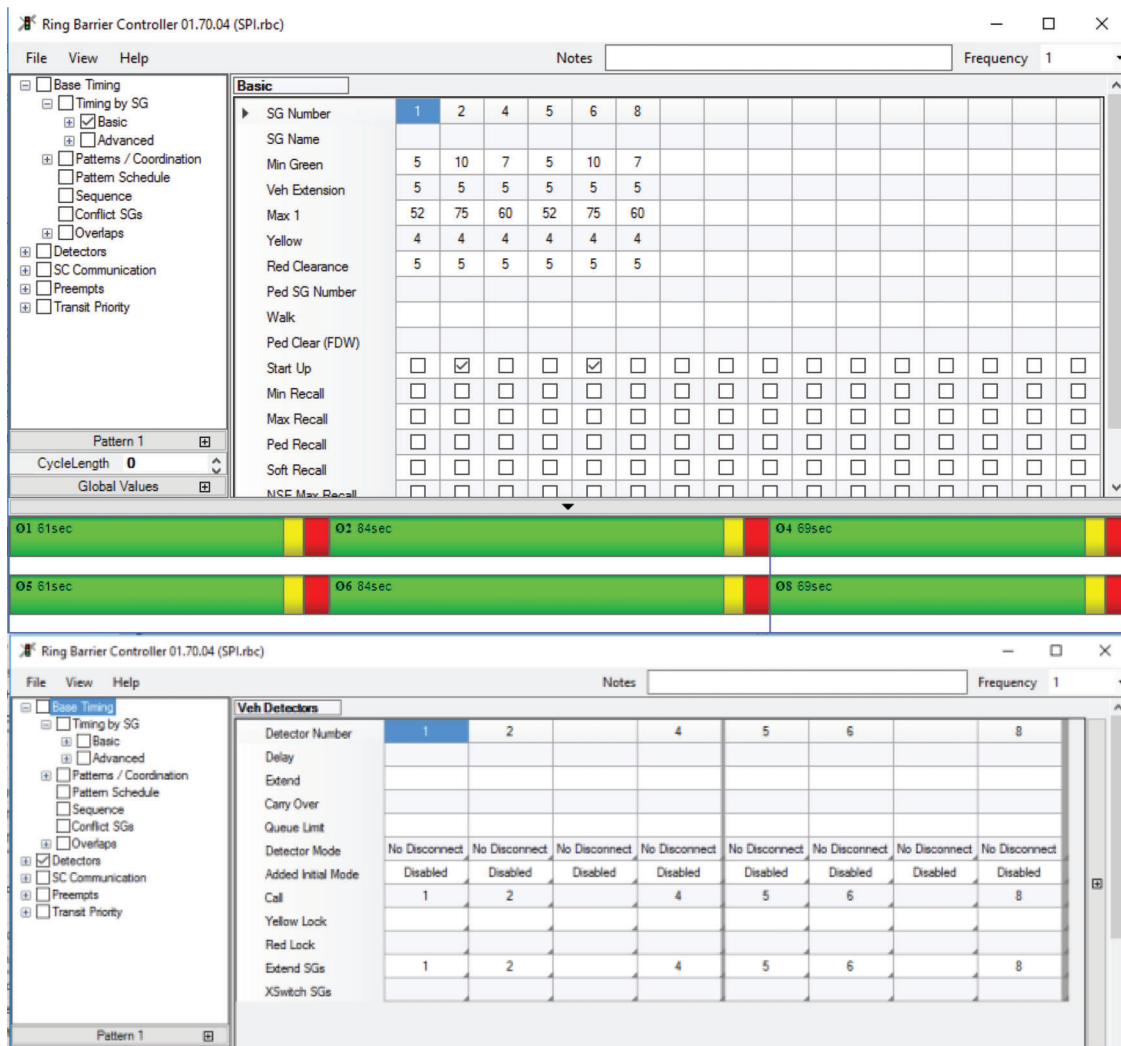
Figure 4.9 Actuated signal settings for SPI.

- 12 non-freeway AADT cases that covered a wide range of traffic demand.
- 40 daily traffic patterns for each non-freeway demand level.
- Daily traffic pattern with the turning volume percentages during the morning peak hour, afternoon peak hour, and an off-peak hour obtained from past traffic studies in Indiana.
- Total number of simulation scenarios: 13,440 = (4x5+2x4) x 12x40.

4.5 Actuated Signal Settings

If the intersection spacing of a diamond interchange is less than 800 ft, then a single controller should be used (Sunkari & Urbanik, 2000). Max3 (Nichols & Bullock, 2000) green time is used during free operation to extend the green interval for an intersection where v/c is unknown. The max3 parameters were as follows:
- Main street max3 = 75 sec
- Main street max ext = 12 sec
- Side street max3 = 60 sec

- Side street max ext = 10 sec
- All left-turn max3 = 52 sec
- All left-turn max ext = 8 sec

An actuated signal control (Hunter, n.d.) was used for designing the signalized alternative interchanges. Fifty-one-foot (51 ft) stop bar detectors have been placed on the signalized approaches (Day, Premachandra, Brennan, Sturdevant, & Bullock, 2010). SPI had three signal phases (Qureshi, Spring, Lasod, & Sugathan, 2004): (1) the first phase controlled both crossing road left-turn movements; (2) in the second phase, both crossing road through movements took place; and (3) in the third phase, both off-ramp left-turn movements were made (see Figure 4.9).

For the DI and TDI signal timing, three phase strategies were used (Sunkari & Urbanik, 2000) (see Figure 4.10). Phase one was for the internal arterial road through-movement and the left turn to the on-ramp. The second phase was the movement from the off-ramp to the arterial road or straight through to the on-ramp. The last phase was the through movements of the crossing roads (Nelson, Bullock, & Urbanik, 2000).
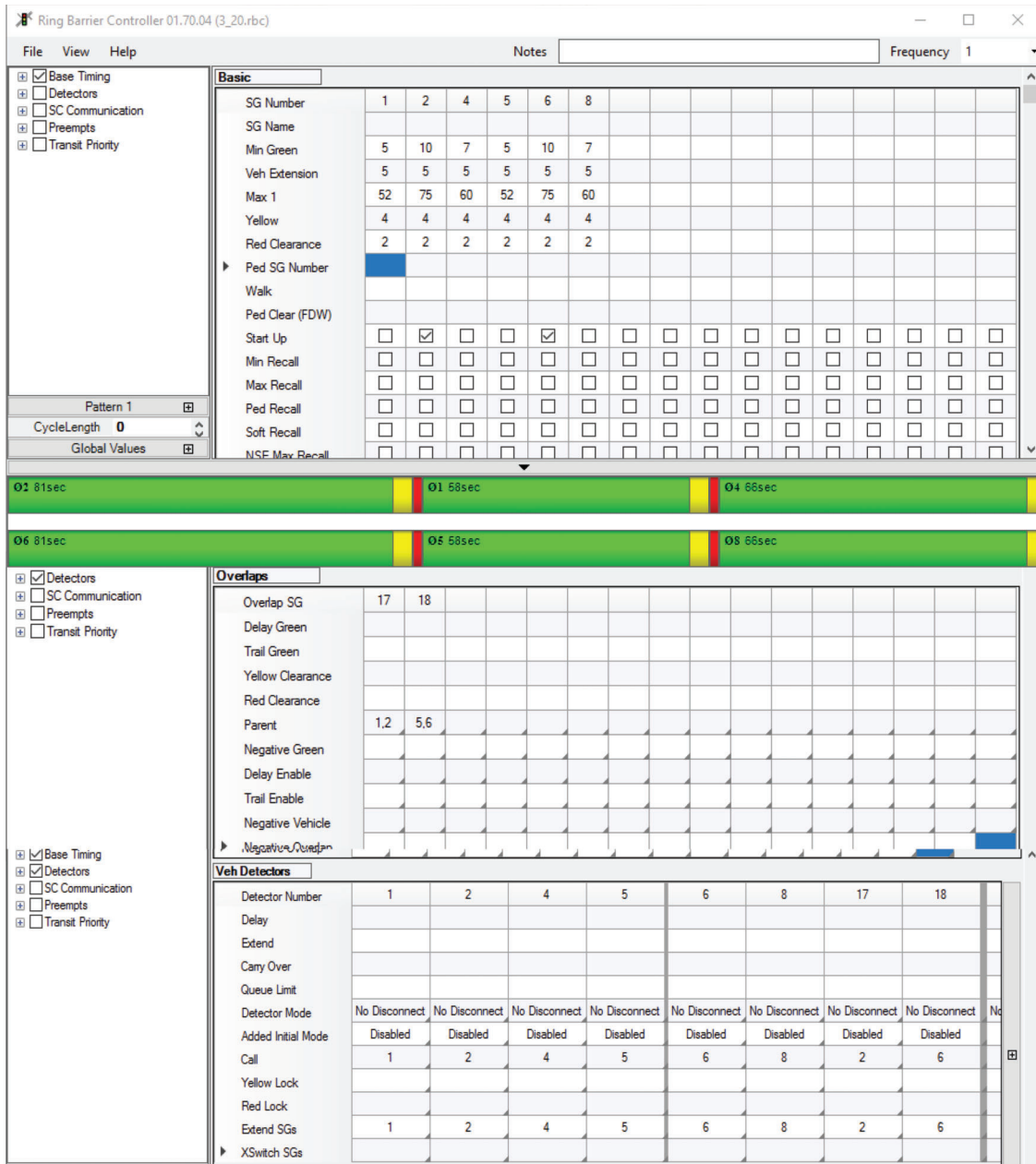
Figure 4.10 Actuated signal settings for diamond.

Typically, DDI signal timing consists of a relatively simple two-phase configuration at each intersection (Hainen et al., 2015) (see Figure 4.11). Ring 1 handled the first intersection and Ring 2 the second intersection, with two even-numbered phases each (2, 4) and (6, 8), respectively.

4.6 VISSIM Objects and Corresponding Evaluation Settings

Network level and intersection level VISSIM objects were used to save the performance measures of the simulation results. Vehicle Input (many vehicles will enter to the system) Vehicle Routing Decision (which route a vehicle will take), Desired Speed, Reduced Speed on the curves, Vehicle Travel Times, Data Collection Points Signal Head, Priority Rules, Detector, Queue Counter (reports the queue length), and Data Collection Points are the important objects that were used in this study.

The delay, data collection, vehicle travel time, and queue counter results were saved after every simulation run. Figure 4.12 shows a snapshot of the evaluation configuration, and Figure 4.13 shows the simulation screen captures of the alternative diamond interchanges.

4.7 Running Simulation with VISSIM through Macro

A large number of simulation runs was required to evaluate the performance of the different interchange
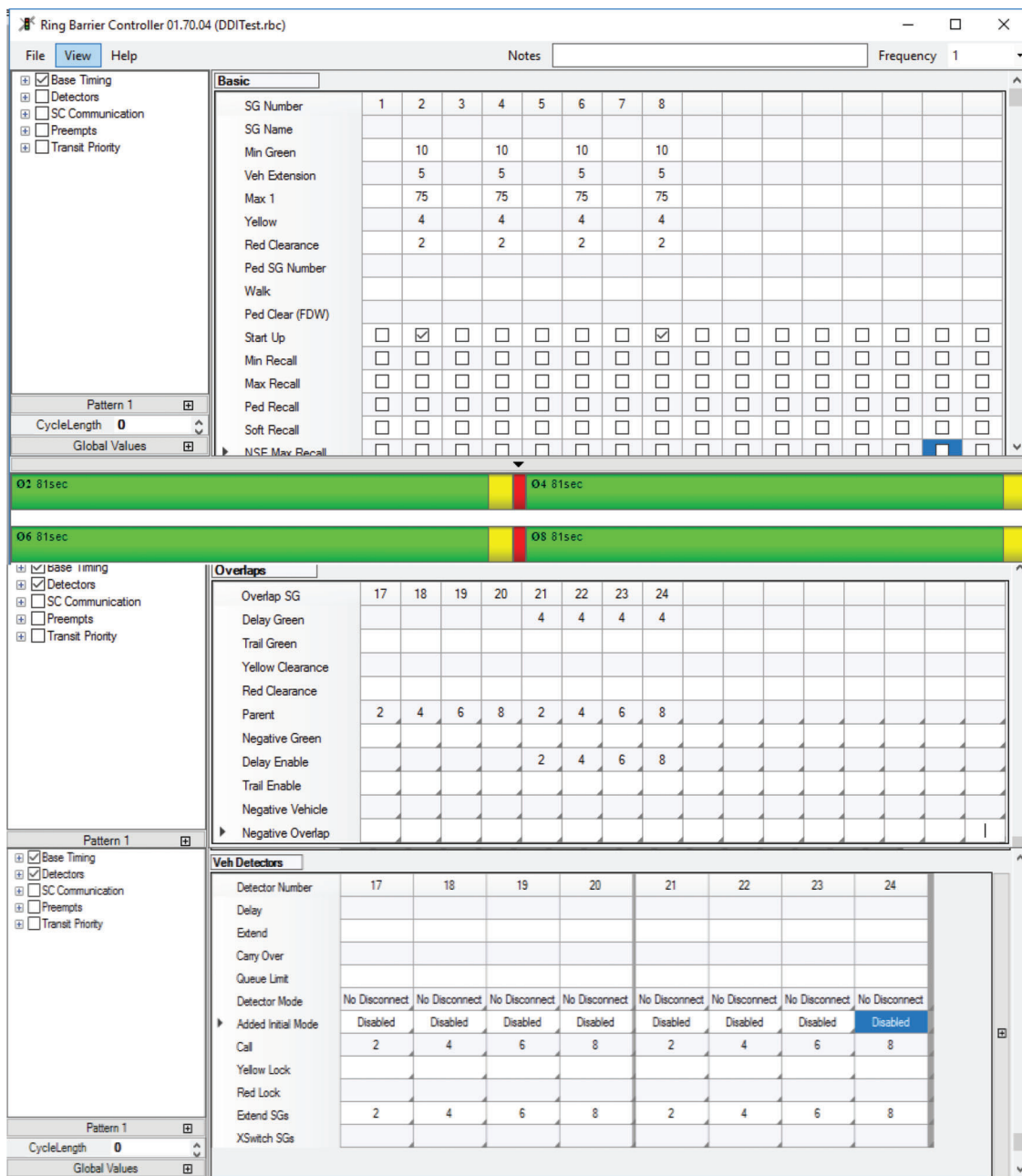
Figure 4.11 Actuated signal settings for DDI.

alternatives. An input editor and simulation manager program was created in order to set the required simulation inputs, control the simulation runs, and save the results.

The input editor and simulation manager were developed in Microsoft Excel using Visual Basic applications (VBA) and the VISSIM component object model (COM) interface, which allows programs to communicate and interact with VISSIM.

4.7.1 Defining Simulation Parameters

The input editor (Figure 4.14) provided the ability to select the geometry alternative, set the non-freeway AADT, the daily traffic profile, and the traffic patterns, the values of which were converted into the corresponding VISSIM inputs.

- Traffic patterns were randomly selected from 200 Indiana four-leg service interchanges.
- The daily traffic distribution was calculated based on a simplified profile.
- Non-freeway AADT was used to obtain different traffic volumes for each traffic pattern.
- A VISSIM model was selected for each geometry alternative.
- The traffic volume and distribution were modified according to the period of the day.
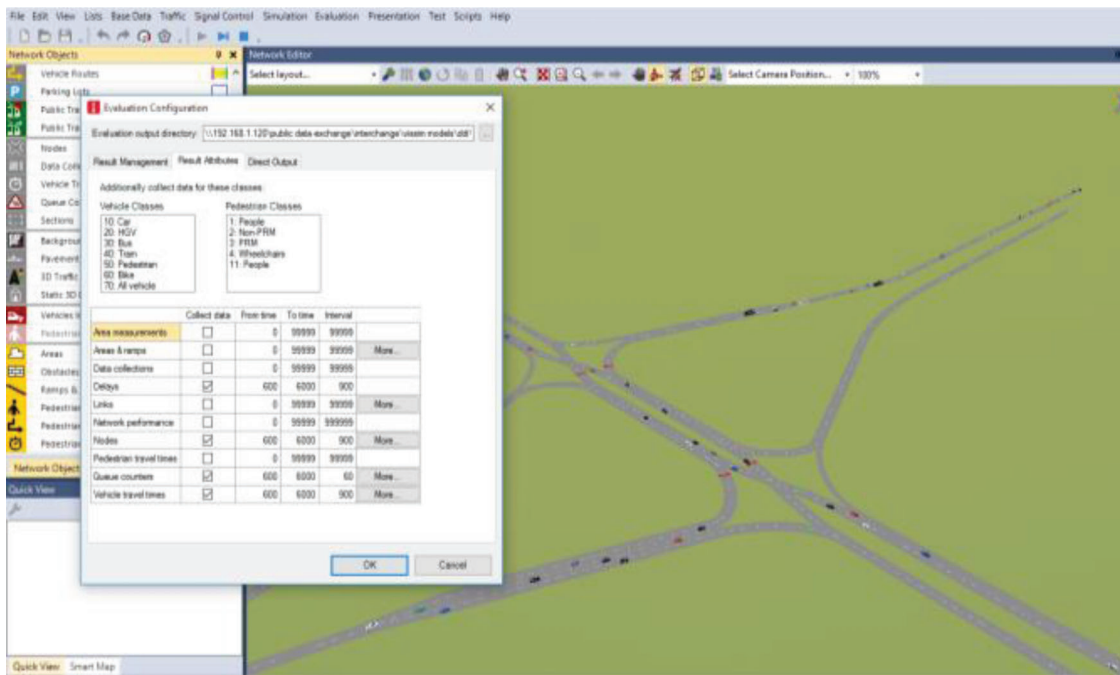
Figure 4.12 VISSIM settings for saving evaluation results.

4.7.2 Selecting the Number of Simulation Runs and Starting Simulation

The simulation manager transferred the defined inputs to VISSIM parameters, ran the simulation, saved the inputs for each run, collected the simulation results, and aggregated and saved the results in a file. For each of the 12 periods that represent the traffic distribution during a day, the simulation inputs included:

- Number of vehicles per entry point.
- Traffic distribution.
- Saturation flow rate parameters.

For each period, the simulation manager set the corresponding parameters, ran the simulations, and obtained the following results:

- Vehicle counts every 15 sec per data collection point.
- Maximum and average queue length every 1 min per queue counter. In each time step, the current queue length was measured upstream by the queue counter, and the maximum and average were then calculated per time interval. A vehicle was considered in the queue if its speed was between 5 and 10 mph. The maximum net distance which can occur between two vehicles in the queue is 65.6 ft.
- Number of stops every 1 min per queue counter: A queue stop occurred when the speed of one vehicle in the queue was below the 5 mph queue forming condition.
- Average travel time every 15 min per movement.
- Average delay per vehicle every 15 min per movement.

Figure 4.15 shows the saved results by the simulation manager. The saved results contains all the raw data from simulation such as delay, travel time for each of the movements, queue length for each approach and total number of stops for the entire interchange.

The simulation manager also summarized the results in 15-min periods and created an output file that included the simulation identification, the inputs, and the results. Once all the simulations were completed, a new set of combined output files were produced in order to create the required statistical inputs based on different levels of aggregation, such as daily, peak hour, and highest 15-min period.

Finally, once the statistical models were obtained, the simulation manager calculated the daily average delay based on the yearly traffic distribution as well as the stops per vehicles (see Figure 4.16). It also calculated the longest queues for both the ramp and the crossing road and generated the corresponding graphs for the various traffic distributions generated.

4.8 Simulation Output

The simulation manager saves the assumed and generated volumes along with the corresponding travel time, number of stops, delays, and queue lengths for the predefined time periods. Table 4.9 shows the sample data collected from each of the simulation runs.

4.9 Simulation Results Adjustments

The delays, stops and queues were measured inside the simulated area but additional delays, stops, and queues occurred outside the simulated area when the queues exceeded the limits of the simulated network. The generated vehicles could not enter the system and thus formed latent queues outside of the simulated network. Fortunately, VISSIM stored these vehicles and entered them into the
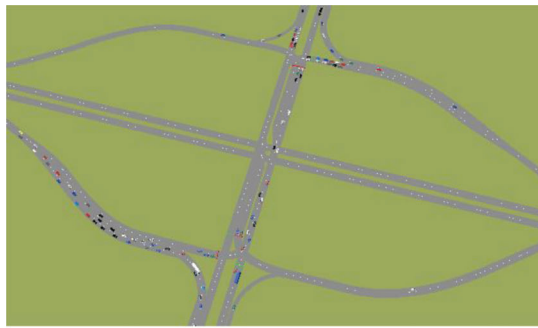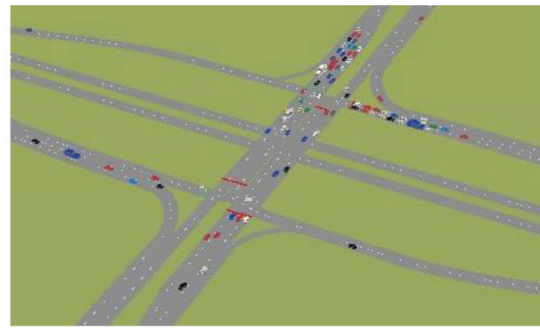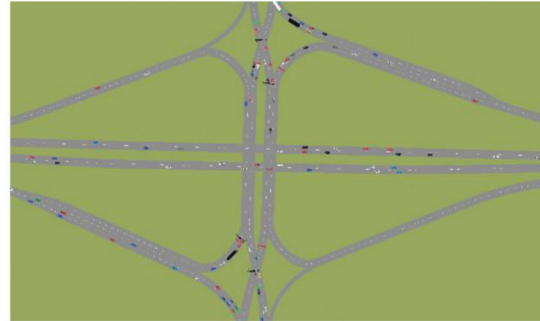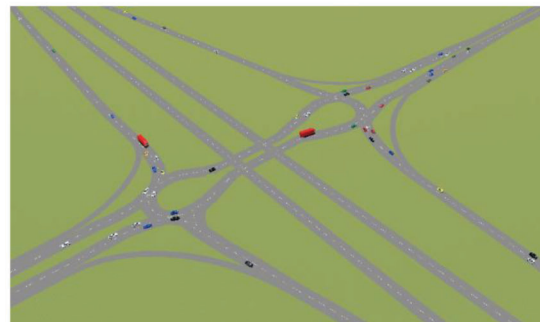
Figure 4.13 Simulation screenshot of the alternative diamond interchange.

simulated network as soon as they reached a position in the queue that was inside the simulated network. Thus, the delays, number of stops, and queue lengths measured along simulated paths were supplemented with the values experienced in the latent queues.

4.9.1 VISSIM Objects for Measuring Additional Delay, Stop and Queue

A vehicle input (VI) object was used to generate the assumed number of vehicles per hour during the simulation interval (15 min) at a given entry point (see Figure 4.17). The option of exact vehicle input was used to reduce the variability of the number of vehicles. The data collection point (DCP) object was placed closely downstream of the VI object to report the actual number of vehicles that entered the system every 15 sec. This number was lower than the generated number if the queue of vehicles reached the system limit (entry

point) and it metered the number of vehicles entering the system. The desired speed decision (DSD) and the vehicle routing decision (VRD) objects were placed between the VI and DCP objects to assign the desired speed and the path (one out of two or three) to vehicles that just entered the system.

The input volume was set to not exceed 95% of the capacity of the uninterrupted flow on the road segment leading towards the interchange. Otherwise, the simulation would not produce meaningful results.

4.9.2 Delay Adjustment

The average delay inside the simulated area was calculated with travel times measured with the VISSIM VTT objects placed at the beginning and the end of the path. The vehicles counted by the DCP object were used to calculate the delay adjustments that represented the additional delay entering the system due to a queue
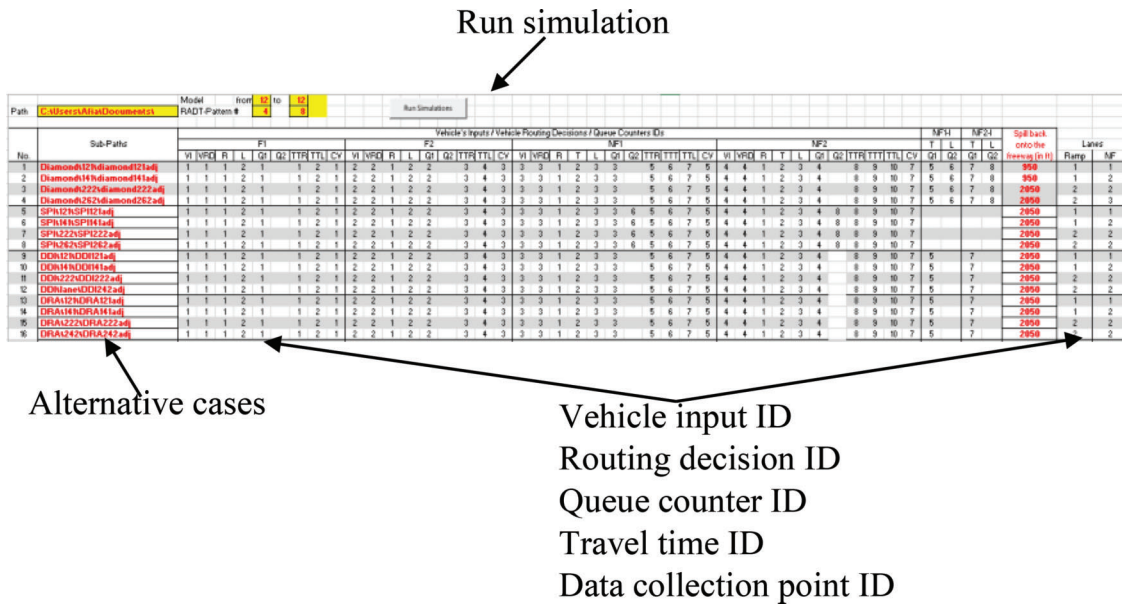
Figure 4.14 Input editor for VISSIM simulation run.
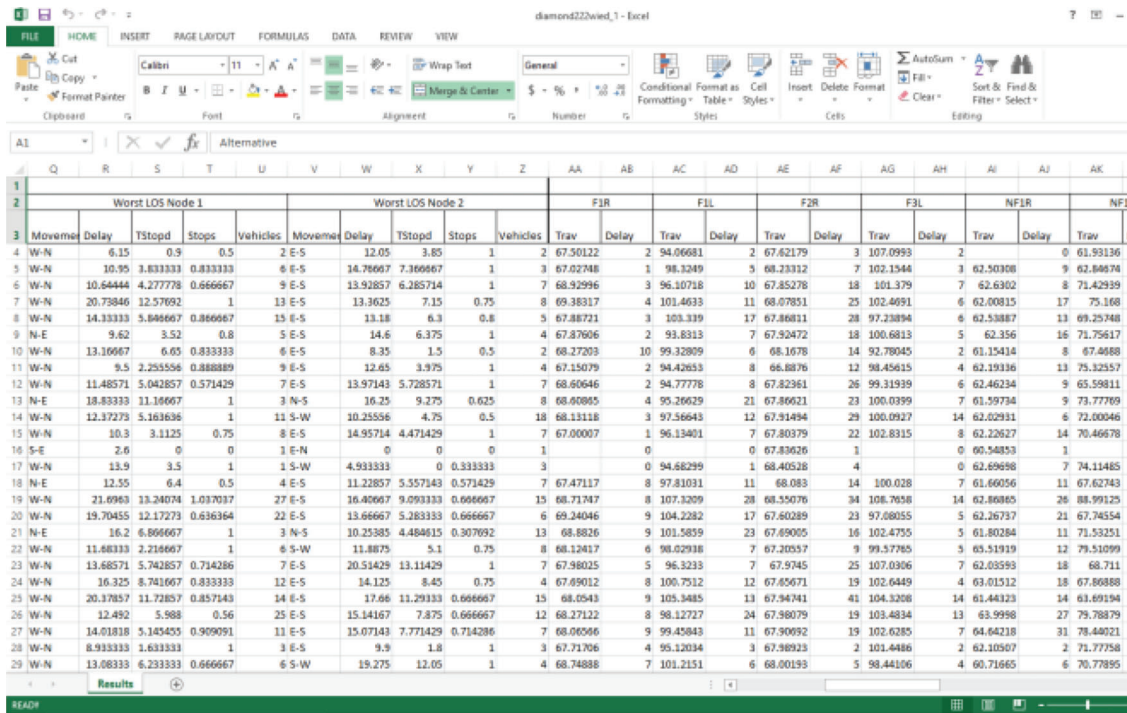
Figure 4.15 Saved results from VISSIM simulation.

blockage at the entry. This additional delay was calculated using the cumulative counts of the vehicles generated and entering the network. Eq. 4.19 through Eq. 4.22 were used to calculate the delay adjustments in 15-min simulation intervals.

Let t_{gi} be the time when a vehicle entering the simulated network at time t_i was generated, Q^* the latent queue at the beginning of the current 15-min simulation interval,

VC_i the number of vehicles entering the network in 15-sec interval i, and VI^* and VI the vehicle inputs in the previous and current simulation intervals in veh/hr, respectively. The estimated time when the first vehicle in the initial latent queue entered the simulated network was:

$$t_{g0} = -\frac{3600 \cdot Q^*}{VI^*} \tag{4.19}$$

Case	From	To	Increment				
242	20	60	10				Create Graphs
Title							
	Number of Continuous Lanes on Crossing Road			4			
	Number of Continuous Lanes on Off-Ramps			2			
	Number of Approach Lanes to the Crossing Road			4			Create PDF
	Percentage of Off-Ramp Volume			[Value]			
	Percentage of Crossing Road Volume			1-[Value]			
							Calculate
Graph 1	AVG						
Title	Delay						
Axis	min	max	Title		Scale		
X	20000	120000	RADT		1000		
Y	0	120	Total Delay				
Parameters		1000	LOG				

Figure 4.16   Automatic graph generating macro.

TABLE 4.9
Output variables from the simulation

Category	Variable Name	Variable Description
General	ID	Identification number
	Alternative	DI, TUDI, SPUI, DDI, DRI, SRI
Traffic	Non-Freeway AADT	AADT on the crossing road and off-ramps
	cr_a	Daily assumed volume on the crossing road
	$ramp_a$	Daily assumed volume on the off-ramps
	pttrn	Proportion 10 movement in relation to non-freeway AADT
	cr_g	Generated volume on the crossing road
	$ramp_g$	Generated volume on the off-ramps
Performance	TT	Total travel time of all the simulated vehicles
	Total_Stop	Total number of stops on interchange during 24 hour
	D_{cm}	Delay on the ten interchange movements
	QL	Longest queue length on the off-ramps and crossing road
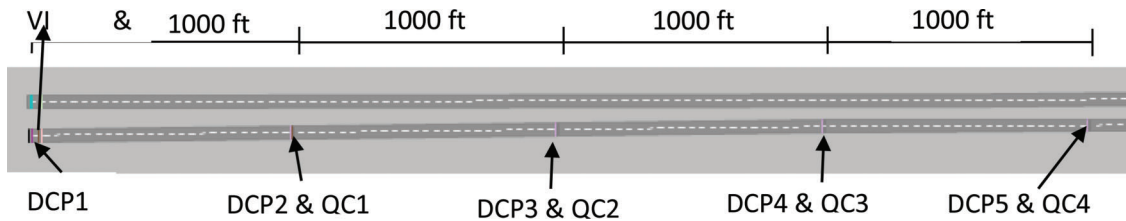
Figure 4.17   VISSIM objects for estimating outflow stops.

The negative sign indicates that the vehicle was generated before the beginning of the current interval. The generation times of other vehicles entering the simulated network before and during the current simulation interval were calculated as follows:

$$t_{gi} = t_{g0} + 3600 \frac{\sum_{j=1}^{60} VC_j}{VI^*} \text{ if } t_{gi} < 0 \quad (4.20)$$

$$t_{gi} = 3600 \frac{\sum_{j=1}^{60} VC_j - Q^*}{VI}, \text{ otherwise.}$$

A delay adjustment of a vehicle entering the network at time $t_i = i \, \Delta t$ was:

$$d_i = t_i - t_{gi} \text{ if } d_i > 0 \quad (4.21)$$

$d_i = 0$, otherwise.

Finally, the average time between generating and entering vehicles into the network during the current simulation interval was:

$$d_{adj} = \frac{\sum_{i=1}^{60} VC_i \cdot (d_{i-1} + d_i)}{2 \sum_{i=1}^{60} VC_i}, \text{ if } d > 0; \quad (4.22)$$

$d = 0$, otherwise.

4.9.3 Number of Stops Adjustment

Figure 4.17 shows the VISSIM objects, data collection points, and queue counters for estimating the overflow stops outside the simulated network. The number of stops adjustment was calculated using Eq. 4.23:

$$S_{adj} = \frac{S_{DCP2-DCP4}}{Segment\ length} \cdot Occupancy_{DCP3-DCP4} \cdot VQ \quad (4.23)$$

where:

S_{adj} = Stops that occurred outside the simulated system,

$S_{DCP3-DCP4}$ = Number of stops between data collection point DCP3 and DCP4

VQ = Number of vehicles outside the simulated system,

$Occupancy_{DCP3-DCP4}$ = Occupancy between data collection point DCP3 and DCP4

4.9.4 Queue Adjustment

To adjust the overflow queue length, only those cases were included where the horizontal queue length exceeded the system entry point. The vehicle count between data collection points DCP2 and DCP4 in Figure 4.17 provided the occupancy (OCC) (i.e., the distance/vehicle in that segment). This vertical queue length then was added to the simulated horizontal maximum queue length.

QL_i is the vertical queue length for the overflow vehicles for the current 15-min simulated interval that could not enter the simulated network. The overflow vehicles were calculated as the difference between the vehicle input for the 15-min interval and the sum of all the vehicle counts at DCP1 in every 15-sec interval during the 15-min interval.

Vertical queue Length, QL_i

$$= (\frac{VI}{4} - \sum_{j=1}^{i} VC1_j + Q^*) \cdot OCC_{avg} \quad (4.24)$$

5. STATISTICAL MODELS

Statistical models were estimated for each geometry case as a convenient way to summarize the simulation results and to compare the performance of the studied alternative interchanges. It is noted that double and single roundabouts were considered as a single group because the difference in their performance was negligible (see Appendix). Five performance measures (daily-average delay, daily-average stops, critical movement delay, longest queue length on off-ramp, and longest queue length on crossing road) were modeled using log-linear or modified log-linear regression. Variables representing the crossing road and off-ramp traffic volumes were included in these models. The statistical models were estimated using statistical software SAS (SAS, 2016).

5.1 Interchange Delay

Delays experienced at an interchange are an important component of user costs. The average road user delay at crossing roads and terminal off-ramp intersections may be used to evaluate the perception of the traffic conditions with the Highway Capacity Manual method. Models for predicting the total daily delay at an interchange therefore were developed in this study.

5.1.1 Delay Model

A model of the total delay on an interchange during a 24-hour period was estimated with the simulated results. Table 5.1 shows the three functional forms utilized. The residual plot for functional form 1 shows the estimation bias that existed, which indicated that functional form 1 was inadequate. The residual plot for functional form 2 also indicated that it also was inadequate. The residual plot for model form 3, however, did not exhibit any obvious bias along the entire range of the dependent variables, and the adjusted R^2 statistic was the highest among all the tested forms. Functional form 3 was selected for the non-freeway daily interchange delay model.

Based on the adjusted R^2 and the residual plots, model form 3 was selected for predicting the non-freeway daily delay.

$$D_{24} = \exp(\beta_0 + \beta_1 CrossVol_{24} + \beta_2 \log(RampVol_{24})) \quad (5.1)$$

where:

D_{24} = daily interchange delay (s),

$CrossVol_{24}$ = assumed daily volume on crossing road,

$RampVol_{24}$ = assumed daily volume on off-ramp,

$\beta_0, \beta_1, \beta_2$ = model parameters.

Table 5.2 presents an example of the estimated relationship between the crossing road volume, the off-ramp volume, and the non-freeway daily interchange delay. The model exhibited very good fitness with an r-square of 0.98. It should be mentioned that the r-square of the daily interchange delay models were above 0.95 for all the geometry cases of the alternative interchanges.

5.1.2 Implementation of the Delay Model

The delay model in Eq. 5.1 calculated the total delay during a day for each geometry case and for a fixed proportion of traffic on the off-ramps. For any given non-freeway AADT at a certain location, by using the daily factor (INDOT, 2014), the traffic volume for a particular day of the year was estimated with Eq. 5.2. Using the delay parameters from Eq. 5.1, for a fixed proportion of traffic on off-ramps, the daily interchange delay was estimated for each day of the year using Eq. 5.3. This estimation was done using the macro explained in Chapter 4. In order to take into account the yearly traffic variation and the non-linear

TABLE 5.1
Functional forms of delay model
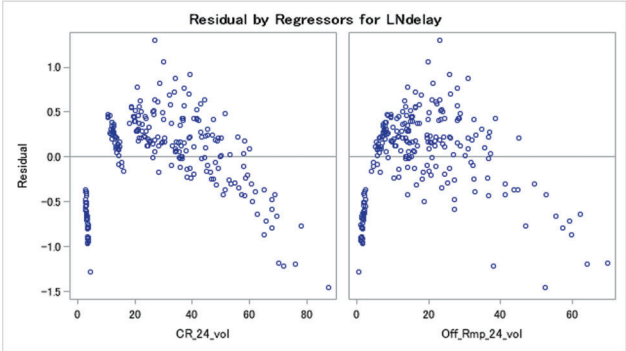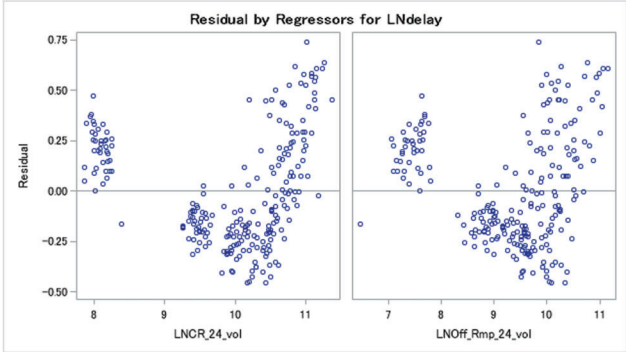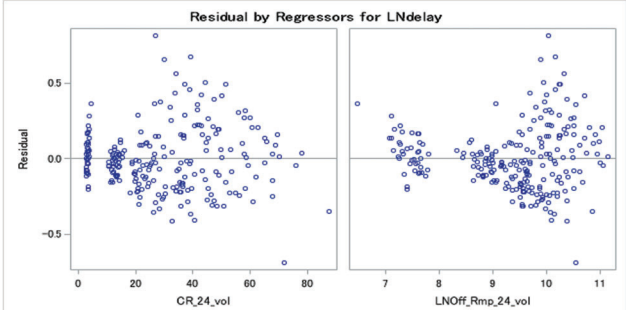
Functional Form	Residual Plot
1. Log-linear Model $Log(D_{24}) = \beta_{do} + \beta_1 (CrossVol_{24}) + \beta_2 (RampVol_{24})$ Adj. $R^2 = 0.89$	
2. Log-log Model $Log(D_{24}) = \beta_{do} + \beta_1 Log(CroosVol_{24}) + \beta_2 log(RampVol_{24})$ Adj. $R^2 = 0.96$	
3. Modified Log-linear Model $Log(D_{24}) = \beta_{do} + \beta_1 (CrossVol_{24}) + \beta_2 log(RampVol_{24})$ Adj. $R^2 = 0.98$	

TABLE 5.2
Example of daily interchange delay model

Parameter	DF	Estimate	Standard Error	t Value	Pr > |t|
Intercept	1	4.23563	0.20778	20.38	<.0001
$CrossVol_{24}$	1	0.02762	0.00137	20.10	<.0001
$Log(RampVol_{24})$	1	0.97652	0.02574	37.93	<.0001
Number of Observations	241				
R-Square	0.9808				
Adj R-Sq	0.9806				

TABLE 5.3
Example of critical movement delay model

Variable	DF	Parameter Estimate	Standard Error	t Value	Pr > |t|
Intercept	1	2.61953	0.03522	74.38	<.0001
$CrossVol_h$	1	0.53985	0.02111	25.57	<.0001
$RampVol_h$	1	0.43609	0.03023	14.43	<.0001

Number of Observations	482
R-Square	0.8885
Adj R-Sq	0.8880

relationship between delay and traffic volume, the average daily interchange delay was calculated using Eq. 5.4. In the graph, the annual-average non-freeway delay per vehicle is plotted against the interchange's non-freeway AADT.

$$Vol_{24i} = (CrossVol_{24} + RampVol_{24})F_i \qquad (5.2)$$

$$D_i = \exp(\beta_0 + \beta_1 CrossVol_{24i} + \beta_2 RampVol_{24i}) \qquad (5.3)$$

$$d_i = \frac{\sum_{i=1}^{365} D_i}{\sum_{i=1}^{365} Vol_{24i}} \qquad (5.4)$$

where:

Vol_{24i} = interchange non-freeway traffic on day i (crossing road and off-ramp traffic), veh/24h,
$CrossVol_{24}$ = AADT on the crossing road, veh/24h,
$RampVol_{24}$ = sum of AADT on the two off-ramps, veh/24h,
DF_i = traffic adjustment factor applicable to day i,
D_i = total delay on the interchange on day i (s),
$\beta_0, \beta_1, \beta_2$ = delay model parameters,
d_i= average delay per vehicle on day i (s/veh).

5.2 Critical Movement Delay

The movement with the highest average vehicle delay among the ten non-freeway interchange movements was considered a critical movement. The critical-movement delay was an indicator of the quality of service at an interchange and an LOS F of this movement indicated the capacity failure of an interchange.

5.2.1 Development of Critical Movement Delay Model

A model of the critical movement delay was estimated for the busiest 15-min morning and afternoon periods. The functional form is presented in Eq. 5.5. The residual plots did not exhibit any pattern; therefore, other functional forms were not investigated.

$$d_{cm} = \exp(\beta_0 + \beta_1 CrossVol_h + \beta_2 RampVol_h) \qquad (5.5)$$

where:
d_{cm} = critical movement delay (s),

$CrossVol_h$ = crossing-road volume during morning or afternoon rush hour (veh/h),
$RampVol_h$ = ramp volume during morning or afternoon rush hour (veh/h),
$\beta_0, \beta_1, \beta_2$ = model parameters.

Table 5.3 shows an example critical movement delay model. The model exhibited very good fitness with an R^2 of 0.88. It should be mentioned that the R^2 of the critical movement delay models were around 0.90 for all the geometry cases of the alternative interchanges. The crossing road volume had a higher impact on the critical movement delay than did the off-ramp volume. Although the critical movement delay predicted with individual turning volumes (see Appendix) yielded slightly better goodness of fit, for the sake of simplicity and ease of use, combined crossing road and off-ramp volumes are presented here.

5.2.2 Implementation of Critical Movement Delay Model

Graphs of the critical movement delay were generated for the range of non-freeway rush hour flow rates and the various percentages of ramp flow rate u_r.

$$d_{cm} = \exp(\beta_0 + \beta_1 Vol_h(1 - u_r) + \beta_{m2} Vol_h u_r) \qquad (5.6)$$

where:
d_{cm} = Average critical movement delay per vehicle during the busiest 15-min interval of the design hour (s),
Vol_h = total hourly volume on the non-freeway part of the interchange (crossing road and off-ramps) during a selected rush hour that represents the design hour in the design year (veh/h),
u_r = proportion of the non-freeway traffic on off-ramps,
$\beta_0, \beta_1, \beta_2$ = model parameters.

5.3 Interchange Stops

The average number of stops at an interchange is another important performance measure for selecting an alternative interchange from an economic point of view. A modified log-linear model was used to estimate the expected number of stops for the entire interchange in a 24-hour period. This expected total number of stops then was used to calculate the daily-average number of stops.

TABLE 5.4
Functional form of stop model

Functional Form	Residual Plot
1. Log-linear Model $Log(S_{24}) = \beta_0 + \beta_1(CrossVol_{24}) + \beta_2(RampVol_{24})$ Adj. R^2 =0.90	
2. Log-log Model $Log(S_{24}) = \beta_0 + \beta_1 Log(CrossVol_{24}) + \beta_2 log(RampVol_{24})$ Adj. R^2 =0.86	
3. Modified Log-linear Model $Log(S_{24})=\beta_0 + \beta_1 (CrossVol_{24}) + \beta_2 log(RampVol_{24})$ Adj. R^2 =0.92	

5.3.1 Stop Model

Daily stops on the interchange were predicted using a modified log-normal regression model for each type of interchange. The number of stops in the entire interchange during a 24-hour period was used as a dependent variable. Table 5.4 shows the functional forms of the stop model investigated.

In model 1, the residual plot shows the estimation bias indicating that the functional form was inadequate. The residual plot in functional form 2 shows that the relation between the dependent and explanatory variables was not log-log, confirming the inadequacy of this form. The residual plot in functional form 3 indicated that no systematic bias existed along the entire range of the dependent variables and that the adjusted R^2 statistic was the highest among all the tested forms. Functional form 3 therefore was selected for predicting the non-freeway daily interchange stops.

Based on the r-square and fit residual plot results, model 3 was selected for predicting the non-freeway daily-average stop.

$$S_{24} = \exp(\beta_0 + \beta_1 \cdot CrossVol_{24} + \beta_2 \cdot \log(RampVol_{24})) \quad (5.7)$$

where:

S_{24}= daily interchange stops
$CR\ volume_{24}$= assumed daily volume on crossing road

TABLE 5.5
Example of daily interchange stops model

Parameter	DF	Estimate	Standard Error	t Value	Pr > |t|
Intercept	1	2.57271	0.40302	6.38	<.0001
CrossVol$_{24}$	1	0.05075	0.00267	19.04	<.0001
Log (RampVol$_{24}$)	1	0.66576	0.04993	13.33	<.0001
Number of Observations	241				
R-Square	0.9405				
Adj R-Sq	0.9400				

Ramp volume$_{24}$ = assumed daily volume on off-ramps $\beta_0, \beta_1, \beta_2$ = stop model parameters.

Table 5.5 shows an example to depict the relationship between the crossing road/ off-ramp volume, and the daily interchange stops. These two variables were positively related to the dependent variable, which means that the probability of stops occurring increased with an increased non-freeway ADT. The model indicates very good fitness with an r-square of 0.94. It should be mentioned that the r-square of the daily interchange stops models were above 0.90 for all the geometry cases of the alternative interchanges. Although the daily interchange stops predicted with individual turning volumes (see Appendix) yielded slightly better goodness of fit, but for the sake of simplicity and ease of use, combined crossing road and off-ramp volumes are presented here.

5.3.2 Implementation of Stop Model

Reference graphs were generated using the stop model developed in Eq. 5.7 for each geometry case and for a fixed proportion of traffic on the off-ramps. For any given non-freeway AADT at a certain location, by using the daily factor (INDOT, 2014), the traffic volume for a particular day of the year was estimated utilizing Eq. 5.8. Using the stop model parameters from Eq. 5.7, for a fixed proportion of traffic on off-ramps, the daily interchange stops was estimated for each day of the year using Eq. 5.9. This estimation was done using the macro explained in Chapter 4. In order to take into account the yearly traffic variation and the non-linear relationship between the stops and the traffic volume, the average daily interchange stops were calculated using Eq. 5.10. Finally, the annual-average non-freeway stops per vehicle were plotted against the annual-average interchange non-freeway daily traffic.

$$Vol_{24i} = (CrossVol_{24} + RampVol_{24}) \cdot DF_i \quad (5.8)$$

$$S_i = \exp(\beta_0 + \beta_1 CrossVol_{24i} + \beta_d RampVol_{24i}) \quad (5.9)$$

$$s_i = \frac{\sum_{i=1}^{365} S_i}{\sum_{i=1}^{365} Vol_{24i}} \quad (5.10)$$

where:
Vol_{24i} = interchange non-freeway traffic on day i (crossing road and off-ramp traffic), veh/24h,

$CrossVol_{24}$ = AADT on the crossing road, veh/24h,
$RampVol_{24}$ = sum of AADT on the two off-ramps, veh/24h,
DF_i = traffic adjustment factor applicable to day i,
S_i = total stops on the interchange on day i,
$\beta_0, \beta_1, \beta_2$ = stops model parameters
s_i = average stops per vehicle on day i.

5.4 Longest Queue on Off-Ramps and Crossing Road

The physical queue length at the external approaches of a crossing road was useful in evaluating the risk of blocking the adjacent non-freeway intersections by the queue spillback from the considered alternative. Moreover, the length of the ramp was a critical design factor - for avoiding a dangerous queue spillback onto the freeway through-lanes. This is a valuable tool for evaluating the risk of queue spillback when the ramp length is known.

5.4.1 Queue Model Development

The longest queues on the off-ramps or crossing road during the busiest 15-min of the morning and afternoon peak hours were predicted using a log-normal regression model. The longest queue on the off-ramps or crossing road during the busiest 15-min of the morning and afternoon peak hours was used as a dependent variable. The crossing road and ramp rush hour volumes were the two variables that were used to predict the queue length. The residual plots did not exhibit any pattern; therefore, other functional forms were not investigated.

$$q_r = \exp(\beta_0 + \beta_1 \cdot CrossVol_h + \beta_2 \cdot RampVol_h) \quad (5.11)$$

$$q_c = \exp(\beta_0 + \beta_1 \cdot CrossVol_h + \beta_2 \cdot RampVol_h) \quad (5.12)$$

where:
q_r, q_c = longest queue on the off-ramp and crossing road,
$CrossVol_h$ = crossing-road volume during morning or afternoon rush hour (veh/h),
$RampVol_h$ = ramp volume during morning or afternoon rush hour (veh/h),
$\beta_0, \beta_1, \beta_2$ = parameters of the model for a maximum queue on an off-ramp and crossing-road.

Table 5.6 and Table 5.7 show examples of the longest queue models on the off-ramp and crossing road,

TABLE 5.6
Example of longest queue on off-ramp model

Variable	DF	Parameter Estimate	Standard Error	t Value	Pr > |t|
Intercept	1	3.61127	0.05122	70.50	<.0001
$CrossVol_h$	1	0.30853	0.03047	10.12	<.0001
$RampVol_h$	1	1.04592	0.04356	24.01	<.0001
Number of Observations	958 (964)				
R-Square	0.7444				
Adj R-Sq	0.7439				

TABLE 5.7
Example of longest queue on crossing model

Variable	DF	Parameter Estimate	Standard Error	t Value	Pr > |t|
Intercept	1	3.22664	0.05751	56.11	<.0001
$CrossVol_h$	1	0.90215	0.03443	26.20	<.0001
$RampVol_h$	1	0.47949	0.04928	9.73	<.0001
Number of Observations	963 (964)				
R-Square	0.8338				
Adj R-Sq	0.8335				

respectively. These two variables were positively related to the dependent variable, which means that the probability of having a longer queue increased with an increased rush hour volume. The crossing road volume had a greater impact on the longest queue crossing road than the off-ramp volume and vice versa.

The model indicated good fitness with an R^2 of 0.74 for the off-ramp model and 0.83 for the crossing road model. It should be mentioned that the R^2 of the off-ramp longest queue models was around 0.75 for all the geometry cases of the alternative interchanges, while the crossing road longest queue models were about 0.80 R^2.

5.4.2 Queue Model Implementation

Graphs of the longest queue were generated for the range of non-freeway rush hour flow rates and the various percentages of ramp flow rate u_r. Rush hour represents the design hour in the analysis year, which can be the hour with the 30 highest hourly volume (30 HV) during the analysis year or a selected rush hour that represents the design hour. Although typically the 30th highest hourly volume is assumed, other ranks are also used. The longest queue length expected on the off-ramps or crossing road was calculated as:

$$q_r = \exp(\beta_0 + \beta_1 Vol_h(1-u_r) + \beta_{m2} Vol_h u_r) \quad (5.13)$$

$$q_c = \exp(\beta_0 + \beta_1 Vol_h(1-u_r) + \beta_{m2} Vol_h u_r) \quad (5.14)$$

where:

q_r, q_c = 15-min maximum queue on off-ramp or crossing road,

Vol_h = total hourly volume on the non-freeway part of the interchange (crossing road and off-ramps) during

a selected rush hour that represents the design hour in the analysis year (veh/h),

u_r = proportion of the non-freeway traffic on off-ramps,

$\beta_0, \beta_1, \beta_2$ = model parameters.

6. DISCUSSION

The 13,440 simulation scenarios in this study included six alternative designs, five lane alternatives, 12 various non-freeway AADT, and 40 traffic patterns for four-lane crossing roads as well as additional scenarios for six-lane crossing roads. Due to the large number required, the simulations were run and the simulated outputs were post-processed into final samples for statistical modeling with limited human participation and computer applications developed for the project.

The statistical models were developed and applied to summarize the simulation results into a convenient format. Graphs were used to directly compare the MOE values of the five diamond alternatives under specific traffic and geometric scenarios. The following five MOEs are presented in the graphs.

1. Daily-average interchange delay represents the overall performance of the interchanges and allows estimation of the user costs.
2. Daily-average number of stops per vehicles on the interchange represents the overall performance of the interchanges and allows estimation of the user costs.
3. Average delay of the critical movement considers the performance of the weakest component of the interchange and its capacity failure.
4. Longest queue on the off-ramps during a rush hour checks whether or not this queue interferes with the high-speed traffic on the freeway mainline lanes.
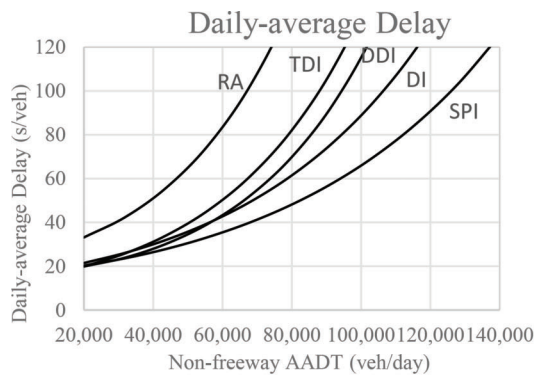
(a) Off-ramp share=30%
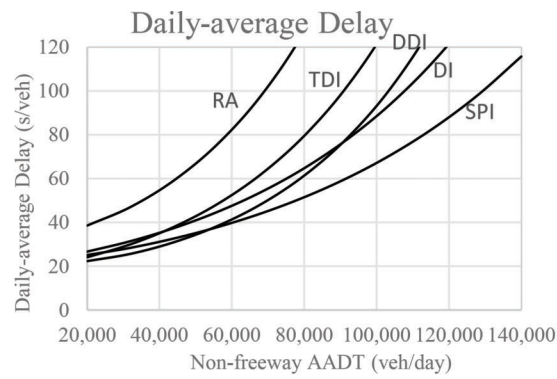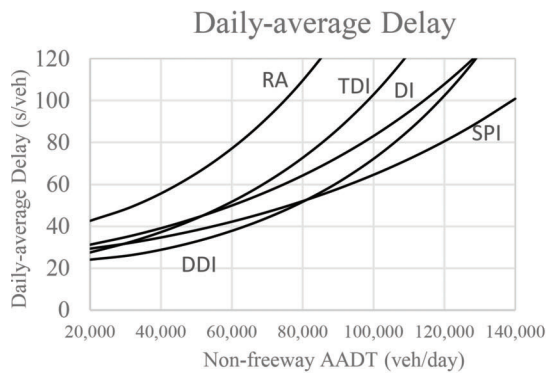
(b) Off-ramp share=40%
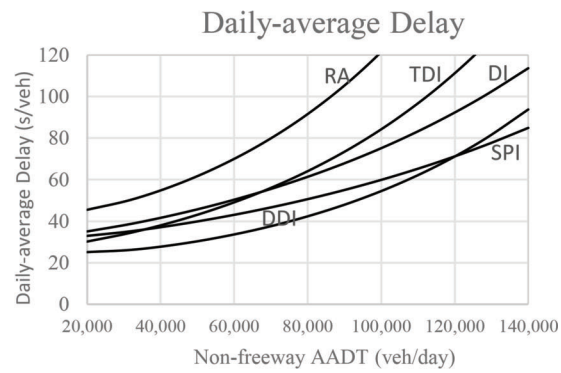
(c) Off-ramp share=50%

(d) Off-ramp share=60%

Figure 6.1 (a-d) Example presentation of the intersection delay.

5. Longest queue on the crossing road to check if the interchange traffic affects operations of the adjacent intersections.

Examples of the results presented in the Guidelines (Volume 2 of this report) are shown in Figure 6.1 through Figure 6.5.

6.1 Daily-Average Delay

Figure 6.1 presents the annual-average interchange delay as a function of the non-freeway AADT. Several such graphs are available for different distributions of traffic between the crossing road and the off-ramps. Overall, the SPI has the lowest delay across different percentages of off-ramp share of non-freeway AADT. The TDI has the highest average delay among the signalized interchanges. The roundabout interchanges have the highest average delay among all the interchange types.

All the interchanges exhibited a tendency toward lower average delays with increasing off-ramp shares under fixed total non-freeway volumes; and this tendency was especially strong for SPI and DDI. DI performed better than DDI when the non-freeway traffic from the off-ramps was up to 30% while DDI

outperformed DI when the off-ramp traffic share increased beyond 30%. Further, when the off-ramp share reached 60%, DDI performed better than SPI up to 120,000 non-freeway AADT. This improvement of DDI performance with a growing off-ramp traffic share is the result of the DDI control that preferentially treats off-ramp traffic. This control makes the DDI perform better than other interchange types when the traffic is balanced between the crossing road and the off-ramps, particularly when the traffic on the off-ramps is heavier than on the crossing road. Several previous researchers, such as (Siromaskul, 2010; Siromaskul & Septh, 2008), also confirmed that DDI experienced lower delays when the ramp interchange traffic was heavy. Overall, there was a tendency toward a growing average delay at 20,000 veh/day with increasing ramp shares.

6.2 Critical Movement Delay and Level of Service

Figure 6.2 presents the critical movement delay as well as the corresponding LOS during the busiest 15-min interval of a rush hour. An 80 seconds for signalized and 50 seconds for unsignalized intersections corresponded to LOS F, at which time the interchange experienced capacity failure. The graphs indicate that SPI had the

(a) Off-ramp share=30%

(b) Off-ramp share=40%

(c) Off-ramp share=50%

(d) Off-ramp share=60%
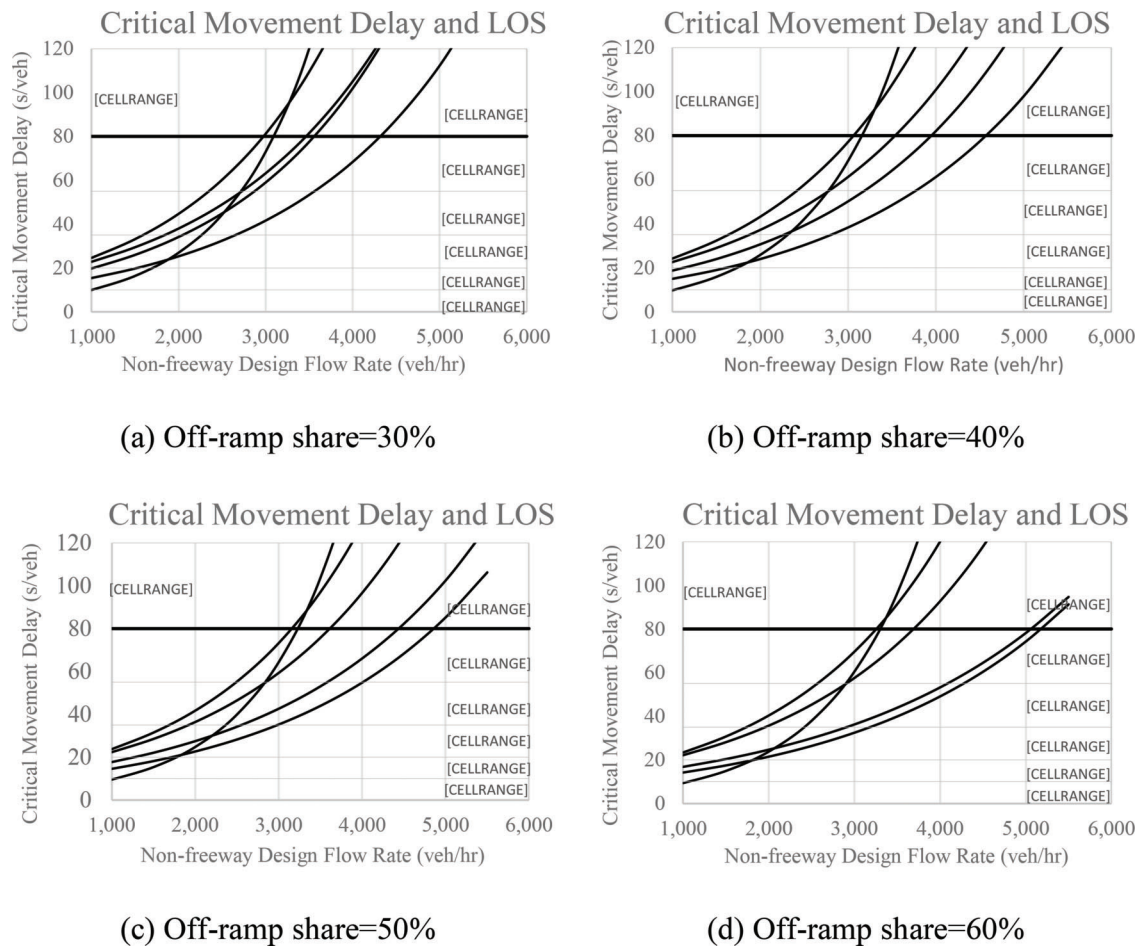
Figure 6.2 **(a-d)** Example presentation of the delay at the critical movement.

highest capacity at all the investigated off-ramp traffic shares. The TDI and roundabout interchanges had the lowest capacity among the studied interchange types. Signalized interchanges exhibited a tendency of decreasing critical movement delay with an increasing off-ramp volume share in non-freeway traffic. This tendency was very strong for SPI and DDI where the capacity failure occurred at 3,500 veh/hr and 30% off-ramp traffic share and at over 5,000 veh/hr at 60% off-ramp traffic share, respectively. This tendency indicated that these two interchanges effectively accommodated the off-ramp volume and also performed well in the balanced traffic flow conditions. The critical movement delay was not affected by the off-ramp traffic share at roundabout interchanges.

6.3 Daily-Average Stops

Figure 6.3 presents the daily-average number of stops per vehicle at an interchange as a function of the non-freeway AADT for various off-ramp traffic shares. SPI had the lowest number of stops except under very low traffic conditions, which was when the roundabouts performed better. This result was not surprising because all the movements in a SPI pass no more than one location where traffic control may

interrupt the motion. Only in low traffic conditions did roundabouts experience lower numbers of stops than all the other diamond interchanges. In rural locations with a low traffic volume up to 30,000 non-freeway AADT, roundabouts were the best alternative in terms of the average number of stops. On the other hand, the number of stops on roundabouts was now growing faster than on other types of diamonds due to the low capacity of the roundabout diamonds, leading to long queues and multiple stops in heavier traffic.

Signalized interchanges tended to have lower average stops when the off-ramp volume increased. This tendency was very strong in SPI and DDI. DI and DDI had almost identical numbers of average stops at 30% off-ramp share, but with an increasing off-ramp share, DDI outperformed DI. At 60% off-ramp share, DDI and SPI had similar numbers of average stops up to 80,000 non-freeway AADT. Daily-average stops on roundabout interchange were not affected by the off-ramp volume share.

6.4 Longest Off-ramp Queue

A sufficient length of off-ramp that accommodates long vehicle queues stretching from the off-ramp

(a) Off-ramp share=30%

(b) Off-ramp share=40%

(c) Off-ramp share=50%

(d) Off-ramp share=60%
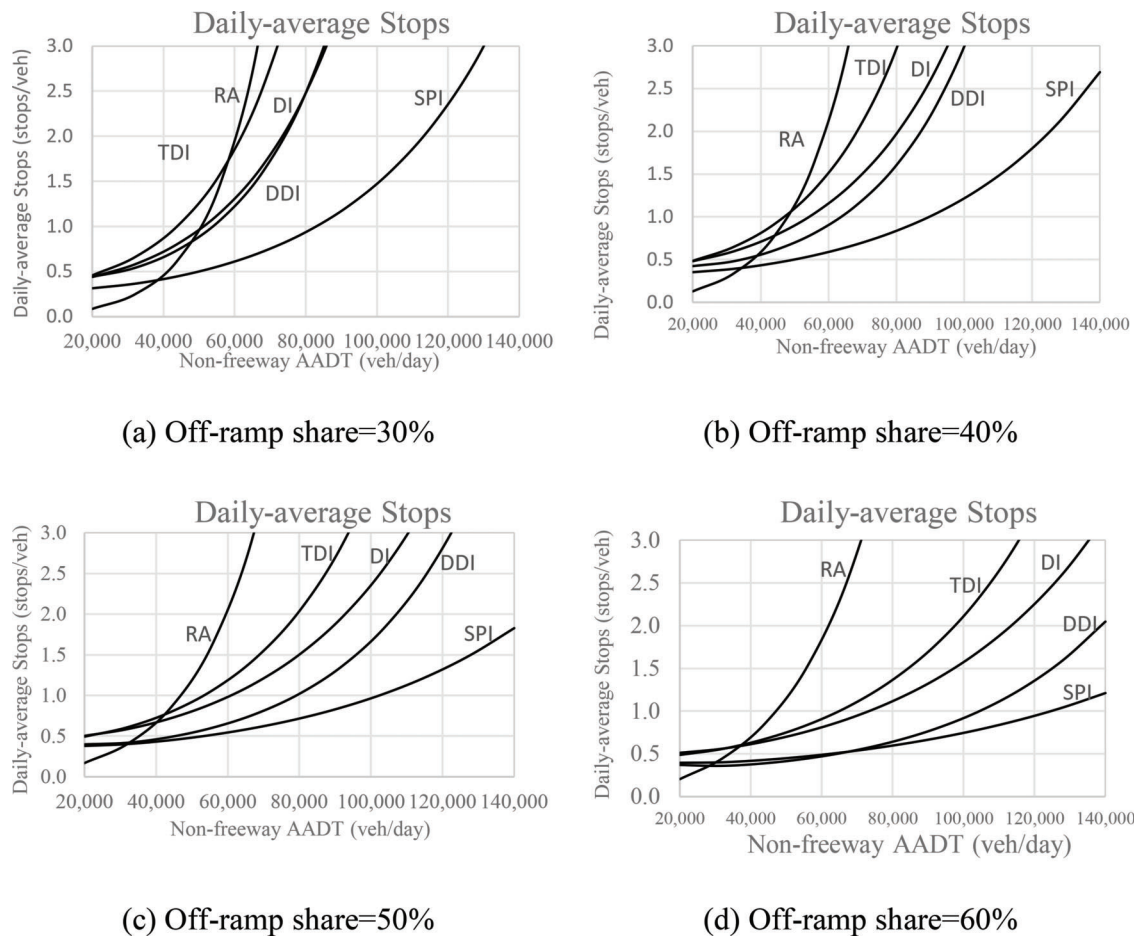
Figure 6.3 (a-d) Example presentation of the number of stops per vehicle.

intersection with the crossing road is critical for safe traffic operations in the freeway area upstream of the ramp gore point. Thus, selection of the proper interchange type is particularly important when the length of the off-ramp is restricted by local conditions. On a typical diagonal ramp with a diamond interchange, a good rule of thumb for a ramp proper is 1,500 feet from the crossing road to the gore. However, in constrained urban conditions they can decrease to 1,000 feet or even 800 feet.

The graphs in Figure 6.4 present the longest queue length during the busiest 15-min interval of a rush hour and indicate that the DDI had the shortest queue across the studied off-ramp traffic shares and at different levels of non-freeway AADT. On the other hand, the roundabout interchanges had the longest queues among all the interchange types. These results were consistent with the lowest capacity and the highest delay at this type of interchange.

The graphs in Figure 6.4 also confirmed that as the off-ramp traffic share increased, the queue length grew on the off-ramps of all the alternative interchanges. Designers should compare the longest off-ramp queue length with the distance from the off-ramp stop line to the point beyond which the safety impact of the queue is expected. There are two possible solutions if this

problem is detected: (1) extend the length of the ramp and (2) use a service interchange with shorter off-ramp queues.

6.5 Longest Crossing Road Queue

Closely spaced intersections around diamond interchanges are common in urban areas. Long queues on the non-freeway crossing road may interfere with traffic on the crossing road intersections adjacent to the interchange. The possibility of such an undesirable effect may be detected by comparing the queue lengths on the crossing road with the available distance between the intersections. A vehicle is assumed moving in a queue if its speed is lower than 10 mph. The graphs in Figure 6.5 provide useful information about the position of the end of the longest queue length expected during the busiest 15 min of the rush hour in the analysis year. The queue end position is measured from the center of the interchange area. This length may be compared to the distance between the center of the interchange and the adjacent intersection.

Figure 6.5 presents the queue lengths on the crossing road as a function of the non-freeway peak flow rate during the rush hour. The graphs indicate that the single point interchange had the shortest crossing

Off-ramp Longest Queue

(a) Off-ramp share=30%

(b) Off-ramp share=40%

(c) Off-ramp share=50%

(d) Off-ramp share=60%
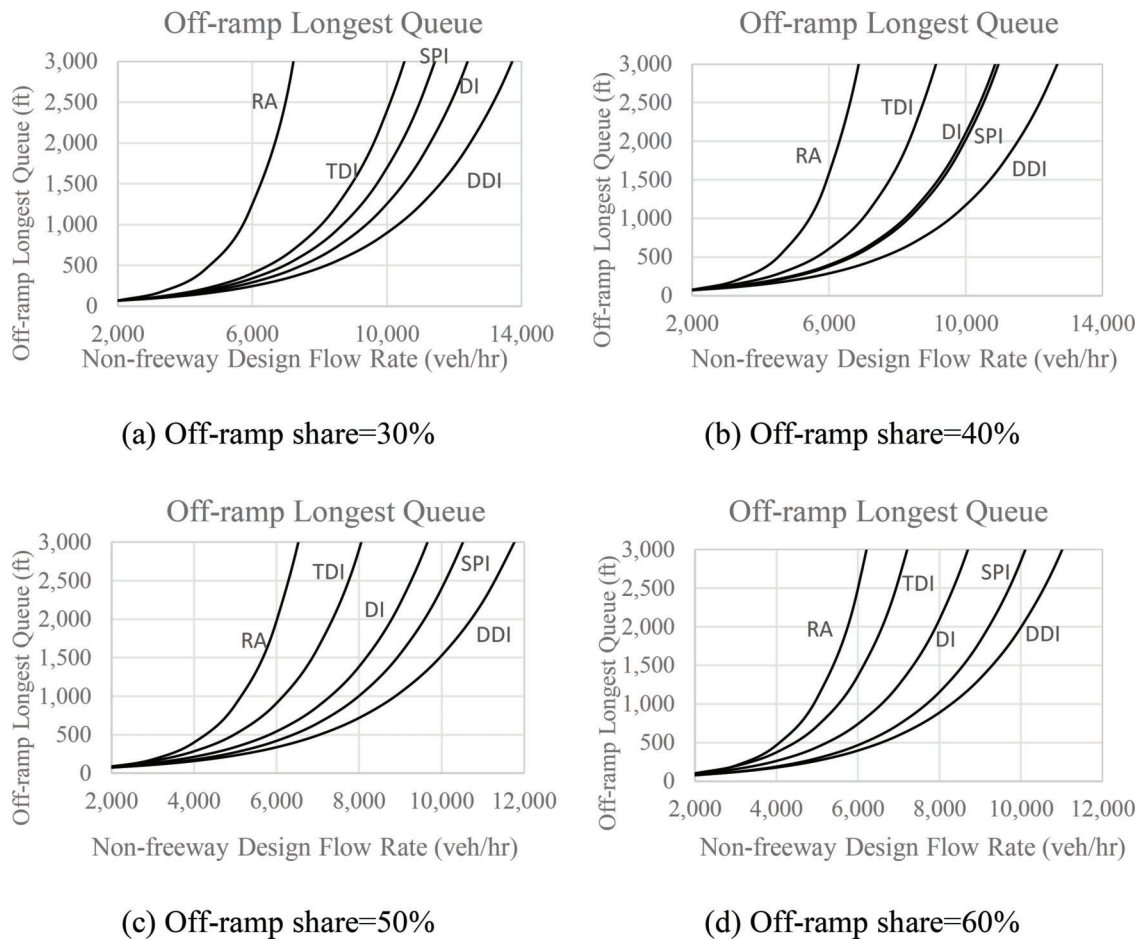
Figure 6.4 **(a-d)** Example presentation of the longest queue on off-ramp.

road queue in various ranges of off-ramp traffic share and at different levels of non-freeway AADT except the 60% off-ramp traffic share. The roundabout interchanges had the longest queue among all the interchange types. An increase in the off-ramp traffic share led to a decrease in the crossing road queue length. DD exhibited this tendency to the strongest extent; previous researchers (Siromaskul, 2010; Siromaskul & Septh, 2008) also confirmed that the most beneficial scenario for the crossing road queues occurred when the ramp interchange traffic was heavy.
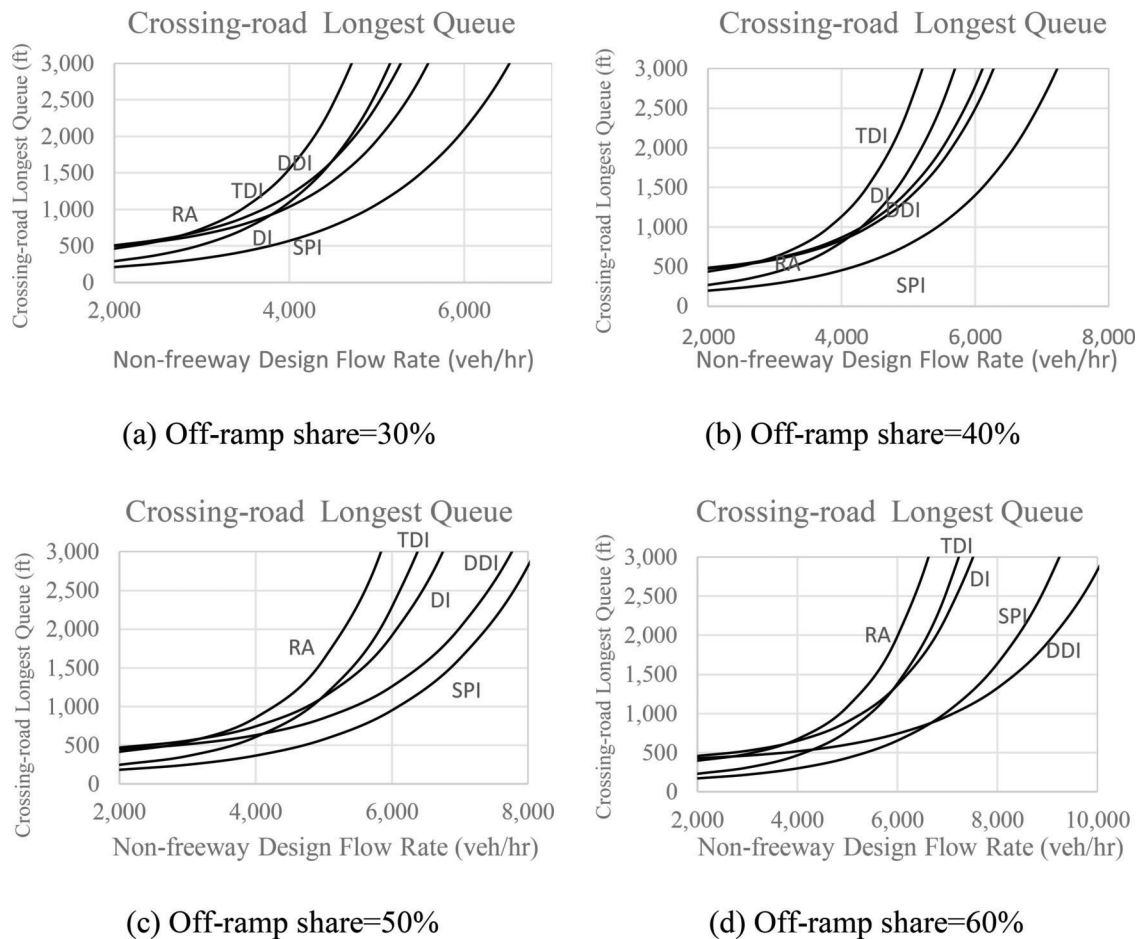
Figure 6.5 (a-d) Example presentation of the longest queue on crossing road.

7. CONCLUSIONS

7.1 Summary

Micro-simulation offers the possibility of evaluating the performance of alternative DIs prior to their construction. Preparing the needed input to simulate preliminary designs of multiple interchanges is time consuming. The purpose of this study was to help designers and planners in the early stage of screening various solutions to identify a few reasonable and feasible forms to reserve for detailed operational analysis. Thirteen thousand simulations of alternative diamond designs were conducted under various geometric and traffic conditions. This report discussed the results, which were also presented in graphical form.

The traffic at 200 Indiana service interchanges was classified into a number of AADT ranges and traffic scenarios that reflected the various shares of traffic movements and their fluctuation during a day. All the alternative interchanges were simulated in the same rectangular area using the Indiana-specific model parameters. The alternative interchanges were compared against five performance measures: (1) LOS of the critical movement, (2) daily-average delay, (3) daily-average number of stops per vehicle, (4) longest queue length on an off-ramp, and (5) longest queue length on a crossing road.

The daily-average delay in non-freeway traffic represents the overall performance of the interchange. The average delay supplemented with the average number of stops can be used to estimate the operational cost of the interchange.

Delays were simulated for ten non-freeway traffic movements. The critical movement with the highest delay and the lowest LOS served as an indicator of the interchange capacity failure if it reached level F.

The longest queues on the crossing road and on the off-ramps determined the "operational footprint" of the interchange. Queue spillback onto the freeway mainline lanes indicated a serious safety problem while queue spillback to the adjacent intersections indicated the undesirable blocking of these intersections and their subsequent poor performance.

Statistical models were developed to predict the five performance measures based on the simulated inputs. **The results are presented graphically in the proposed guidelines (Volume 2 of this report)**. The results exhibit that none of the alternative interchanges were superior across the five performance measures and traffic conditions of the off-ramp and crossing road. Overall, SPI tended to performs better than the other interchanges but was outperformed by DDI depending on the traffic condition. Conventional DI did not outperform SPI

and DDI. TDI performed worst among the signalized interchanges and across all the performance measures and off-ramp traffic shares. Roundabout interchanges proved to be the best solutions at the low non-freeway AADT locations and their performance was only weakly affected by the off-ramp traffic share.

The research conducted and the knowledge acquired in this study will be useful for selecting good alternative interchanges that perform satisfactorily for given geometric and traffic conditions. These results were implemented as Guidelines (Volume 2 of this report) in the form of a complete set of graphs for a wide range of geometric and traffic scenarios. The guidelines should be used to select reasonable alternatives for further analysis and detailing. The final selection should be supported with micro-simulation of the preliminarily designed alternatives and supplemented with discussion of other implications of the local conditions and agency cost for construction along with other factors considered in such decision making which was not included in the simulation results.

7.2 Findings

The obtained daily-average delays at the alternative interchanges were consistent with expectations. Roundabouts had the highest average delay across all the off-ramp and crossing road traffic shares; TDI had the second highest average delay; and with an increase in the off-ramp volume share, DDI exhibited a lower average delay. Overall, SPI had the lowest average delay among all the alternatives.

Roundabouts had the lowest number of average stops among all the alternatives up to 30,000 non-freeway AADT across all the off-ramp and crossing road traffic shares. DI, TDI, and roundabouts had almost double the number of stops of DDI and SPI. With an increase in the off-ramp traffic share, DDI exhibited a smaller numbers of stops. Overall, SPI had the lowest number of average stops among all the alternatives.

Roundabouts outperformed DI and TDI in terms of critical movement delay for 20 and 30 percent off-ramp volumes in the lower range of non-freeway flow rates. With the increased share of off-ramp traffic, DDI exhibited lower critical movement delays. With 50 percent and 60 percent off-ramp shares, DDI exhibited lower critical movement delays than SPI.

DDI had the shortest and roundabouts had the longest queues on the off-ramp among all the alternatives across all the off-ramp and crossing road traffic shares. With an increased share of off-ramp traffic, SPI exhibited queues on off-ramps shorter than DI and TDI.

TDI had shorter queues on the crossing road DDI, DI, and roundabouts up to 2,500 veh/hr across all the off-ramp and crossing road traffic shares. With the increased share of off-ramp traffic, DDI exhibited shorter queues on the crossing road. Overall, SPI had the shortest queues among all the alternatives.

7.3 Future Research Needs

The alternative diamond interchanges were investigated in this study as isolated from the surrounding road network. It is likely that an interchange with closely spaced surface intersections performs differently than an isolated interchange. Although investigation of this effect is difficult due to the enormous number of possible cases, even a limited study may help assess how much the relative comparison of isolated alternative diamonds remains applicable under the presence of closely spaced surface intersections.

The safety of the alternative diamond forms could not be included in this study due to the lack of a suitable research method. Such a study should be undertaken in the future when the studied forms of diamond interchanges are constructed and the crash data or other surrogate traffic safety data are available.

REFERENCES

AASHTO. (2001). *A policy on geometric design of highways and streets* (4th ed., p. 158). Washington, DC: American Association of State Highway and Transportation Officials.

Afshar, A. M., Bared, J. G., Wolf, S., & Edara, P. K. (2009). Traffic operational comparison of single-point and diverging diamond interchanges (No. 09-2939). In *TRB 88th annual meeting compendium of papers DVD*. Washington, DC: Transportation Research Board.

Bared, J. G., & Kaisar, E. I. (2000, June 14–17). Comparison of diamond interchanges with roundabout interchanges (No. FGSV 002/67, pp. 513–521). In *2nd International Symposium on Highway Geometric Design*. Cologne, Germany: Forschungsgesellschaft fur Strassen- und Verkehrswesen (FGSV) [Road and Transportation Research Association].

Bared, J., Edara, P., & Jagannathan, R. (2005). Design and operational performance of double crossover intersection and diverging diamond interchange. *Transportation Research Record: Journal of the Transportation Research Board*, (1912), 31–38.

Benoit, K. (2011). *Linear regression models with logarithmic transformations*. London, England: London School of Economics. Retrieved from Lecture Notes Online Web site http://www.kenbenoit.net/courses/ME104/logmodels2.pdf

Bonneson, J. A., & Messer, C. J. (1989). *A national survey of single point urban interchanges* (Report No. TTI-2–18–88–1148–1). College Station, TX: Texas Transportation Institute.

Bonneson, J., & Lee, S. (2002). Technique for comparing operation of alternative interchange types. *Transportation Research Record: Journal of the Transportation Research Board*, (1802), 7–15. https://doi.org/10.3141/1802-02

Chilukuri, V., Siromaskul, S., Trueblood, M., & Ryan, T. (2011). *Diverging diamond interchange: performance evaluation (I-44 and Route 13)* (No. OR11-012). Retrieved from https://library.modot.mo.gov/RDT/reports/TRyy1013/or11012.pdf

Chlewicki, G. (2003, July). New interchange and intersection designs: the synchronized split-phasing intersection and the diverging diamond interchange. In *2nd Urban Street Symposium: Uptown, Downtown, or Small Town: Designing Urban Streets That Work*, Anaheim, CA.

Click, S., Berry, C., & Mahendran, A. (2010). Evaluation of traditional and nontraditional interchange treatments to preserve service life of narrow over-and underpass roadways. *Transportation Research Record: Journal of the Transportation Research Board*, (2171), 21–32.

Day, C., Premachandra, H., Brennan Jr, T., Sturdevant, J., & Bullock, D. (2010). Operational evaluation of wireless magnetometer vehicle detectors at signalized intersection. *Transportation Research Record: Journal of the Transportation Research Board*, (2192), 11–23.

Fang, C. F. (2008). Simulation modeling of traffic operations at single point and diamond urban interchanges. In *Logistics: The emerging frontiers of transportation and development in China* (pp. 3810–3815). Reston, VA: American Society of Civil Engineers.

FHWA. (2012). *Interchange design (new construction and reconstruction) prompt-list for assessing key geometric features*. Retrieved from http://www.fhwa.dot.gov/modiv/programs/intersta/docs/interchange_design_promptlist.pdf

Fowler, B. (1993). An operational comparison of the single-point urban and tight-diamond interchanges. *ITE Journal*, *64*(4), 19–26.

Garber, N. J., & Fontaine, M. D. (2000, June 14–17). Guidelines for the selection of the optimum interchange type for a specific location. In *2nd International Symposium on Highway Geometric Design* (No. FGSV 002/67), Mainz, Germany.

Gitbooks. (2015). *Double and single roundabout interchanges*. Retrieved from https://attap.gitbooks.io/muid/content/grade-separated_&_unsignalized/double_roundabout_interchange.html

Hainen, A. M., Stevens, A. L., Day, C. M., Li, H., Mackey, J., Luker, M., & Bullock, D. M. (2015). Performance measures for optimizing diverging interchanges and outcome assessment with drone video. *Transportation Research Record: Journal of the Transportation Research Board*, (2487), 31–43.

Hughes, W., Jagannathan, R., Sengupta, D., & Hummer, J. E. (2010). Alternative intersections/interchanges: Informational report (AIIR) (No. FHWA-HRT-09-060). Retrieved from https://www.fhwa.dot.gov/publications/research/safety/09060/

Hunter, M. (n.d.). *Actuated signal control manual*. Retrieved from http://transportation.ce.gatech.edu/sites/

INDOT. (2002). *Indiana interchange planning study: Final summary report*. Indianapolis, IN: Parsons Brinckerhoff (in association with Bernardin Lochmueller & Associates, Inc. and Cambridge Systematics, Inc.)

INDOT. (2014). *Latest INDOT traffic adjustment factors*. Retrieved August 16, 2016, from https://www.in.gov/indot/files/TrafficStatistics_2014_AADT_AdjustementFactors_06102015.pdf

Jones, E., & Selinger, M. (2003). Comparison of operations of single-point and tight urban diamond interchanges. *Transportation Research Record: Journal of the Transportation Research Board*, (1847), 29–35. https://doi.org/10.3141/1847-04

LeBas, M. A. (2015). *A comparative analysis of roundabouts and traffic signals through a corridor* (Doctoral dissertation). Louisiana State University, Baton Rouge, LA. Retrieved from http://digitalcommons.lsu.edu/gradschool_theses/3753/

Leisch, P., Urbanik, T., & James, P. O. (1989). A comparison of two diamond interchange forms in urban areas. *ITE Journal*, *5*(59), 21–27.

Leong, L. V., Mahdi, M. B., & Chin, K. K. (2015). Microscopic simulation on the design and operational performance of diverging diamond interchange. *Transportation Research Procedia*, *6*, 198–212.

Li, Z., DeAmico, M., Chitturi, M. V., Bill, A. R., & Noyce, D. A. (2013). Calibrating VISSIM roundabout model using a critical gap and follow-up headway approach (RS4C 2013). In *Road safety on four continents: 16th international conference, Beijing, China, 15-17 May 2013. Proceedings.*

Linköping, Sweden: Swedish National Road and Transport Research Institute (VTI).

Matin, S. & Tarko, A. P. (2015). Capacity-related driver behavior on roundabouts built on high-speed roads (No. 15-3150). In *TRB 94th annual meeting compendium of papers*. Washington, DC: Transportation Research Board.

Nelson, E. J., Bullock, D., & Urbanik, T. (2000). Implementing actuated control of diamond interchanges. *Journal of Transportation Engineering*, *126*(5), 390–395.

Nichols, A. P., & Bullock, D. M. (2001). *Design guidelines for deploying closed loop systems*. Retrieved from http://docs.lib.purdue.edu/cgi/viewcontent.cgi?article=1520&context=jtrp

Perez-Cartagena, R. I., & Tarko, A. P. (2004). *Predicting traffic conditions at Indiana signalized intersections*. Retrieved from http://docs.lib.purdue.edu/cgi/viewcontent.cgi?article=1642&context=jtrp

PTV. (2014). VISSIM 7.4 User Manual.

Qureshi, M., Spring, G., Lasod, R., & Sugathan, N. (2004). *Design of single point urban interchanges* (No. RDT 04-011). Retrieved from https://library.modot.mo.gov/RDT/reports/RI02015/RDT04011.pdf

SAS Institute. (2016). *SAS user's guide* (Release 9.4). Cary, NC: SAS Institute Inc.

Sharma, S., & Chatterjee, I. (2007). Performance evaluation of the diverging diamond interchange in comparison with the conventional diamond interchange. In *Compendium of student papers presented at the Transportation Scholars Conference, Iowa State University, November 9, 2007*. Ames, IA: Iowa State University.

Sharp, W. H., & Selinger, M. J. (2000). Comparison of SPUI & TUDI interchange alternatives with computer simulation modeling. In *ITE 2000 annual meeting: Compendium of technical papers*. Washington, DC: Institute of Transportation Engineers.

Siromaskul, S. (2010, August 8–11). Diverging diamond interchange design 101: Things to know before you start. In *ITE 2010 annual meeting and exhibit*. Washington, DC: Institute of Transportation Engineers.

Siromaskul, S., & Speth, S. B. (2008). A comparative analysis of diverging diamond interchange operations. In *ITE 2008 annual meeting and exhibit: Compendium of technical papers*. Washington, DC: Institute of Transportation Engineers.

Smith, M., & Garber, N. (1998). Guidelines for selecting single-point urban and diamond interchanges: Nationwide survey and literature review. *Transportation Research Record: Journal of the Transportation Research Board*, (1612), 48–54. https://doi.org/10.3141/1612-07

Sunkari, S. R., & Urbanik, I. I. (2000). *Signal design manual for diamond interchanges* (No. FHWA/TX-01/1439-6). College Station, TX: Texas Transportation Institute, Texas Department of Transportation and Federal Highway Administration. Retrieved from http://static.tti.tamu.edu/tti.tamu.edu/documents/1439-6.pdf

Tarko, A. P., Inerowicz, M., & Lang, B. (2008). *Safety and operational impacts of alternative intersections* (Joint Transportation Research Program Publication No. FHWA/IN/JTRP-2008/23). West Lafayette, IN: Purdue University https://doi.org/10.5703/1288284314313

TRB. (2010). *Highway capacity manual*. Washington, DC: Transportation Research Board.

APPENDIX A: MODEL JUSTIFICATION

Roundabout Model Estimation

The traffic control and operation of the DRI and the SRI were identical in this study. As a result, the reported performance for the two roundabouts also were similar. The statistical models of the performance measures had very similar coefficient estimates; therefore, a simple T-test was performed in order to check whether or not the coefficients of the two models were identical. None of the performance measures of the two roundabout models had significant T-test values to indicate that the models should be separated so the single and double roundabout performance prediction models were combined. Table A.1 shows the t-test results for the critical movement delay model for the single and double roundabouts.

Justification for Reduced Model for Critical Movement Delay

The average delay on the critical movement full model consisted of all the traffic movement volumes from the crossing road and off-ramps. The reduced model had two variables: the combined volumes from the traffic movements of the crossing road and off-ramps. The off-ramp traffic volume indicated a negative correlation with the critical movement delay for DDI. The relationship between the off-ramp volume and the critical movement delay is complex. Depending on the traffic pattern for a certain level of non-freeway ADT, the critical movement may switch from the crossing road movements to the off-ramp movements. The traffic volume itself has an impact on the delay and it also affects the delay through signal timing, which can lead to seemingly counterintuitive results. To confirm this phenomena, the full model was run to determine if there was any systematic bias for predicting the critical movement delay. Figure A.1 shows the average delay on the critical movement from the full model and the reduced model.

For simplicity and practicality in the procedure, the reduced models were used to generate the graphs, but full models should be used for specific situations. Table A.2 shows the full model results for the DDI. The full model consists of all ten interchanges movement volumes.

Table A.3 shows that a log linear relationship between the crossing road volume, off-ramp volume, and critical movement delay in both the full and reduced models. The difference between the r-square of the full model and the reduced model was small.

Justification for Reduced Model for Stops

The full model, which determined the total number of stops for the entire interchange during a 24-hour period, consisted of all the traffic movement volumes from the crossing road and the off-ramps as independent variables. The reduced model had only two variables combining the traffic movements of the crossing road and off-ramps. The off-ramp traffic volume indicated a negative correlation with the total number of stops. This relationship between the off-ramp volume and the total number of stops was very complex. The traffic volume itself had an impact on the total number of stops and also affected the total number of stops through the signal timing. These totals led to seemingly counterintuitive results. To confirm this phenomenon, the full model was run to confirm the existence of any systematic bias for predicting the critical movement delay. Figure A.2 shows the total number of stops from both the full and reduced models.

The reduced model was used to generate the reference graphs for this case study, but for specific projects, the full models should be used. Table A.4 shows the full model for the DDI. The parameters for NF1L, NF2R, and NF2L were set to 0 since the variables are a linear combination of other variables in the model.

Table A.5 shows that the relationship between the crossing road volume and the stops was log-linear and the off-ramp volume and stops were log-log in the reduced model. The relationship between the crossing road movement volumes, off-ramp volumes, and stops was log-linear in the full model. The difference between the r-square of the full model and the reduced model was negligible.

TABLE A.1
T-test for combining roundabout models

Critical Movement Delay Model: Double Roundabout					
Intercept	1	0.60582	0.10115	5.99	<.0001
CrossVol$_h$	1	2.2519	0.12477	18.05	<.0001
RampVol$_h$	1	1.11478	0.17865	6.24	<.0001
Critical Movement Delay Model: Single Roundabout					
Intercept	1	0.5325	0.10343	5.15	<.0001
CrossVol$_h$	1	2.09246	0.12814	16.33	<.0001
RampVol$_h$	1	1.4182	0.18328	7.74	<.0001
T-test for β					
t$_{int}$	$t\frac{\beta_1-\beta_2}{\sqrt{se_1^2+se_2^2}}$			0.506812	
T$_{CR}$	$t\frac{\beta_1-\beta_2}{\sqrt{se_1^2+se_2^2}}$			0.891472	
t$_{ramp}$	$t\frac{\beta_1-\beta_2}{\sqrt{se_1^2+se_2^2}}$			1.185493	
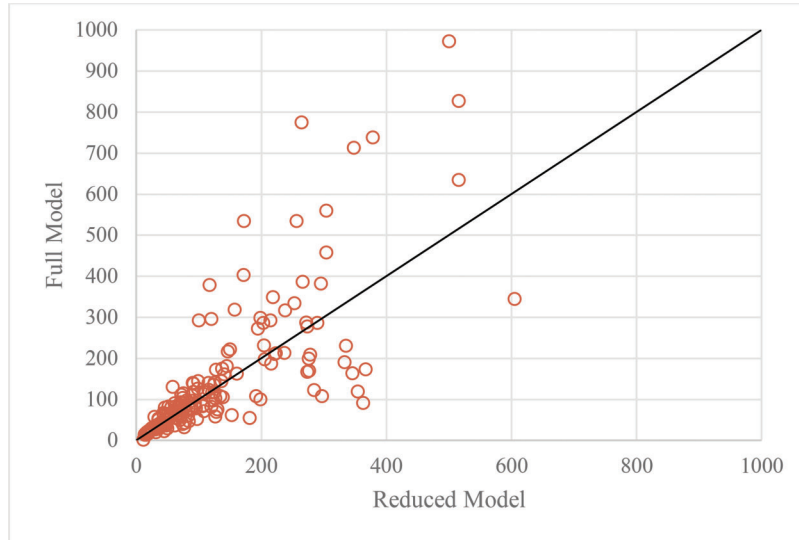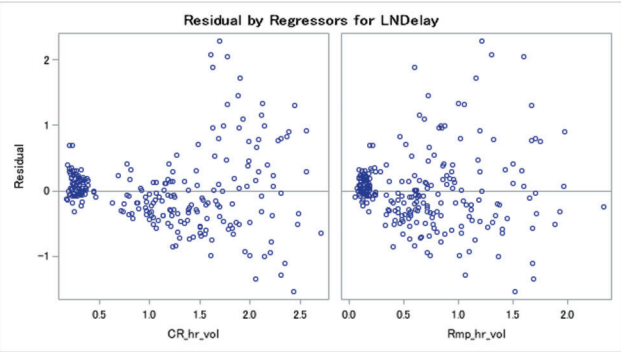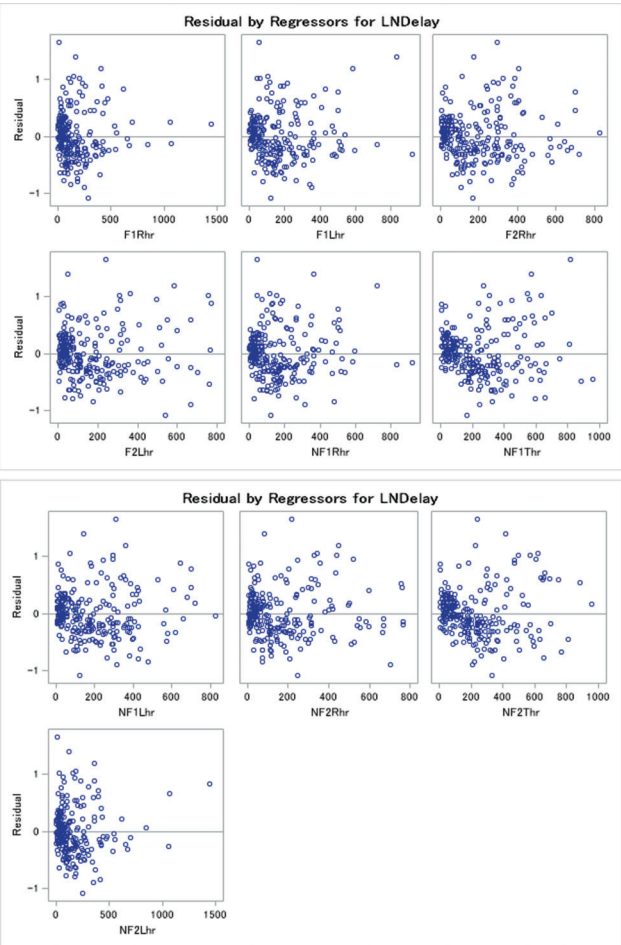
Figure A.1 Average delay on the critical movement

TABLE A.2
Example results of the full model of critical movement delay

Variable	DF	Parameter Estimate	Standard Error	t Value	Pr > |t|
Intercept	1	2.38066	0.05075	46.91	<.0001
$RampVol_{h(1R)}$	1	-0.00035136	0.00021912	-1.60	0.1102
$RampVol_{h(1L)}$	1	0.00142	0.00030971	4.57	<.0001
$RampVol_{h(2R)}$	1	-0.00102	0.00029043	-3.52	0.0005
$RampVol_{h(2L)}$	1	0.00214	0.00029041	7.36	<.0001
$CrossVol_{h(1R)}$	1	-0.00062838	0.00031155	-2.02	0.0448
$CrossVol_{h(1T)}$	1	0.00185	0.00023582	7.84	<.0001
$CrossVol_{h(1L)}$	1	0.00204	0.00030037	6.78	<.0001
$CrossVol_{h(2R)}$	1	-0.00101	0.00028529	-3.55	0.0005
$CrossVol_{h(2T)}$	1	0.00248	0.00023190	10.70	<.0001
$CrossVol_{h(2L)}$	1	0.00154	0.00021971	7.03	<.0001

Number of Observations	244
R-Square	0.878
Adj R-Sq	0.873

TABLE A.3
Fit diagnostics for reduced and full model of critical movement delay

Independent variable	Residual plot
$\log(D_{cm}) = CrossVol_h + RampVol_h$ Adj. $R^2 = 0.77$	
$\log(D_{cm}) = RampVol_{h(1R)} + RampVol_{h(1L)} + RampVol_{h(2R)} + RampVol_{h(2L)} + CrossVol_{h(1R)} + CrossVol_{h(1T)} + CrossVol_{h(1L)} + CrossVol_{h(2R)} + CrossVol_{h(2T)} + CrossVol_{h(2L)}$ Adj. $R^2 = 0.87$	
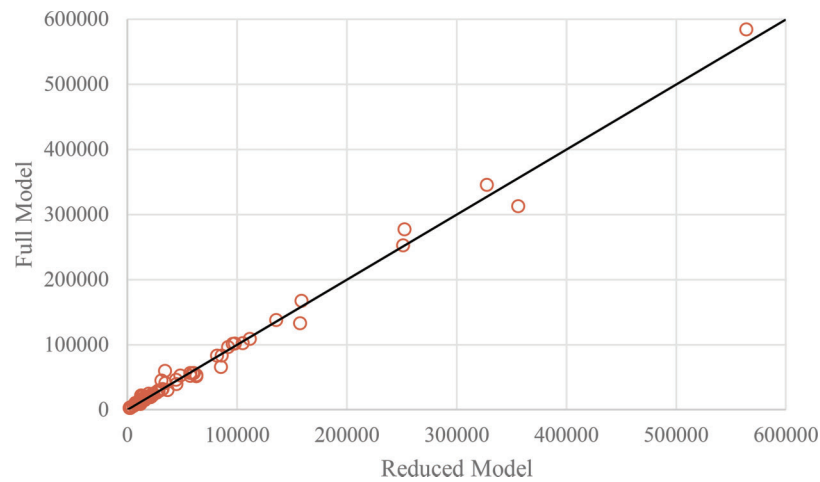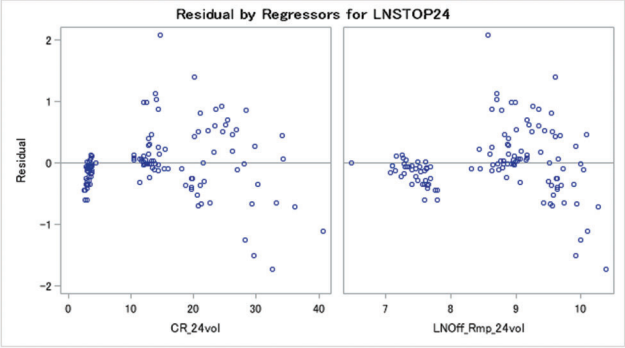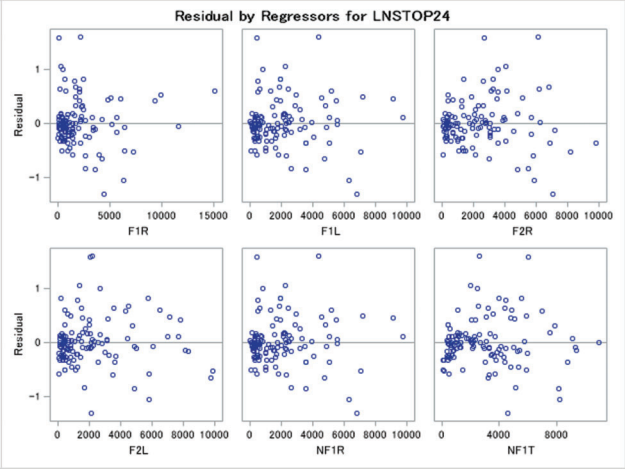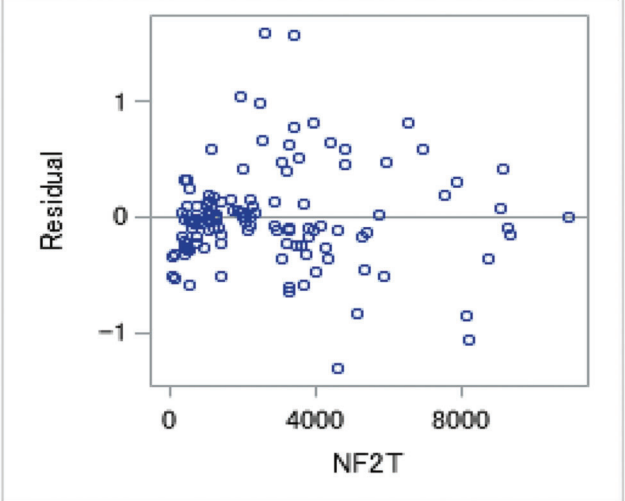
Figure A.2   Number of stops (stops/24 hour).

TABLE A.4
Example results of full model for total number of stops.

Variable	DF	Parameter Estimate	Standard Error	t Value	Pr > |t|
Intercept	1	7.47897	0.07258	103.04	<.0001
$\text{RampVol}_{h(1R)}$	1	0.00014915	0.00002084	7.16	<.0001
$\text{RampVol}_{h(1L)}$	1	0.00306	0.01251	2.24	0.08069
$\text{RampVol}_{h(2R)}$	1	0.00011502	0.00002778	4.14	<.0001
$\text{RampVol}_{h(2L)}$	1	0.00007394	0.00002293	3.22	0.0016
$\text{CrossVol}_{h(1R)}$	1	-0.00298	0.01251	-3.04	0.08119
$\text{CrossVol}_{h(1T)}$	1	0.00028874	0.00005789	4.99	<.0001
$\text{CrossVol}_{h(2T)}$	1	0.00010756	0.00005607	1.92	0.0576

Number of Observations	240
R-Square	0.9095
Adj R-Sq	0.9039

TABLE A.5
Fit diagnostics for reduced and full model of of a example case

Independent Variables	Fit Diagonostics
log(Stops)=CRvolume$_{24}$+Log(Rampvolume$_{24}$ Model R-sq=0.86	
log(S$_{24}$)=RampVol$_{h(1R)}$+RampVol$_{h(1L)}$+RampVol$_{h(2R)}$+ RampVol$_{h(2L)}$+CrossVol$_{h(1R)}$+CrossVol$_{h(1T)}$+CrossVol$_{h(2T)}$ Model R-sq=0.90	

APPENDIX B: STATISTICAL MODELS

Conventional Diamond Interchange

TABLE B.1
Delay Diamond CR2R1A2

Parameter	DF	Estimate	Standard Error	t Value	Pr > |t|
Intercept	1	5.06323	0.26333	19.23	<.0001
CrossVol$_{24}$	1	0.05472	0.00347	15.76	<.0001
RampVol$_{24}$	1	0.85538	0.03535	24.20	<.0001

Number of Observations	122
R-Square	0.9846
Adj R-Sq	0.9843

TABLE B.2
Delay Diamond CR4R1A4

Parameter	DF	Estimate	Standard Error	t Value	Pr > |t|
Intercept	1	4.20891	0.19514	21.57	<.0001
CrossVol$_{24}$	1	0.03168	0.00141	22.44	<.0001
RampVol$_{24}$	1	0.95532	0.02444	39.09	<.0001

Number of Observations	192
R-Square	0.9835
Adj R-Sq	0.9833

TABLE B.3
Delay Diamond CR4R2A2

Parameter	DF	Estimate	Standard Error	t Value	Pr > |t|
Intercept	1	4.23563	0.20778	20.38	<.0001
CrossVol$_{24}$	1	0.02762	0.00137	20.10	<.0001
RampVol$_{24}$	1	0.97652	0.02574	37.93	<.0001

Number of Observations	241
R-Square	0.9808
Adj R-Sq	0.9806

TABLE B.4
Delay Diamond CR4R2A4

Parameter	DF	Estimate	Standard Error	t Value	Pr > |t|
Intercept	1	4.44848	0.17230	25.82	<.0001
CrossVol$_{24}$	1	0.02648	0.00114	23.24	<.0001
RampVol$_{24}$	1	0.93677	0.02135	43.88	<.0001

Number of Observations	241
R-Square	0.9856
Adj R-Sq	0.9855

TABLE B.5
Delay Diamond CR6R2A4

Parameter	DF	Estimate	Standard Error	t Value	Pr > |t|
Intercept	1	4.05244	0.16183	25.04	<.0001
$CrossVol_{24}$	1	0.02020	0.00070819	28.53	<.0001
$RampVol_{24}$	1	1.00147	0.01908	52.49	<.0001

Number of Observations	332
R-Square	0.9818
Adj R-Sq	0.9817

TABLE B.6
Stop Diamond CR2R1A2

Parameter	DF	Estimate	Standard Error	t Value	Pr > |t|
Intercept	1	2.63296	0.64595	4.08	<.0001
$CrossVol_{24}$	1	0.09656	0.00852	11.34	<.0001
$RampVol_{24}$	1	0.63485	0.08670	7.32	<.0001

Number of Observations	122
R-Square	0.9329
Adj R-Sq	0.9318

TABLE B.7
Stop Diamond CR4R1A4

Parameter	DF	Estimate	Standard Error	t Value	Pr > |t|
Intercept	1	2.59473	0.43949	5.90	<.0001
$CrossVol_{24}$	1	0.05667	0.00318	17.82	<.0001
$RampVol_{24}$	1	0.65847	0.05505	11.96	<.0001

Number of Observations	192
R-Square	0.9328
Adj R-Sq	0.9321

TABLE B.8
Stop Diamond CR4R2A2

Parameter	DF	Estimate	Standard Error	t Value	Pr > |t|
Intercept	1	1.08452	0.50042	2.17	0.0312
$CrossVol_{24}$	1	0.04696	0.00331	14.19	<.0001
$RampVol_{24}$	1	0.85028	0.06200	13.71	<.0001

Number of Observations	241
R-Square	0.9214
Adj R-Sq	0.9208

TABLE B.9
Stop Diamond CR4R2A4

Parameter	DF	Estimate	Standard Error	t Value	Pr > |t|
Intercept	1	2.57271	0.40302	6.38	<.0001
$CrossVol_{24}$	1	0.05075	0.00267	19.04	<.0001
$RampVol_{24}$	1	0.66576	0.04993	13.33	<.0001

Number of Observations	241
R-Square	0.9405
Adj R-Sq	0.9400

TABLE B.10
Stop Diamond CR6R2A4

Parameter	DF	Estimate	Standard Error	t Value	Pr > |t|
Intercept	1	1.00433	0.40633	2.47	0.0140
$CrossVol_{24}$	1	0.03739	0.00178	21.03	<.0001
$RampVol_{24}$	1	0.86453	0.04790	18.05	<.0001

Number of Observations	332
R-Square	0.9256
Adj R-Sq	0.9251

TABLE B.11
Critical movement Diamond CR2R1A2

Variable	DF	Parameter Estimate	Standard Error	t Value	Pr > |t|
Intercept	1	2.63031	0.05314	49.50	<.0001
$CrossVol_h$	1	1.07932	0.06555	16.47	<.0001
$RampVol_h$	1	0.78732	0.09386	8.39	<.0001

Number of Observations	244
R-Square	0.8614
Adj R-Sq	0.8602

TABLE B.12
Critical movement Diamond CR4R1A4

Variable	DF	Parameter Estimate	Standard Error	t Value	Pr > |t|
Intercept	1	2.73681	0.04043	67.69	<.0001
$CrossVol_h$	1	0.58206	0.02809	20.72	<.0001
$RampVol_h$	1	0.56109	0.05464	10.27	<.0001

Number of Observations	384
R-Square	0.8631
Adj R-Sq	0.8624

TABLE B.13
Critical movement Diamond CR4R2A2

Variable	DF	Parameter Estimate	Standard Error	t Value	Pr > |t|
Intercept	1	2.73765	0.04803	57.00	<.0001
$CrossVol_h$	1	0.42297	0.02879	14.69	<.0001
$RampVol_h$	1	0.70271	0.04122	17.05	<.0001

Number of Observations	482
R-Square	0.8326
Adj R-Sq	0.8319

TABLE B.14
Critical movement Diamond CR4R2A4

Variable	DF	Parameter Estimate	Standard Error	t Value	Pr > |t|
Intercept	1	2.61953	0.03522	74.38	<.0001
$CrossVol_h$	1	0.53985	0.02111	25.57	<.0001
$RampVol_h$	1	0.43609	0.03023	14.43	<.0001

Number of Observations	482
R-Square	0.8885
Adj R-Sq	0.8880

TABLE B.15
Critical movement Diamond CR4R2A4

Variable	DF	Parameter Estimate	Standard Error	t Value	Pr > |t|
Intercept	1	2.82252	0.03245	86.97	<.0001
$CrossVol_h$	1	0.36232	0.01264	28.68	<.0001
$RampVol_h$	1	0.48733	0.02123	22.95	<.0001

Number of Observations	664
R-Square	0.8961
Adj R-Sq	0.8958

TABLE B.16
Queue on the Ramp Diamond CR2R1A2

Variable	DF	Parameter Estimate	Standard Error	t Value	Pr > |t|
Intercept	1	3.18549	0.06950	45.84	<.0001
$CrossVol_h$	1	0.45350	0.08487	5.34	<.0001
$RampVol_h$	1	1.95872	0.12135	16.14	<.0001

Number of Observations	483 (488)
R-Square	0.7010
Adj R-Sq	0.6998

TABLE B.17
Queue on the Ramp Diamond CR4R1A4

Variable	DF	Parameter Estimate	Standard Error	t Value	Pr > |t|
Intercept	1	3.48037	0.03636	95.72	<.0001
$CrossVol_h$	1	0.23096	0.02516	9.18	<.0001
$RampVol_h$	1	0.76475	0.04894	15.63	<.0001

Number of Observations	768 (765)
R-Square	0.6667
Adj R-Sq	0.6658

TABLE B.18
Queue on the Ramp Diamond CR4R2A2

Variable	DF	Parameter Estimate	Standard Error	t Value	Pr > |t|
Intercept	1	3.61127	0.05122	70.50	<.0001
$CrossVol_h$	1	0.30853	0.03047	10.12	<.0001
$RampVol_h$	1	1.04592	0.04356	24.01	<.0001

Number of Observations	958 (964)
R-Square	0.7444
Adj R-Sq	0.7439

TABLE B.19
Queue on the Ramp Diamond CR4R2A4

Variable	DF	Parameter Estimate	Standard Error	t Value	Pr > |t|
Intercept	1	3.49419	0.03974	87.92	<.0001
$CrossVol_h$	1	0.20875	0.02361	8.84	<.0001
$RampVol_h$	1	0.72614	0.03376	21.51	<.0001

Number of Observations	957 (964)
R-Square	0.6972
Adj R-Sq	0.6966

TABLE B.20
Queue on the Ramp Diamond CR6R2A4

Variable	DF	Parameter Estimate	Standard Error	t Value	Pr > |t|
Intercept	1	3.60542	0.04678	77.08	<.0001
$CrossVol_h$	1	0.05031	0.01800	2.80	0.0053
$RampVol_h$	1	0.94468	0.02976	31.75	<.0001

Number of Observations	1328 (1325)
R-Square	0.6720
Adj R-Sq	0.6715

TABLE B.21
Queue on the CR Diamond CR2R1A2

Variable	DF	Parameter Estimate	Standard Error	t Value	Pr > |t|
Intercept	1	3.19727	0.07231	44.21	<.0001
$CrossVol_h$	1	2.15221	0.08866	24.27	<.0001
$RampVol_h$	1	0.06553	0.12671	0.52	0.6053

Number of Observations	488 (485)
R-Square	0.7706
Adj R-Sq	0.7697

TABLE B.22
Queue on the CR Diamond CR4R1A4

Variable	DF	Parameter Estimate	Standard Error	t Value	Pr > |t|
Intercept	1	3.20870	0.05351	59.96	<.0001
$CrossVol_h$	1	1.17191	0.03713	31.56	<.0001
$RampVol_h$	1	0.30961	0.07219	4.29	<.0001

Number of Observations	768 (4608)
R-Square	0.8154
Adj R-Sq	0.8149

TABLE B.23
Queue on the CR Diamond CR4R2A2

Variable	DF	Parameter Estimate	Standard Error	t Value	Pr > |t|
Intercept	1	3.22664	0.05751	56.11	<.0001
$CrossVol_h$	1	0.90215	0.03443	26.20	<.0001
$RampVol_h$	1	0.47949	0.04928	9.73	<.0001

Number of Observations	963 (964)
R-Square	0.7649
Adj R-Sq	0.7644

TABLE B.24
Queue on the CR Diamond CR4R2A4

Variable	DF	Parameter Estimate	Standard Error	t Value	Pr > |t|
Intercept	1	2.96188	0.05109	57.97	<.0001
$CrossVol_h$	1	1.10219	0.03059	36.03	<.0001
$RampVol_h$	1	0.35494	0.04378	8.11	<.0001

Number of Observations	963 (964)
R-Square	0.8338
Adj R-Sq	0.8335

TABLE B.25
Queue on the CR Diamond CR6R2A4

Variable	DF	Parameter Estimate	Standard Error	t Value	Pr > |t|
Intercept	1	3.12970	0.04994	62.67	<.0001
$CrossVol_h$	1	0.76022	0.01927	39.44	<.0001
$RampVol_h$	1	0.42723	0.03188	13.40	<.0001

Number of Observations	1328 (1328)
R-Square	0.8191
Adj R-Sq	0.8188

Single-Point Interchange

TABLE B.26
Delay SP CR2R1A2

Parameter	DF	Estimate	Standard Error	t Value	Pr > |t|
Intercept	1	4.83162	0.24632	19.61	<.0001
CrossVol$_{24}$	1	0.04078	0.00325	12.55	<.0001
RampVol$_{24}$	1	0.87127	0.03306	26.35	<.0001

Number of Observations	122
R-Square	0.9838
Adj R-Sq	0.9835

TABLE B.27
Delay SP CR4R1A4

Parameter	DF	Estimate	Standard Error	t Value	Pr > |t|
Intercept	1	4.55830	0.18924	24.09	<.0001
CrossVol$_{24}$	1	0.03173	0.00137	23.17	<.0001
RampVol$_{24}$	1	0.90152	0.02370	38.03	<.0001

Number of Observations	192
R-Square	0.9833
Adj R-Sq	0.9831

TABLE B.28
Delay SP CR4R2A2

Parameter	DF	Estimate	Standard Error	t Value	Pr > |t|
Intercept	1	5.01745	0.19065	26.32	<.0001
CrossVol$_{24}$	1	0.02576	0.00127	20.22	<.0001
RampVol$_{24}$	1	0.87517	0.02365	37.00	<.0001

Number of Observations	241
R-Square	0.9800
Adj R-Sq	0.9798

TABLE B.29
Delay SP CR4R2A4

Parameter	DF	Estimate	Standard Error	t Value	Pr > |t|
Intercept	1	4.77218	0.17060	27.97	<.0001
CrossVol$_{24}$	1	0.02338	0.00113	20.72	<.0001
RampVol$_{24}$	1	0.89832	0.02114	42.50	<.0001

Number of Observations	241
R-Square	0.9838
Adj R-Sq	0.9837

TABLE B.30
Delay SP CR6R2A4

Parameter	DF	Estimate	Standard Error	t Value	Pr > |t|
Intercept	1	4.33559	0.17077	25.39	<.0001
CrossVol$_{24}$	1	0.02073	0.00074732	27.74	<.0001
RampVol$_{24}$	1	0.95208	0.02013	47.29	<.0001

Number of Observations	332
R-Square	0.9788
Adj R-Sq	0.9787

TABLE B.31
Stop SP CR2R1A2

Parameter	DF	Estimate	Standard Error	t Value	Pr > |t|
Intercept	1	3.21980	0.47044	6.84	<.0001
$CrossVol_{24}$	1	0.06336	0.00620	10.21	<.0001
$RampVol_{24}$	1	0.54863	0.06315	8.69	<.0001

Number of Observations	122
R-Square	0.9344
Adj R-Sq	0.9333

TABLE B.32
Stop SP CR4R1A4

Parameter	DF	Estimate	Standard Error	t Value	Pr > |t|
Intercept	1	2.82000	0.34851	8.09	<.0001
$CrossVol_{24}$	1	0.04818	0.00252	19.11	<.0001
$RampVol_{24}$	1	0.60634	0.04365	13.89	<.0001

Number of Observations	192
R-Square	0.9445
Adj R-Sq	0.9439

TABLE B.33
Stop SP CR4R2A2

Parameter	DF	Estimate	Standard Error	t Value	Pr > |t|
Intercept	1	3.25926	0.21256	15.33	<.0001
$CrossVol_{24}$	1	0.02144	0.00142	15.09	<.0001
$RampVol_{24}$	1	0.70722	0.02637	26.82	<.0001

Number of Observations	241
R-Square	0.9633
Adj R-Sq	0.9630

TABLE B.34
Stop SP CR4R2A4

Parameter	DF	Estimate	Standard Error	t Value	Pr > |t|
Intercept	1	2.55928	0.33665	7.60	<.0001
$CrossVol_{24}$	1	0.03661	0.00223	16.44	<.0001
$RampVol_{24}$	1	0.65197	0.04171	15.63	<.0001

Number of Observations	241
R-Square	0.9394
Adj R-Sq	0.9389

TABLE B.35
Stop SP CR6R2A4

Parameter	DF	Estimate	Standard Error	t Value	Pr > |t|
Intercept	1	1.80655	0.32693	5.53	<.0001
$CrossVol_{24}$	1	0.03183	0.00143	22.25	<.0001
$RampVol_{24}$	1	0.74631	0.03854	19.36	<.0001

Number of Observations	332
R-Square	0.9338
Adj R-Sq	0.9334

TABLE B.36
Critical movement delay SP CR2R1A2

Variable	DF	Parameter Estimate	Standard Error	t Value	Pr > |t|
Intercept	1	2.22392	0.05581	39.85	<.0001
CrossVol$_h$	1	1.06357	0.06885	15.45	<.0001
RampVol$_h$	1	0.34276	0.09858	3.48	0.0006

Number of Observations	244
R-Square	0.7884
Adj R-Sq	0.7866

TABLE B.37
Critical movement delay SP CR4R1A4

Variable	DF	Parameter Estimate	Standard Error	t Value	Pr > |t|
Intercept	1	2.32445	0.04477	51.92	<.0001
CrossVol$_h$	1	0.68633	0.03110	22.07	<.0001
RampVol$_h$	1	0.39788	0.06050	6.58	<.0001

Number of Observations	384
R-Square	0.8460
Adj R-Sq	0.8452

TABLE B.38
Critical movement delay SP CR4R2A2

Variable	DF	Parameter Estimate	Standard Error	t Value	Pr > |t|
Intercept	1	2.36811	0.05463	43.35	<.0001
CrossVol$_h$	1	0.49539	0.03276	15.12	<.0001
RampVol$_h$	1	0.47913	0.04692	10.21	<.0001

Number of Observations	482
R-Square	0.7610
Adj R-Sq	0.7600

TABLE B.39
Critical movement delay SP CR4R2A4

Variable	DF	Parameter Estimate	Standard Error	t Value	Pr > |t|
Intercept	1	2.23836	0.04022	55.66	<.0001
CrossVol$_h$	1	0.57926	0.02411	24.03	<.0001
RampVol$_h$	1	0.30344	0.03451	8.79	<.0001

Number of Observations	482
R-Square	0.8450
Adj R-Sq	0.8443

TABLE B.40
Critical movement delay SP CR6R2A4

Variable	DF	Parameter Estimate	Standard Error	t Value	Pr > |t|
Intercept	1	2.34006	0.04210	55.58	<.0001
CrossVol$_h$	1	0.42369	0.01625	26.08	<.0001
RampVol$_h$	1	0.38391	0.02687	14.29	<.0001

Number of Observations	664
R-Square	0.8383
Adj R-Sq	0.8378

TABLE B.41
Queue on the Ramp SP CR2R1A2

Variable	DF	Parameter Estimate	Standard Error	t Value	Pr > |t|
Intercept	1	3.20734	0.05992	53.52	<.0001
$CrossVol_h$	1	0.70655	0.07321	9.65	<.0001
$RampVol_h$	1	1.15469	0.10466	11.03	<.0001

Number of Observations	483 (488)
R-Square	0.6788
Adj R-Sq	0.6775

TABLE B.42
Queue on the Ramp SP CR4R1A4

Variable	DF	Parameter Estimate	Standard Error	t Value	Pr > |t|
Intercept	1	3.43701	0.03775	91.05	<.0001
$CrossVol_h$	1	0.29398	0.02596	11.32	<.0001
$RampVol_h$	1	0.67360	0.05049	13.34	<.0001

Number of Observations	762 (768)
R-Square	0.6917
Adj R-Sq	0.6908

TABLE B.43
Queue on the Ramp SP CR4R2A2

Variable	DF	Parameter Estimate	Standard Error	t Value	Pr > |t|
Intercept	1	3.54074	0.05593	63.30	<.0001
$CrossVol_h$	1	0.39695	0.03331	11.92	<.0001
$RampVol_h$	1	0.86381	0.04764	18.13	<.0001

Number of Observations	957 (964)
R-Square	0.6905
Adj R-Sq	0.6899

TABLE B.44
Queue on the Ramp SP CR4R2A4

Variable	DF	Parameter Estimate	Standard Error	t Value	Pr > |t|
Intercept	1	3.43274	0.04322	79.43	<.0001
$CrossVol_h$	1	0.34802	0.02574	13.52	<.0001
$RampVol_h$	1	0.52198	0.03683	14.17	<.0001

Number of Observations	958 (964)
R-Square	0.6832
Adj R-Sq	0.6825

TABLE B.45
Queue on the Ramp SP CR6R2A4

Variable	DF	Parameter Estimate	Standard Error	t Value	Pr > |t|
Intercept	1	3.53834	0.04821	73.39	<.0001
$CrossVol_h$	1	0.20192	0.01850	10.91	<.0001
$RampVol_h$	1	0.64076	0.03060	20.94	<.0001

Number of Observations	1322 (1328)
R-Square	0.6469
Adj R-Sq	0.6463

TABLE B.46
Queue on the CR SP CR2R1A2

Variable	DF	Parameter Estimate	Standard Error	t Value	Pr > |t|
Intercept	1	3.52954	0.05948	59.34	<.0001
CrossVol$_h$	1	1.64564	0.07337	22.43	<.0001
RampVol$_h$	1	-0.13349	0.10506	-1.27	0.2045

Number of Observations	488 (488)
R-Square	0.7570
Adj R-Sq	0.7559

TABLE B.47
Queue on the CR SP CR4R1A4

Variable	DF	Parameter Estimate	Standard Error	t Value	Pr > |t|
Intercept	1	3.43024	0.05374	63.83	<.0001
CrossVol$_h$	1	1.02589	0.03734	27.47	<.0001
RampVol$_h$	1	0.35242	0.07262	4.85	<.0001

Number of Observations	768 (768)
R-Square	0.7807
Adj R-Sq	0.7801

TABLE B.48
Queue on the CR SP CR4R2A2

Variable	DF	Parameter Estimate	Standard Error	t Value	Pr > |t|
Intercept	1	3.66843	0.05004	73.31	<.0001
CrossVol$_h$	1	0.68476	0.03001	22.82	<.0001
RampVol$_h$	1	0.13684	0.04297	3.18	0.0015

Number of Observations	964 (964)
R-Square	0.7099
Adj R-Sq	0.7091

TABLE B.49
Queue on the CR SP CR4R2A4

Variable	DF	Parameter Estimate	Standard Error	t Value	Pr > |t|
Intercept	1	3.26231	0.05190	62.85	<.0001
CrossVol$_h$	1	0.93607	0.03111	30.09	<.0001
RampVol$_h$	1	0.22554	0.04454	5.06	<.0001

Number of Observations	964 (964)
R-Square	0.7631
Adj R-Sq	0.7626

TABLE B.50
Queue on the CR SP CR6R2A4

Variable	DF	Parameter Estimate	Standard Error	t Value	Pr > |t|
Intercept	1	3.29187	0.05149	63.93	<.0001
CrossVol$_h$	1	0.73572	0.01987	37.02	<.0001
RampVol$_h$	1	0.30842	0.03287	9.38	<.0001

Number of Observations	1328 (1328)
R-Square	0.7799
Adj R-Sq	0.7796

Diverging Diamond

TABLE B.51
Delay DDI CR2R1A2

Parameter	DF	Estimate	Standard Error	t Value	Pr > |t|
Intercept	1	7.89222	0.43431	18.17	<.0001
Crossroad _24_vol	1	0.08386	0.00573	14.64	<.0001
Off_Ramp_24_vol	1	0.46887	0.05830	8.04	<.0001

Number of Observations	122
R- Square	0.9537
Adj R-Square	0.9529

TABLE B.52
Delay DDI CR4R1A4

Parameter	DF	Estimate	Standard Error	t Value	Pr > |t|
Intercept	1	6.57155	0.23585	27.86	<.0001
$CrossVol_{24}$	1	0.04843	0.00171	28.38	<.0001
$RampVol_{24}$	1	0.65432	0.02954	22.15	<.0001

Number of Observations	192
R- Square	0.9755
Adj R-Square	0.9753

TABLE B.53
Delay DDI CR4R2A2

Parameter	DF	Estimate	Standard Error	t Value	Pr > |t|
Intercept	1	6.43340	0.27371	23.50	<.0001
$CrossVol_{24}$	1	0.04037	0.00181	22.30	<.0001
$RampVol_{24}$	1	0.69838	0.03391	20.59	<.0001

Number of Observations	241
R-Sq	0.9652
Adj R-Square	0.9649

TABLE B.54
Delay DDI CR4R2A4

Parameter	DF	Estimate	Standard Error	t Value	Pr > |t|
Intercept	1	6.41043	0.25676	24.97	<.0001
$CrossVol_{24}$	1	0.03942	0.00170	23.22	<.0001
$RampVol_{24}$	1	0.68148	0.03181	21.42	<.0001

Number of Observations	241
R-Square	0.9678
Adj R-Sq	0.9675

TABLE B.55
Delay DDI CR6R2A4

Parameter	DF	Estimate	Standard Error	t Value	Pr > |t|
Intercept	1	5.65928	0.19902	28.44	<.0001
$CrossVol_{24}$	1	0.02775	0.00087096	31.86	<.0001
$RampVol_{24}$	1	0.78026	0.02346	33.25	<.0001

Number of Observations	332
R-Square	0.9718
Adj R-Sq	0.9717

TABLE B.56
Stop DDI CR2R1A2

Parameter	DF	Estimate	Standard Error	t Value	Pr > |t|
Intercept	1	8.68752	0.84141	10.32	<.0001
$CrossVol_{24}$	1	0.15281	0.01110	13.77	<.0001
$RampVol_{24}$	1	-0.15576	0.11294	-1.38	0.1704

Number of Observations	122
R-Square	0.8689
Adj R-Sq	0.8667

TABLE B.57
Stop DDI CR4R1A4

Parameter	DF	Estimate	Standard Error	t Value	Pr > |t|
Intercept	1	5.19806	0.42849	12.13	<.0001
$CrossVol_{24}$	1	0.07624	0.00310	24.59	<.0001
$RampVol_{24}$	1	0.27697	0.05367	5.16	<.0001

Number of Observations	192
R-Square	0.9349
Adj R-Sq	0.9342

TABLE B.58
Stop DDI CR4R2A2

Parameter	DF	Estimate	Standard Error	t Value	Pr > |t|
Intercept	1	5.69397	0.44253	12.87	<.0001
$CrossVol_{24}$	1	0.06470	0.00293	22.11	<.0001
$RampVol_{24}$	1	0.30582	0.05483	5.58	<.0001

Number of Observations	153
R-Square	0.9222
Adj R-Sq	0.9215

TABLE B.59
Stop DDI CR4R2A4

Parameter	DF	Estimate	Standard Error	t Value	Pr > |t|
Intercept	1	5.64718	0.40790	13.84	<.0001
$CrossVol_{24}$	1	0.06259	0.00270	23.20	<.0001
$RampVol_{24}$	1	0.29384	0.05054	5.81	<.0001

Number of Observations	241
R-Square	0.8447
Adj R-Sq	0.8428

TABLE B.60
Stop DDI CR6R2A4

Parameter	DF	Estimate	Standard Error	t Value	Pr > |t|
Intercept	1	2.01564	0.37288	5.41	<.0001
$CrossVol_{24}$	1	0.04515	0.00163	27.67	<.0001
$RampVol_{24}$	1	0.64554	0.04396	14.68	<.0001

Number of Observations	332
R-Square	0.9365
Adj R-Sq	0.9361

TABLE B.61
Critical movement delay DDI CR2R1A2

Variable	DF	Parameter Estimate	Standard Error	t Value	Pr > |t|
Intercept	1	2.44156	0.06629	36.83	<.0001
$CrossVol_h$	1	1.67483	0.08177	20.48	<.0001
$RampVol_h$	1	-0.40571	0.11709	-3.46	0.0006

Number of Observations	244
R-Square	0.7798
Adj R-Sq	0.7780

TABLE B.62
Critical movement delay DDI CR4R1A4

Variable	DF	Parameter Estimate	Standard Error	t Value	Pr > |t|
Intercept	1	2.47480	0.04344	56.97	<.0001
$CrossVol_h$	1	0.98430	0.03018	32.61	<.0001
$RampVol_h$	1	-0.28153	0.05870	-4.80	<.0001

Number of Observations	384
R-Square	0.8579
Adj R-Sq	0.8572

TABLE B.63
Critical movement delay DDI CR4R2A2

Variable	DF	Parameter Estimate	Standard Error	t Value	Pr > |t|
Intercept	1	2.77587	0.05016	55.34	<.0001
$CrossVol_h$	1	0.70248	0.03007	23.37	<.0001
$RampVol_h$	1	0.19130	0.04305	4.44	<.0001

Number of Observations	482
R-Square	0.8010
Adj R-Sq	0.8002

TABLE B.64
Critical movement delay DDI CR4R2A4

Variable	DF	Parameter Estimate	Standard Error	t Value	Pr > |t|
Intercept	1	2.43709	0.03708	65.73	<.0001
$CrossVol_h$	1	0.70892	0.02223	31.90	<.0001
$RampVol_h$	1	0.16790	0.03182	5.28	<.0001

Number of Observations	482
R-Square	0.8785
Adj R-Sq	0.8780

TABLE B.65
Critical movement delay DDI CR6R2A4

Variable	DF	Parameter Estimate	Standard Error	t Value	Pr > |t|
Intercept	1	2.49712	0.04976	50.18	<.0001
$CrossVol_h$	1	0.52826	0.01920	27.51	<.0001
$RampVol_h$	1	0.03009	0.03176	0.95	0.3438

Number of Observations	664
R-Square	0.7403
Adj R-Sq	0.7395

TABLE B.66
Queue on the Ramp DDI CR2R1A2

Variable	DF	Parameter Estimate	Standard Error	t Value	Pr > |t|
Intercept	1	3.17691	0.06093	52.14	<.0001
$CrossVol_h$	1	0.70434	0.07343	9.59	<.0001
$RampVol_h$	1	0.86970	0.10465	8.31	<.0001

Number of Observations	473 (4888)
R-Square	0.6144
Adj R-Sq	0.6128

TABLE B.67
Queue on the Ramp DDI CR4R1A4

Variable	DF	Parameter Estimate	Standard Error	t Value	Pr > |t|
Intercept	1	3.54924	0.04287	82.78	<.0001
$CrossVol_h$	1	0.31537	0.02915	10.82	<.0001
$RampVol_h$	1	0.51487	0.05670	9.08	<.0001

Number of Observations	754 (768)
R-Square	0.5732
Adj R-Sq	0.5730

TABLE B.68
Queue on the Ramp DDI CR4R2A2

Variable	DF	Parameter Estimate	Standard Error	t Value	Pr > |t|
Intercept	1	3.46094	0.05600	61.81	<.0001
$CrossVol_h$	1	0.11347	0.03325	3.41	0.0007
$RampVol_h$	1	1.30161	0.04753	27.39	<.0001

Number of Observations	956 (964)
R-Square	0.7137
Adj R-Sq	0.7131

TABLE B.69
Queue on the Ramp DDI CR4R2A4

Variable	DF	Parameter Estimate	Standard Error	t Value	Pr > |t|
Intercept	1	3.56287	0.04699	75.82	<.0001
$CrossVol_h$	1	0.24411	0.02764	8.83	<.0001
$RampVol_h$	1	0.50966	0.03941	12.93	<.0001

Number of Observations	949 (964)
R-Square	0.5668
Adj R-Sq	0.5659

TABLE B.70
Queue on the Ramp DDI CR6R2A4

Variable	DF	Parameter Estimate	Standard Error	t Value	Pr > |t|
Intercept	1	3.70515	0.04787	77.40	<.0001
$CrossVol_h$	1	0.14949	0.01809	8.26	<.0001
$RampVol_h$	1	0.52936	0.02988	17.72	<.0001

Number of Observations	1306 (1328)
R-Square	0.5399
Adj R-Sq	0.5397

TABLE B.71
Queue on the CR DDI CR2R1A2

Variable	DF	Parameter Estimate	Standard Error	t Value	Pr > |t|
Intercept	1	3.35970	0.07713	43.56	<.0001
CrossVol$_h$	1	2.50361	0.09514	26.31	<.0001
RampVol$_h$	1	-0.71187	0.13624	-5.23	<.0001

Number of Observations	488 (488)
R-Square	0.7347
Adj R-Sq	0.7336

TABLE B.72
Queue on the CR DDI CR4R1A4

Variable	DF	Parameter Estimate	Standard Error	t Value	Pr > |t|
Intercept	1	3.14537	0.05278	59.59	<.0001
CrossVol$_h$	1	1.52529	0.03667	41.59	<.0001
RampVol$_h$	1	-0.29746	0.07133	-4.17	<.0001

Number of Observations	768 (768)
R-Square	0.8408
Adj R-Sq	0.8404

TABLE B.73
Queue on the CR DDI CR4R2A2

Variable	DF	Parameter Estimate	Standard Error	t Value	Pr > |t|
Intercept	1	3.26993	0.05970	54.77	<.0001
CrossVol$_h$	1	1.37427	0.03574	38.45	<.0001
RampVol$_h$	1	-0.13815	0.05115	-2.70	0.0070

Number of Observations	963 (964)
R-Square	0.7843
Adj R-Sq	0.7838

TABLE B.74
Queue on the CR DDI CR4R2A4

Variable	DF	Parameter Estimate	Standard Error	t Value	Pr > |t|
Intercept	1	3.06632	0.05906	51.92	<.0001
CrossVol$_h$	1	1.34942	0.03540	38.12	<.0001
RampVol$_h$	1	-0.10948	0.05068	-2.16	0.0310

Number of Observations	964 (964)
R-Square	0.7851
Adj R-Sq	0.7846

TABLE B.75
Queue on the CR DDI CR6R2A4

Variable	DF	Parameter Estimate	Standard Error	t Value	Pr > |t|
Intercept	1	2.77631	0.06540	42.45	<.0001
CrossVol$_h$	1	0.91796	0.02366	38.80	<.0001
RampVol$_h$	1	0.13251	0.03879	3.42	0.0007

Number of Observations	1267 (1328)
R-Square	0.7478
Adj R-Sq	0.7474

Tight Diamond

TABLE B.76
Delay TDI CR2R1A2

Parameter	DF	Estimate	Standard Error	t Value	Pr > |t|
Intercept	1	5.68397	0.30132	18.86	<.0001
CrossVol$_{24}$	1	0.06245	0.00397	15.72	<.0001
RampVol$_{24}$	1	0.78867	0.04045	19.50	<.0001

Number of Observations	122
R-Square	0.9802
Adj R-Sq	0.9798

TABLE B.77
Delay TDI CR4R1A4.

Parameter	DF	Estimate	Standard Error	t Value	Pr > |t|
Intercept	1	5.20365	0.20946	24.84	<.0001
CrossVol$_{24}$	1	0.03768	0.00152	24.86	<.0001
RampVol$_{24}$	1	0.85504	0.02623	32.59	<.0001

Number of Observations	192
R-Square	0.9810
Adj R-Sq	0.9808

TABLE B.78
Delay TDI CR4R2A2

Parameter	DF	Estimate	Standard Error	t Value	Pr > |t|
Intercept	1	4.20294	0.26232	16.02	<.0001
CrossVol$_{24}$	1	0.04082	0.00173	23.53	<.0001
RampVol$_{24}$	1	0.93819	0.03250	28.87	<.0001

Number of Observations	241
R-Square	0.9764
Adj R-Sq	0.9762

TABLE B.79
Delay TDI CR4R2A4

Parameter	DF	Estimate	Standard Error	t Value	Pr > |t|
Intercept	1	4.44818	0.24459	18.19	<.0001
CrossVol$_{24}$	1	0.03565	0.00162	22.04	<.0001
RampVol$_{24}$	1	0.91302	0.03030	30.13	<.0001

Number of Observations	241
R-Square	0.9762
Adj R-Sq	0.9760

TABLE B.80
Delay TDI CR6R2A4

Parameter	DF	Estimate	Standard Error	t Value	Pr > |t|
Intercept	1	3.76649	0.18267	20.62	<.0001
CrossVol$_{24}$	1	0.02523	0.00079942	31.56	<.0001
RampVol$_{24}$	1	1.00051	0.02154	46.46	<.0001

Number of Observations	332
R-Square	0.9803
Adj R-Sq	0.9802

TABLE B.81
Stop TDI CR2R1A2

Parameter	DF	Estimate	Standard Error	t Value	Pr > |t|
Intercept	1	2.05512	0.77456	2.65	0.0091
$CrossVol_{24}$	1	0.11186	0.01021	10.95	<.0001
$RampVol_{24}$	1	0.69709	0.10397	6.70	<.0001

Number of Observations	122
R-Square	0.9257
Adj R-Sq	0.9244

TABLE B.82
Stop TDI CR4R1A4

Parameter	DF	Estimate	Standard Error	t Value	Pr > |t|
Intercept	1	3.00782	0.49401	6.09	<.0001
$CrossVol_{24}$	1	0.06879	0.00357	19.24	<.0001
$RampVol_{24}$	1	0.59757	0.06187	9.66	<.0001

Number of Observations	192
R-Square	0.9294
Adj R-Sq	0.9287

TABLE B.83
Stop TDI CR4R2A2

Parameter	DF	Estimate	Standard Error	t Value	Pr > |t|
Intercept	1	2.55458	0.50823	5.03	<.0001
$CrossVol_{24}$	1	0.06948	0.00336	20.67	<.0001
$RampVol_{24}$	1	0.65120	0.06297	10.34	<.0001

Number of Observations	241
R-Square	0.9359
Adj R-Sq	0.9354

TABLE B.84
Stop TDI CR4R2A4

Parameter	DF	Estimate	Standard Error	t Value	Pr > |t|
Intercept	1	2.67547	0.50477	5.30	<.0001
$CrossVol_{24}$	1	0.06235	0.00334	18.68	<.0001
$RampVol_{24}$	1	0.63959	0.06254	10.23	<.0001

Number of Observations	241
R-Square	0.9268
Adj R-Sq	0.9262

TABLE B.85
Stop TDI CR6R2A4

Parameter	DF	Estimate	Standard Error	t Value	Pr > |t|
Intercept	1	1.45298	0.38623	3.76	0.0002
$CrossVol_{24}$	1	0.04257	0.00169	25.19	<.0001
$RampVol_{24}$	1	0.80286	0.04553	17.63	<.0001

Number of Observations	241
R-Square	0.9374
Adj R-Sq	0.9370

TABLE B.86
Critical movement delay TDI CR2R1A2

Variable	DF	Parameter Estimate	Standard Error	t Value	Pr > |t|
Intercept	1	2.34330	0.06201	37.79	<.0001
$CrossVol_h$	1	1.37217	0.07648	17.94	<.0001
$RampVol_h$	1	0.82500	0.10952	7.53	<.0001

Number of Observations	244
R-Square	0.8680
Adj R-Sq	0.8669

TABLE B.87
Critical movement delay TDI CR4R1A4

Variable	DF	Parameter Estimate	Standard Error	t Value	Pr > |t|
Intercept	1	2.58635	0.04347	59.50	<.0001
$CrossVol_h$	1	0.74166	0.03020	24.56	<.0001
$RampVol_h$	1	0.56507	0.05874	9.62	<.0001

Number of Observations	384
R-Square	0.8855
Adj R-Sq	0.8849

TABLE B.88
Critical movement delay TDI CR4R2A2

Variable	DF	Parameter Estimate	Standard Error	t Value	Pr > |t|
Intercept	1	2.57190	0.04822	53.34	<.0001
$CrossVol_h$	1	0.69460	0.02890	24.03	<.0001
$RampVol_h$	1	0.57261	0.04138	13.84	<.0001

Number of Observations	482
R-Square	0.8771
Adj R-Sq	0.8766

TABLE B.89
Critical movement delay TDI CR4R2A4

Variable	DF	Parameter Estimate	Standard Error	t Value	Pr > |t|
Intercept	1	2.60580	0.04541	57.38	<.0001
$CrossVol_h$	1	0.64810	0.02722	23.81	<.0001
$RampVol_h$	1	0.47738	0.03897	12.25	<.0001

Number of Observations	482
R-Square	0.8666
Adj R-Sq	0.8660

TABLE B.90
Critical movement delay TDI CR6R2A4

Variable	DF	Parameter Estimate	Standard Error	t Value	Pr > |t|
Intercept	1	2.70555	0.03774	71.69	<.0001
$CrossVol_h$	1	0.40697	0.01456	27.94	<.0001
$RampVol_h$	1	0.52213	0.02409	21.68	<.0001

Number of Observations	664
R-Square	0.8859
Adj R-Sq	0.8855

TABLE B.91
Queue on the Ramp TDI CR2R1A2

Variable	DF	Parameter Estimate	Standard Error	t Value	Pr > |t|
Intercept	1	3.19602	0.06852	46.65	<.0001
$CrossVol_h$	1	0.56612	0.08339	6.79	<.0001
$RampVol_h$	1	1.75611	0.11911	14.74	<.0001

Number of Observations	488 (481)
R-Square	0.6994
Adj R-Sq	0.6981

TABLE B.92
Queue on the Ramp TDI CR4R1A4

Variable	DF	Parameter Estimate	Standard Error	t Value	Pr > |t|
Intercept	1	3.51861	0.04226	83.27	<.0001
$CrossVol_h$	1	0.18274	0.02920	6.26	<.0001
$RampVol_h$	1	0.88092	0.05680	15.51	<.0001

Number of Observations	764 (768)
R-Square	0.6093
Adj R-Sq	0.6083

TABLE B.93
Queue on the Ramp TDI CR4R2A2

Variable	DF	Parameter Estimate	Standard Error	t Value	Pr > |t|
Intercept	1	3.55320	0.05100	69.68	<.0001
$CrossVol_h$	1	0.30247	0.03045	9.93	<.0001
$RampVol_h$	1	1.24498	0.04359	28.56	<.0001

Number of Observations	960 (964)
R-Square	0.7893
Adj R-Sq	0.7888

TABLE B.94
Queue on the Ramp TDI CR4R2A4

Variable	DF	Parameter Estimate	Standard Error	t Value	Pr > |t|
Intercept	1	3.33386	0.05103	65.33	<.0001
$CrossVol_h$	1	0.24138	0.03045	7.93	<.0001
$RampVol_h$	1	0.91871	0.04357	21.08	<.0001

Number of Observations	960 (964)
R-Square	0.6793
Adj R-Sq	0.6786

TABLE B.95
Queue on the Ramp TDI CR6R2A4

Variable	DF	Parameter Estimate	Standard Error	t Value	Pr > |t|
Intercept	1	3.55289	0.04834	73.50	<.0001
$CrossVol_h$	1	0.08563	0.01852	4.62	<.0001
$RampVol_h$	1	0.91812	0.03062	29.99	<.0001

Number of Observations	1321 (1328)
R-Square	0.6678
Adj R-Sq	0.6673

TABLE B.96
Queue on the CR TDI CR2R1A2

Variable	DF	Parameter Estimate	Standard Error	t Value	Pr > |t|
Intercept	1	3.05697	0.07563	40.42	<.0001
$CrossVol_h$	1	2.28791	0.09329	24.52	<.0001
$RampVol_h$	1	0.47459	0.13358	3.55	0.0004

Number of Observations	488 (488)
R-Square	0.8057
Adj R-Sq	0.8049

TABLE B.97
Queue on the CR TDI CR4R1A4

Variable	DF	Parameter Estimate	Standard Error	t Value	Pr > |t|
Intercept	1	3.20950	0.05533	58.00	<.0001
$CrossVol_h$	1	1.23969	0.03838	32.30	<.0001
$RampVol_h$	1	0.46486	0.07465	6.23	<.0001

Number of Observations	767 (768)
R-Square	0.8343
Adj R-Sq	0.8339

TABLE B.98
Queue on the CR TDI CR4R2A2

Variable	DF	Parameter Estimate	Standard Error	t Value	Pr > |t|
Intercept	1	3.04579	0.05361	56.81	<.0001
$CrossVol_h$	1	1.29042	0.03214	40.15	<.0001
$RampVol_h$	1	0.31134	0.04601	6.77	<.0001

Number of Observations	964 (964)
R-Square	0.8516
Adj R-Sq	0.8513

TABLE B.99
Queue on the CR TDI CR4R2A4

Variable	DF	Parameter Estimate	Standard Error	t Value	Pr > |t|
Intercept	1	3.04192	0.05207	58.42	<.0001
$CrossVol_h$	1	1.22739	0.03113	39.42	<.0001
$RampVol_h$	1	0.31457	0.04454	7.06	<.0001

Number of Observations	962 (964)
R-Square	0.8488
Adj R-Sq	0.8485

TABLE B.100
Queue on the CR TDI CR6R2A4

Variable	DF	Parameter Estimate	Standard Error	t Value	Pr > |t|
Intercept	1	3.11056	0.04833	64.35	<.0001
$CrossVol_h$	1	0.80583	0.01863	43.25	<.0001
$RampVol_h$	1	0.44811	0.03082	14.54	<.0001

Number of Observations	1327 (1328)
R-Square	0.8441
Adj R-Sq	0.8438

Roundabout Interchange

TABLE B.101
Delay RA CR2R1A2

Parameter	DF	Estimate	Standard Error	t Value	Pr > |t|
Intercept	1	6.32896	0.29801	21.24	<.0001
$CrossVol_{24}$	1	0.06619	0.00393	16.84	<.0001
$RampVol_{24}$	1	0.73916	0.04000	18.48	<.0001

Number of Observations	244
R-Square	0.9608
Adj R-Sq	0.9605

TABLE B.102
Delay RA CR4R1A4

Parameter	DF	Estimate	Standard Error	t Value	Pr > |t|
Intercept	1	6.45593	0.16003	40.34	<.0001
$CrossVol_{24}$	1	0.04628	0.00116	39.96	<.0001
$RampVol_{24}$	1	0.72960	0.02004	36.40	<.0001

Number of Observations	384
R-Square	0.9783
Adj R-Sq	0.9782

TABLE B.103
Delay RA CR4R2A2

Parameter	DF	Estimate	Standard Error	t Value	Pr > |t|
Intercept	1	5.44500	0.17593	30.95	<.0001
$CrossVol_{24}$	1	0.03905	0.00116	33.56	<.0001
$RampVol_{24}$	1	0.85495	0.02180	39.22	<.0001

Number of Observations	482
R-Square	0.9754
Adj R-Sq	0.9753

TABLE B.104
Delay RA CR4R2A4

Parameter	DF	Estimate	Standard Error	t Value	Pr > |t|
Intercept	1	5.85602	0.17450	33.56	<.0001
$CrossVol_{24}$	1	0.03974	0.00115	34.43	<.0001
$RampVol_{24}$	1	0.80325	0.02162	37.15	<.0001

Number of Observations	482
R-Square	0.9746
Adj R-Sq	0.9745

TABLE B.105
Stop RA CR2R1A2

Parameter	DF	Estimate	Standard Error	t Value	Pr > |t|
Intercept	1	-9.46847	1.15878	-8.17	<.0001
$CrossVol_{24}$	1	0.14068	0.01528	9.21	<.0001
$RampVol_{24}$	1	1.86534	0.15554	11.99	<.0001

Number of Observations	244
R-Square	0.8984
Adj R-Sq	0.8976

TABLE B.106
Stop RA CR4R1A4

Parameter	DF	Estimate	Standard Error	t Value	Pr > |t|
Intercept	1	-2.98853	1.10407	-2.71	0.0071
$CrossVol_{24}$	1	0.08305	0.00799	10.39	<.0001
$RampVol_{24}$	1	1.18738	0.13828	8.59	<.0001

Number of Observations	384
R-Square	0.7362
Adj R-Sq	0.7348

TABLE B.107
Stop RA CR4R2A2

Parameter	DF	Estimate	Standard Error	t Value	Pr > |t|
Intercept	1	-10.73882	0.62974	-17.05	<.0001
$CrossVol_{24}$	1	0.07093	0.00417	17.03	<.0001
$RampVol_{24}$	1	1.97741	0.07802	25.34	<.0001

Number of Observations	482
R-Square	0.9309
Adj R-Sq	0.9306

TABLE B.108
Stop RA CR4R2A4

Parameter	DF	Estimate	Standard Error	t Value	Pr > |t|
Intercept	1	-10.11605	0.61525	-16.44	<.0001
$CrossVol_{24}$	1	0.07284	0.00407	17.90	<.0001
$RampVol_{24}$	1	1.89787	0.07623	24.90	<.0001

Number of Observations	482
R-Square	0.9321
Adj R-Sq	0.9319

TABLE B.109
Critical movement RA CR2R1A2

Variable	DF	Parameter Estimate	Standard Error	t Value	Pr > |t|
Intercept	1	0.56916	0.07225	7.88	<.0001
$CrossVol_h$	1	2.17274	0.08931	24.33	<.0001
$RampVol_h$	1	1.26579	0.12781	9.90	<.0001

Number of Observations	482
R-Square	0.8559
Adj R-Sq	0.8553

TABLE B.110
Critical movement RA CR4R1A4

Variable	DF	Parameter Estimate	Standard Error	t Value	Pr > |t|
Intercept	1	0.72998	0.06197	11.78	<.0001
$CrossVol_h$	1	1.08438	0.04305	25.19	<.0001
$RampVol_h$	1	1.52993	0.08374	18.27	<.0001

Number of Observations	768
R-Square	0.8594
Adj R-Sq	0.8591

TABLE B.111
Critical movement RA CR4R2A2

Variable	DF	Parameter Estimate	Standard Error	t Value	Pr > |t|
Intercept	1	1.44447	0.07138	20.24	<.0001
CrossVol$_h$	1	1.08371	0.04279	25.33	<.0001
RampVol$_h$	1	0.84640	0.06126	13.82	<.0001

Number of Observations	964
R-Square	0.7920
Adj R-Sq	0.7916

TABLE B.112
Critical movement RA CR4R2A4

Variable	DF	Parameter Estimate	Standard Error	t Value	Pr > |t|
Intercept	1	1.30275	0.06403	20.35	<.0001
CrossVol$_h$	1	1.05824	0.03838	27.57	<.0001
RampVol$_h$	1	0.84966	0.05495	15.46	<.0001

Number of Observations	964
R-Square	0.8213
Adj R-Sq	0.8210

TABLE B.113
Queue on the off-ramp RA CR2R1A2

Variable	DF	Parameter Estimate	Standard Error	t Value	Pr > |t|
Intercept	1	2.81671	0.10293	27.37	<.0001
CrossVol$_h$	1	1.13198	0.10062	11.25	<.0001
RampVol$_h$	1	1.81649	0.13699	13.26	<.0001

Number of Observations	783 (976)
R-Square	0.5780
Adj R-Sq	0.5769

TABLE B.114
Queue on the off-ramp RA CR4R1A4

Variable	DF	Parameter Estimate	Standard Error	t Value	Pr > |t|
Intercept	1	1.96200	0.09932	19.75	<.0001
CrossVol$_h$	1	0.73500	0.04835	15.20	<.0001
RampVol$_h$	1	1.56156	0.09449	16.53	<.0001

Number of Observations	1171 (1536)
R-Square	0.5723
Adj R-Sq	0.5715

TABLE B.115
Queue on the off-ramp RA CR4R2A2

Variable	DF	Parameter Estimate	Standard Error	t Value	Pr > |t|
Intercept	1	3.17777	0.06166	51.54	<.0001
CrossVol$_h$	1	0.60221	0.03285	18.33	<.0001
RampVol$_h$	1	1.15158	0.04570	25.20	<.0001

Number of Observations	1775 (1928)
R-Square	0.6853
Adj R-Sq	0.6850

TABLE B.116
Queue on the off-ramp RA CR4R2A4

Variable	DF	Parameter Estimate	Standard Error	t Value	Pr > |t|
Intercept	1	2.79682	0.07164	39.04	<.0001
CrossVol$_h$	1	0.60542	0.03707	16.33	<.0001
RampVol$_h$	1	0.99265	0.05117	19.40	<.0001

Number of Observations	9685 (11568)
R-Square	0.5919
Adj R-Sq	0.5914

TABLE B.117
Queue on the crossing road RA CR2R1A2

Variable	DF	Parameter Estimate	Standard Error	t Value	Pr > |t|
Intercept	1	2.65676	0.08507	31.23	<.0001
CrossVol$_h$	1	2.59368	0.09845	26.35	<.0001
RampVol$_h$	1	0.12950	0.13872	0.93	0.3508

Number of Observations	917 (976)
R-Square	0.6673
Adj R-Sq	0.6666

TABLE B.118
Queue on the crossing road RA CR4R1A4

Variable	DF	Parameter Estimate	Standard Error	t Value	Pr > |t|
Intercept	1	2.64398	0.05504	48.04	<.0001
CrossVol$_h$	1	1.52807	0.03442	44.39	<.0001
RampVol$_h$	1	0.43469	0.06693	6.49	<.0001

Number of Observations	1424 (1536)
R-Square	0.8082
Adj R-Sq	0.8079

TABLE B.119
Queue on the crossing road RA CR4R2A2

Variable	DF	Parameter Estimate	Standard Error	t Value	Pr > |t|
Intercept	1	2.69689	0.05765	46.78	<.0001
CrossVol$_h$	1	1.47229	0.03110	47.35	<.0001
RampVol$_h$	1	0.25157	0.04333	5.81	<.0001

Number of Observations	1775 (1928)
R-Square	0.7794
Adj R-Sq	0.7792

TABLE B.120
Queue on the crossing road RA CR4R2A4

Variable	DF	Parameter Estimate	Standard Error	t Value	Pr > |t|
Intercept	1	2.74133	0.05855	46.82	<.0001
CrossVol$_h$	1	1.40684	0.03192	44.08	<.0001
RampVol$_h$	1	0.36148	0.04456	8.11	<.0001

Number of Observations	1788 (1928)
R-Square	0.7713
Adj R-Sq	0.7710

About the Joint Transportation Research Program (JTRP)

On March 11, 1937, the Indiana Legislature passed an act which authorized the Indiana State Highway Commission to cooperate with and assist Purdue University in developing the best methods of improving and maintaining the highways of the state and the respective counties thereof. That collaborative effort was called the Joint Highway Research Project (JHRP). In 1997 the collaborative venture was renamed as the Joint Transportation Research Program (JTRP) to reflect the state and national efforts to integrate the management and operation of various transportation modes.

The first studies of JHRP were concerned with Test Road No. 1—evaluation of the weathering characteristics of stabilized materials. After World War II, the JHRP program grew substantially and was regularly producing technical reports. Over 1,600 technical reports are now available, published as part of the JHRP and subsequently JTRP collaborative venture between Purdue University and what is now the Indiana Department of Transportation.

Free online access to all reports is provided through a unique collaboration between JTRP and Purdue Libraries. These are available at: http://docs.lib.purdue.edu/jtrp

Further information about JTRP and its current research program is available at: http://www.purdue.edu/jtrp

About This Report

An open access version of this publication is available online. This can be most easily located using the Digital Object Identifier (doi) listed below. Pre-2011 publications that include color illustrations are available online in color but are printed only in grayscale.

The recommended citation for this publication is: